



# OAK RIDGE NATIONAL LABORATORY

managed by  
MARTIN MARIETTA ENERGY SYSTEMS, INC.  
for the  
U.S. DEPARTMENT OF ENERGY

## RSIC DATA LIBRARY COLLECTION

### SAILOR

Coupled, Self-Shielded, 47-Neutron, 20-Gamma-Ray, P<sub>3</sub>,  
Cross Section Library for Light Water Reactors

Contributed by

Science Applications, Inc.  
La Jolla, California  
Oak Ridge National Laboratory  
Oak Ridge, Tennessee  
and  
Electric Power Research Institute  
Palo Alto, California

RADIATION SHIELDING INFORMATION CENTER



**Legal Notice:** This report was prepared as an account of Government sponsored work and describes a code system or data library which is one of a series collected by the Radiation Shielding Information Center (RSIC). These codes/data were developed by various Government and private organizations who contributed them to RSIC for distribution; they did not normally originate at RSIC. RSIC is informed that each code system has been tested by the contributor, and, if practical, sample problems have been run by RSIC. Neither the United States Government, nor the Department of Energy, nor Martin Marietta Energy Systems, Inc., nor any person acting on behalf of the Department of Energy or Energy Systems, makes any warranty, expressed or implied, or assumes any legal liability or responsibility for the accuracy, completeness, usefulness or functioning of any information code/data and related material, or represents that its use would not infringe privately owned rights. Reference herein to any specific commercial product, process, or service by trade name, trademark, manufacturer, or otherwise, does not necessarily constitute or imply its endorsement, recommendation, or favoring by the United States Government, the Department of Energy, Energy Systems, nor any person acting on behalf of the Department of Energy or Energy Systems.

This code/data package is a part of the collections of the Radiation Shielding Information Center (RSIC) developed by various government and private organizations and contributed to RSIC for distribution. Any further distribution by any holder, unless otherwise specifically provided for is prohibited by the U.S. Dept. of Energy without the approval of RSIC, P.O. Box 2008, Oak Ridge, TN 37831-6362.

Documentation for DLC-76/SAILOR Data Package

	PAGE
RSIC Data Library Abstract .....	iii
G. L. Simmons, "Analysis of the Browns Ferry Unit 3 Irradiation Experiments," EPRI NP-3719 (November 1984) .....	1

(Total Pages 124; July 1987)



## RSIC DATA LIBRARY DLC-76

1. **NAME AND TITLE OF DATA LIBRARY**  
SAILOR: Coupled, Self-Shielded, 47 Neutron, 20 Gamma-Ray,  $P_3$ , Cross Section Library for Light Water Reactors.
2. **NAME AND TITLE OF DATA RETRIEVAL PROGRAMS**  
BCDBIN: Conversion Program to Make an ANISN Library.
3. **CONTRIBUTORS**  
Science Applications, Inc., La Jolla, California.  
Oak Ridge National Laboratory, Oak Ridge, Tennessee.  
Electric Power Research Institute, Palo Alto, California.  
Battelle, Columbus, Ohio.
4. **HISTORICAL BACKGROUND AND INFORMATION**  
The ANS 6.1.2 Working Group developed a Standard for specification of a multigroup cross-section library for LWR shielding applications. The DLC-47/BUGLE library, produced by collapse from DLC-41/VITAMIN-C, was the first attempt at providing a library that conformed. Comparison of BUGLE results with several multigroup libraries for a concrete slab problem and an LWR model revealed deficiencies that limited its usefulness as a cross-section library for use in various LWR shielding applications.  
It was recognized that changes to the group structure, self shielding appropriate to specific geometries and compositions, proper treatment of temperature effects, and collapse with appropriate energy spectra would be required to develop a broad group library for application to specific LWR problems. From this perspective, a multigroup cross section library called SAILOR (Shielded and Application Independent Libraries for Operating Reactors) was developed. The DLC-75/BUGLE80 library, which used the same group structure as SAILOR, was ultimately cited in the ANS 6.1.2 Standard. Delay in the release of SAILOR precluded its inclusion in the Standard.
5. **APPLICATION OF THE DATA**  
One-dimensional cylindrical models of a Pressurized Water Reactor (PWR) and a Boiling Water Reactor (BWR) were used as the focal point for the determination of reference spectra. These calculated spectra were then used in making comparisons between various cross section libraries and also as the source of weighting spectra for collapsing the VITAMIN-C library. The models were used to represent conditions at the reactor mid-plane and served as the basis for determining the neutron and gamma-ray spectra at various radial locations. The BWR model consisted of seven concentric regions and the PWR model eight. It is expected that actual reactors with configurations near that of the SAILOR models can be analyzed well with this library.

6. **SOURCE AND SCOPE OF DATA**

Data are provided for the range of materials needed in the analysis of LWR shielding applications, including the pressure vessel dosimetry problem. Microscopic cross sections for individual elements and isotopes are provided for each region of the PWR and BWR models. These transport cross sections are based on self-shielded data collapsed from DLC-41/VITAMIN-C (based on ENDF/B-IV) AMPX-II system. In addition, dosimetry cross sections from ENDF/B-IV are also included.

7. **DISCUSSION OF THE DATA RETRIEVAL PROGRAM**

The BCDBIN program has the single purpose of converting the card image form of the SAILOR cross-section library into the unformatted form that is known as an ANISN Library.

8. **DATA FORMAT AND COMPUTER**

BCD/EBCDIC card images; IBM 370/3033, PC 386, PC 486.

9. **TYPICAL RUNNING TIME**

Conversion takes less than one minute on an IBM 3033.  
On a PC 386, the conversion program took about 9 minutes.

10. **REFERENCES**

a. Included with package

G. L. Simmons, "Analysis of the Browns Ferry Unit 3 Irradiation Experiments," EPRI NP-3719 (November 1984).

b. Background information

American Nuclear Society Standards Committee Working Group ANS-6.1.2, "American National Standard Neutron and Gamma-Ray Cross Sections for Nuclear Radiation Protection Calculations for Nuclear Power Plants," ANSI/ANS-6.1.2-1983 (August 1983).

11. **CONTENTS OF LIBRARY**

Included are the document in 10.a. and a reel of magnetic tape which contains the cross sections, the input data for BCDBIN, sample DD cards, and the printed output from BCDBIN; total records 41,087. The PC 386 and PC 486 version is available on two DS/HD 5.25-inch diskette (1.2MB).

12. **DATE OF ABSTRACT**

April 1985; July 1987; April 1991.

**KEYWORDS:** ANISN FORMAT; COUPLED NEUTRON-GAMMA-RAY CROSS SECTIONS;  
MICROCOMPUTER; MULTIGROUP CROSS SECTIONS BASED ON ENDF/B

SUBJECTS	Corrosion, chemistry, and radiation transport / Reliability, operations, maintenance, and human factors / Plant materials / Safety analysis	
TOPICS	Pressure vessels BWRs Neutron transport	Neutron dosimetry Computer calculations DOT code
AUDIENCE	Generation engineers / R&D scientists	

**Analysis of the Browns Ferry Unit 3  
Irradiation Experiments**

A technique for calculating neutron radiation in and around LWR pressure vessels proved accurate enough to replace actual measurement in most applications. In the course of validating this technique, researchers developed the SAILOR cross-section library of data on power reactor shielding.

BACKGROUND	The steel walls of the nuclear reactor pressure vessels in LWR power plants are subject to gradual embrittlement induced by neutron irradiation from the core. Reliable methods for predicting neutron fluences and neutron spectra at various locations within a reactor vessel are important for establishing the integrity of pressure boundaries in existing plants and for demonstrating compliance with licensing requirements in new ones. In addition, these neutron flux parameters may have significance for personnel safety. A neutron transport calculation method using the discrete ordinates procedure with the Oak Ridge National Laboratory (ORNL) DOT and ANISN computer codes (EPRI reports NP-152 and NP-155) needed validation for this application.
OBJECTIVE	To demonstrate the validity of a neutron transport calculation method for determining neutron fluence and neutron spectra at various locations in a BWR pressure containment system.
APPROACH	Using the neutron transport method, analysts performed a series of one- and two-dimensional computations of fast neutron fluence for a particular core source term at the Browns Ferry (Alabama) Unit 3 BWR. For this work they prepared a cross-section library from ORNL data on neutron interaction. They compared the calculations to neutron fluence and neutron spectra data obtained inside the reactor pressure vessel and in the cavity just outside the vessel at the Browns Ferry BWR from November 1976 to August 1979 (EPRI report NP-1997). The measurements of radiation parameters had been made by activating metal foils sensitive to neutrons above various energy thresholds in the range up to 6 MeV.
RESULTS	The calculated in-vessel neutron fluence values demonstrated that this calculation method can effectively predict the measured results, when the calculations include required corrections for photofission and power distributions near the detector. In the vessel cavity, the DOT and ANISN codes

---

predicted values within approximately 50% at the midplane of the core and within a factor of 2 at the plane of the core top. The chief uncertainty in the calculations is the poorly understood distribution of voids (steam bubbles) in and around the core. The 70-group Shielding- and Application-Independent Libraries for Operating Reactors (SAILOR) cross-section library, developed in this study, is documented in the report.

---

**EPRI PERSPECTIVE**

The in-vessel results of this study are particularly pertinent to PWRs, which are more vulnerable than BWRs to neutron embrittlement processes. (Because PWR pressure vessels are smaller in diameter, they provide less water shielding than BWRs.) These calculations are not sufficiently rigorous to serve as benchmarks, but they do support the general belief in the invulnerability of BWR pressure vessels to neutron-induced embrittlement. Because the uncertainties concerning BWR steam bubble void distribution will probably persist, some measurements using foil activation will continue to be needed. For most purposes, however, these calculations are sufficient, since BWR pressure vessels are not exposed to embrittling neutron doses over their expected lifetimes. In particular, this technique can be useful in predicting radiation levels in those areas of reactor containments where people work on rare but significant occasions. The SAILOR cross-section library, available from the ORNL Radiation-Shielding Information Center, can be used for LWR pressure vessel dosimetry and shielding. Engineers concerned with neutron embrittlement in pressure vessels and with personnel exposure to neutrons within reactor containments will find this report useful.

---

# Analysis of the Browns Ferry Unit 3 Irradiation Experiments

---

NP-3719  
Research Project 827-1

Final Report, November 1984

Prepared by

SCIENCE APPLICATIONS, INC.  
Post Office Box 2351  
La Jolla, California 92038

Principal Investigator  
G. L. Simmons

Contributors  
T. E. Albert  
W. K. Hagan

Prepared for

Electric Power Research Institute  
3412 Hillview Avenue  
Palo Alto, California 94304

EPRI Project Managers  
T. O. Passell  
H. Till

Chemistry, Radiation, and Waste Processing Program  
Nuclear Power Division

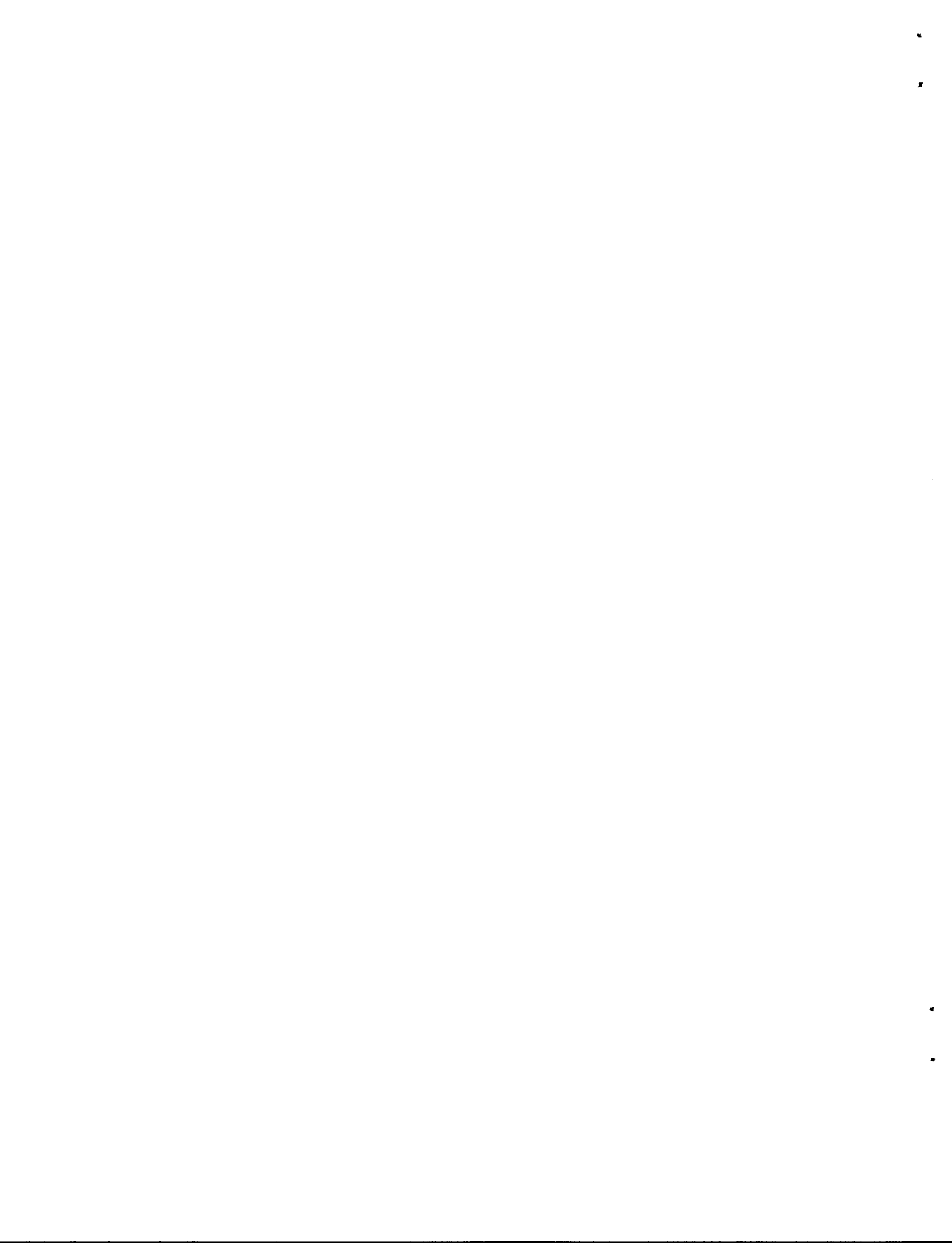


## Table of Contents

	Page
Section	
1. Introduction .....	1-1
2. The Analysis of the BF <sub>3</sub> In-Vessel Experiment .....	2-1
3. The Analysis of the BF <sub>3</sub> Cavity Neutron Measurements .....	3-1
Comparison of Vessel Leakage Energy Spectra from One-and Two-Dimensional Calculations .....	3-2
Calculations of the Axial Distribution of the Neutron Flux in the Cavity .....	3-17
R-Z Calculation .....	3-26
4. References .....	4-1
Appendix A: SAILOR - A Coupled Multigroup Cross Section Light Water Reactors .....	A-1
Appendix B: AMPX-II - Job Streams Used to Generate the SAILOR Library .....	B-1

## ILLUSTRATIONS

<u>Figure</u>	<u>Page</u>
3-1 Case 2 vs Middle Case/Theta 1	3-4
3-2 Case 2 vs Middle Case/Theta 5	3-5
3-3 Case 2 vs Middle Case/Theta 10	3-6
3-4 Case 2 vs Middle Case/Theta 15	3-7
3-5 Case 2 vs Middle Case/Theta 20	3-8
3-6 Case 2 vs Middle Case/Theta 25	3-9
3-7 Case 2 vs Middle Case/Theta 30	3-10
3-8 Case 2 vs Middle Case/Theta 35	3-11
3-9 Case 2 vs Middle Case/Theta 40	3-12
3-10 Case 2 vs Middle Case/Theta 1	3-13
3-11 Case 4 vs Middle Case/Theta 1	3-14
3-12 Case 5 vs Middle Case/Theta 1	3-15
3-13 Case 6 vs Middle Case/Theta 1	3-16
3-14 Case 2 vs Top Case/Theta 1	3-18
3-15 Case 3 vs Top Case/Theta 1	3-19
3-16 Case 4 vs Top Case/Theta 1	3-20
3-17 Case 5 vs Top Case/Theta 1	3-21
3-18 Case 6 vs Top Case/Theta 1	3-22
3-19 Comparison of One- and Two-Dimensional Calculated Spectrum with Unfolded Experimentally Derived Spectrum	3-23
3-20 Comparison of Calculated and Measured Integral Flux $\rightarrow$ 1 MeV	3-25
3-21 Nickel Activation Ratio (relative to core midplane) vs Distance from Core Midplane	3-27

<u>Figure</u>	<u>Page</u>
3-22 Assumed Axial Variation of Void Fraction in Core	3-28
3-23 Nickel Activation Ratio (relative to core midplane): Comparison of Experiment with R-Z Calculations	3-29

#### TABLES

<u>Table</u>	<u>Page</u>
2-1 Power Distribution at the Core Midplane	2-3
2-2 Power Distribution at the Top of the Reactor Core - Three Inches from the Top of the Fuel	2-4
2-3 Power Distribution at Node 23 - Nine Inches from the Top of the Fuel	2-5
2-4 Representative Axial Power Distributions	2-6
2-5 Integral Flux Comparisons $\phi > E$ for BF3	2-8
3-1 PV Leakage Azimuthal Distribution from MIDDLE Case Power Distribution	3-24
3-2 Integral Flux Comparison's $\phi > E$	3-31

## ABSTRACT

The results of the analysis of two experiments performed at the Browns Ferry-3 reactor are presented. These calculations utilize state-of-the-art neutron transport techniques and a new neutron cross-section library that has been developed for LWR applications. The calculations agree well with the experimental data obtained in irradiations inside the reactor vessel. For the measurements performed in the reactor cavity, the calculations agree well at the reactor midplane. Accurate determination of the axial distribution of the neutron fluence in the reactor cavity depends on having a concise representation of the axial-void distribution in the core.

Detailed data are presented describing the procedures used in the generation of the new cross-section library that has been named SAILOR. This library is available from the Radiation-Shielding Information Center.

## ACKNOWLEDGMENTS

The authors would like to thank the personnel at the Radiation-Shielding Information Center for their assistance in the course of this project. In particular, Dr. R. W. Roussin provided invaluable help in preparing the new cross-section library. We would like to thank EPRI project managers Drs. F. Rahn, H. Till, and T. O. Passell for their encouragement and suggestions during the long course of this project. Thanks also to Dr. G. C. Martin at General Electric for providing much of his data prior to publication and for many stimulating discussions during the project.

## SUMMARY

Determining the neutron energy spectra and neutron fluence at critical locations within the steel pressure vessel of light water reactors is of interest in predicting the useful lifetime of the vessel under neutron irradiation. The information contained in this report describes a method of calculation that has been developed in support of the larger program at EPRI directed toward the continued assurance of LWR pressure boundaries and the ability of new and existing plants to meet licensing and technical specification requirements. This methodology is designed to provide accurate predictions of these neutron parameters at critical locations in the pressure containment system, particularly in regions where surveillance capsules are not available.

Concurrent with the development of a calculational methodology is a program to perform measurements of the neutron spectra at locations of interest at the Browns Ferry Unit 3 and McGuire Unit 1 nuclear reactors. These measurements serve as validation data for the analysis methods and, in particular, the comparisons with the Browns Ferry data are discussed in detail in this report. The calculational methodology uses the well known discrete ordinates procedure for solving the neutron transport equation and has been described in detail in a previous EPRI Report, NP 155. In refining this methodology, a completely new coupled neutron and gamma ray cross section library, named SAILOR, has been created for use in LWR pressure vessel dosimetry and shielding applications. This library should be useful for both boiling water and pressurized water reactor types. The complete procedure that was used in generating this library is contained in an Appendix of this report.

For the Browns Ferry reactor, measurements were carried out both inside the reactor vessel and in the reactor vessel cavity. The in-vessel experiment is of most interest for neutron embrittlement considerations, while the cavity measurements are of interest for neutron streaming studies. The conclusion of our analysis of the in-vessel experiments is that the methods used can effectively predict the measured results, provided that all the corrections associated with photofission and power distributions near the detector are

included. For the cavity experiments, the procedures used to perform the analysis provided results that agreed well with the measured data at the core mid-plane. At other locations, the calculated results were quite sensitive to the assumptions made concerning the void distribution that was assumed in the core. Overall, the procedures used in the analysis should provide an excellent tool for determining the neutron spectra and fluence at critical locations in light water reactors.

Section 1  
INTRODUCTION

Since 1977, Science Applications, Inc. (SAI) has supported the EPRI program for pressure vessel embrittlement studies in the development of a calculational methodology. The methodology has evolved, consisting of a collection of radiation transport computer programs, cross section data, albedo scattering data, and a set of procedures for utilizing these codes and data. The methodology was first expounded in an analysis of PWR and BWR radiation environments for radiation damage studies (1). In subsequent projects the methodology was refined and extended to in-vessel neutron spectral analysis and to cavity streaming problems.

The development of a calculational methodology supported the larger program at EPRI directed toward the continued assurance of LWR pressure boundaries and the ability of new and existing plants to meet licensing and technical specification requirements. The role and value of the calculational methodology is to provide accurate predictions of the neutron flux and energy spectrum at critical locations in the pressure containment system, particularly in regions where surveillance capsules are not available.

A high priority objective of the EPRI program was obtaining precision dosimetric measurements, in part, for the validation of the calculational methods and data. A measurement program for characterizing the neutron flux and spectrum inside the pressure vessel and in the cavity of a BWR operating at high power was conducted by the General Electric (GE) Company. The measurements were performed at the Browns Ferry Unit 3 (BF3) reactor between November 1976 and August 1979, and reported in August 1980 (2) and in August 1981 (3).

A parallel series of measurements were planned by IRT Corporation to obtain data in a PWR, specifically the McGuire Reactor (4). However, no results have been reported at the present time from the PWR measurement program.

The objective of this report is to provide a comparison of calculated results with the available measurements.

Section 2  
THE ANALYSIS OF THE BF3 IN-VESSEL EXPERIMENT

The in-vessel experiments at BF3 consisted of threshold foil measurements at three locations inside the reactor pressure vessel. At each of the three positions, the reaction rates were obtained at several radial locations between the reactor barrel and the pressure vessel. The three positions for the measures are designated as: G-1 at the core top on the core flats; G-3 at core midplane on the flats; and G-4 at the core midplane and 45 degrees from the flats. The details of this experiment and the procedures used by GE to obtain the final spectral data are described in Reference 2 and will not be repeated here. Because unfolding techniques were used in obtaining the neutron spectra, some of our results were used by GE to perform various corrections to the activation results. These corrections included both the effects of local power histories and the enhanced activation of the foils due to localized photo fission events. Our contributions are noted in both References 2 and 3. We also provided trial spectra for use by GE in the unfolding procedures.

The procedures used to perform the analysis of the in-vessel experiment are described in Reference 1. The primary deviation from these procedures involves the use of a newer cross section set that was specifically generated for LWR pressure vessel applications. The detailed discussion of the cross section library is contained in Appendix A, along with some comparisons between other libraries. As discussed in Reference 1, the input to the analysis is primarily the reactor geometry and the power distribution.

The power distribution for both the in-vessel and cavity calculations were taken from data supplied to SAI by engineers at TVA. These data consisted of results from both predictive three-dimensional core performance calculations and operating data from the plant process computer. The data that was used in the analysis was obtained converting the three-dimensional burn-up distribution at the end of the irradiation cycle into a power distribution. This burn-up distribution should provide a reasonable representation of the average power distribution over the burn-up cycle. This is a convenient method for reducing

the number of calculations that would have to be carried out if power distributions obtained at different times during the burn-up cycle were used to synthesize the time history of irradiation. The data on the power and burn-up distributions were obtained at 24 evenly spaced axial nodes for each of the 764 fuel assemblies in the reactor.

The measurements were obtained at the core midplane, positions G-3 and G-4, and at the G-1 position near the top of the core. Note that there was a detector set at the top of the core, corresponding to the G-4 position, but it was lost during the irradiation. The data in Table 2-1 represents the power distribution that was used in the calculation of the neutron spectra at the core midplane location. These data are normalized to a unit power distribution at this location and must then be modified by the axial peaking associated with the core midplane. The data in Tables 2-2 and 2-3 represent the power distribution at the top of the core near the G-1 position. An examination of these tables indicates that the power distribution is changing quite rapidly between these two positions and, therefore, will introduce some error in the associated analysis.

Data presented in Table 2-4 represents the axial power distributions over the entire core and for selected fuel assemblies. The fuel assemblies were chosen because of their proximity to the various detector locations. The power distribution information at each axial node represents an average over the fuel assembly. It is well documented that for calculations of neutron spectra and fluence at the reactor pressure vessel, the power distribution for the individual pins may be required. This is particularly true for those fuel assemblies that are on the outer edge of the core and near the location of maximum fluence. It is precisely for these fuel assemblies that there is potentially the least amount of confidence in these predicted results of core analysis. This lack of knowledge of these parameters introduces a source of error in the analysis that is difficult to quantify.

Using these power distributions, a series of one-dimensional transport calculations were performed as a first step in the analysis. The core was represented as a cylinder and the neutron spectra were obtained for a variety of power distributions and core conditions. These data served a two-fold purpose. First, they provided a set of data for comparison with the two-dimensional R-







Table 2-4  
Representative Axial Power Distributions

Axial Node	Core Average	Core Flat A*	45 Degree Position		
			B*	C	D
Core Bottom → 1	0.591	0.533	0.499	0.569	0.572
2	0.903	0.855	0.858	0.919	0.889
3	1.027	1.037	1.062	1.101	1.061
4	1.127	1.158	1.165	1.212	1.195
5	1.168	1.210	1.239	1.265	1.252
6	1.172	1.208	1.226	1.250	1.262
7	1.150	1.189	1.184	1.220	1.248
8	1.175	1.209	1.198	1.234	1.270
9	1.165	1.188	1.177	1.204	1.243
10	1.150	1.172	1.159	1.169	1.221
11	1.157	1.174	1.147	1.172	1.223
12	1.160	1.164	1.156	1.169	1.203
13	1.120	1.117	1.126	1.127	1.144
14	1.068	1.056	1.092	1.074	1.085
15	1.075	1.069	1.102	1.079	1.078
16	1.075	1.061	1.094	1.075	1.068
17	1.019	1.057	1.044	1.013	0.997
18	1.022	1.053	1.023	1.010	1.000
19	1.014	1.024	1.008	0.972	0.961
20	0.949	0.938	0.934	0.884	0.850
21	0.870	0.846	0.819	0.779	0.757
22	0.831	0.775	0.751	0.700	0.668
23	0.619	0.567	0.579	0.499	0.463
Core Top → 24	0.388	0.338	0.358	0.298	0.278

\*The location on the core map is shown in Table 2-1.

theta transport calculations. Secondly, they provided a reasonably detailed flux profile and distribution across the water gap between the core barrel and the reactor pressure vessel. This region of the reactor contains the jet pumps and also the fluence detectors used in the measurements. These radial flux profiles, coupled with experimental data, served as a mechanism for obtaining an estimate of the neutron spectra at a single point within the jet pump region.

Following the one-dimensional analysis, a series of two-dimensional calculations were performed. These R-theta calculations resulted in the detailed data that were used in a direct comparison with the experimental results obtained by GE. Table 2-5 presents some of these data for integral flux parameters above a certain energy threshold. Included in this table is an estimate of the experimental error at various thresholds. The comparisons between the calculated results and the experiment is really quite good. Note that for high-energy thresholds, the calculations consistently over predict the experiment, indicating a somewhat harder spectra. Upon examination of the foil unfolding procedure used in the experiment, the representation of the spectra at high energies in the unfolding code may be a partial cause of this discrepancy. In general, it appears that current analytical techniques would yield neutron spectra that compare quite favorably with results obtained from the in-vessel experiment in a very complicated geometry. What is difficult to quantify is the uncertainty that is associated with these calculations, given the difficulty in determining the uncertainty in the basic neutron source at the edge of the reactor core.

Table 2-5

Integral Flux Comparisons  $\phi > E$  for BF3

Measurement Position: Near-Shroud or Core Barrel

E(MeV)	Mid-Plane		Top of Core		Measurement Error
	SAI <sup>1</sup>	GE <sup>2</sup>	SAI	GE	
6	6.1x10 <sup>9</sup>	5.6x10 <sup>9</sup>	3.4x10 <sup>9</sup>	2.9x10 <sup>9</sup>	
4	1.5x10 <sup>10</sup>	1.8x10 <sup>10</sup>	8.5x10 <sup>9</sup>	9.8x10 <sup>9</sup>	
3	2.2x10 <sup>10</sup>	2.9x10 <sup>10</sup>	1.2x10 <sup>10</sup>	1.9x10 <sup>10</sup>	+15%
2	3.7x10 <sup>10</sup>	4.7x10 <sup>10</sup>	2.1x10 <sup>10</sup>	3.2x10 <sup>10</sup>	
1	5.8x10 <sup>10</sup>	7.6x10 <sup>10</sup>	3.2x10 <sup>10</sup>	5.0x10 <sup>10</sup>	+25%
0.1	1.1x10 <sup>11</sup>	1.5x10 <sup>11</sup>	5.9x10 <sup>10</sup>	9.4x10 <sup>10</sup>	+35%

Measurement Position: Near-Vessel

E(MeV)	Mid-Plane		Top of Core		Measurement Error
	SAI	GE	SAI	GE	
6	1.3x10 <sup>8</sup>	7.7x10 <sup>7</sup>	8.5x10 <sup>7</sup>	4.0x10 <sup>7</sup>	
4	2.5x10 <sup>8</sup>	1.2x10 <sup>8</sup>	1.6x10 <sup>8</sup>	1.0x10 <sup>8</sup>	
3	3.2x10 <sup>8</sup>	2.8x10 <sup>8</sup>	2.0x10 <sup>8</sup>	1.5x10 <sup>8</sup>	+15%
2	4.3x10 <sup>8</sup>	3.8x10 <sup>8</sup>	2.7x10 <sup>8</sup>	2.0x10 <sup>8</sup>	
1	5.6x10 <sup>8</sup>	5.2x10 <sup>8</sup>	3.5x10 <sup>8</sup>	2.7x10 <sup>8</sup>	+30%
0.1	7.9x10 <sup>8</sup>	9.0x10 <sup>8</sup>	4.9x10 <sup>8</sup>	4.7x10 <sup>8</sup>	+35%

Measurement Position: Vessel Surface

E(MeV)	Mid-Plane		Top of Core		Measurement Error
	SAI	GE	SAI	GE	
6	7.5x10 <sup>7</sup>	5.2x10 <sup>7</sup>	4.7x10 <sup>7</sup>	2.8x10 <sup>7</sup>	
4	1.4x10 <sup>8</sup>	1.3x10 <sup>8</sup>	8.4x10 <sup>7</sup>	7.0x10 <sup>7</sup>	
3	1.8x10 <sup>8</sup>	1.9x10 <sup>8</sup>	1.2x10 <sup>8</sup>	1.0x10 <sup>8</sup>	+20%
2	2.6x10 <sup>8</sup>	2.6x10 <sup>8</sup>	1.6x10 <sup>8</sup>	1.4x10 <sup>8</sup>	
1	3.8x10 <sup>8</sup>	3.5x10 <sup>8</sup>	2.8x10 <sup>8</sup>	1.9x10 <sup>8</sup>	+35%
0.1	6.7x10 <sup>8</sup>	6.1x10 <sup>8</sup>	4.2x10 <sup>8</sup>	3.3x10 <sup>8</sup>	+40%

<sup>1</sup>Calculated

<sup>2</sup>Measured

Section 3  
THE ANALYSIS OF THE BF3 CAVITY NEUTRON MEASUREMENTS

The objectives of the BF3 cavity neutron measurements were:

- To help verify the long-term integrity and service life of the BWR pressure vessel,
- To determine the fast neutron energy spectra and flux levels in a BWR cavity region during high power operating conditions, and
- To establish a data base for cavity radiation levels as a benchmark for calculations.

The measurement program included dosimetry specimens within the pressure vessel, in addition to dosimetry measurements in the cavity. If a validation of the calculations were obtained, the EPRI program may obviate the need for in-vessel specimens.

The cavity measurements consisted of a series of capsules suspended on nickel wires strung in the cavity between the feedwater nozzle insulation and the recirculation inlet nozzle insulation. The capsules consisted of several types of dosimeter wires and disks. In addition, the nickel wire stringer was cut into one-inch segments and was analyzed for Co-58 activity. Neutron spectra were determined from an unfolding of the dosimetric data at the capsule locations. In addition, the nickel wire disintegration and reaction rates were tabulated for the one-inch segments as a function of axial and azimuthal locations. This subset of the experimental results comprise the basis for the comparison with the calculations reported in this report.

The methodology used for analysis of radiation fields in the cavity of an LWR consists of one- or two-dimensional discrete ordinates calculations from the core through the pressure vessel. For cavity streaming calculations, the leakage from the pressure vessel is used as a source term for three-dimensional Monte Carlo calculations outside of the pressure vessel.

It is desirable for reasons of economy to utilize one-dimensional calculations in the core and pressure vessel. Reference 1 reported good comparisons of the

integral flux on the outside surface of the pressure vessel at the core midplane for one- and two-dimensional discrete ordinate calculations. However, the two-dimensional R-Z calculations are only able to approximate the shape of the core and it is known that the power distribution in the outer assemblies strongly affect vessel fluences. Two-dimensional R-theta calculations are able to represent the geometry of the core and pressure vessel with good fidelity in a plane perpendicular to the axis of the vessel, but does not consider the axial power distribution in the core. Although three-dimensional discrete ordinates codes have recently been developed they have not been considered as part of the EPRI calculational methodology. Therefore, in practice, the leakage from the pressure vessel is calculated approximately by a composite of one- and two-dimensional discrete ordinates results.

The availability of measured neutron spectra as a function of axial and azimuthal location in the reactor cavity afforded the opportunity to test the various approximate methods of calculating the neutron fluence and spectra at the surface of the pressure vessel. Four types of calculations were performed for comparison with the measurements:

- One-dimensional calculations for comparisons at the core midplane.
- Two-dimensional calculations in R-theta geometry using power distributions at the middle and top of the core for comparison with the one-dimensional and the azimuthal measurements.
- Cavity streaming calculations in three dimensions using a pressure vessel leakage source term reconstructed from the one-dimensional calculation and axial and azimuthal power distributions.
- Two-dimensional calculations in R-Z geometry for comparison with axial locations of the measured dosimetric data.

#### COMPARISON OF VESSEL LEAKAGE ENERGY SPECTRA FROM ONE- AND TWO-DIMENSIONAL CALCULATIONS

Several calculations of the neutron flux distributions in the BF<sub>3</sub> reactor vessel have been made. Both one-dimensional calculations have been made using the ANISN code, as well as two-dimensional R-theta calculations using the DOT code. The ultimate objective is to calculate the neutron flux in the reactor cavity, and it is desirable to utilize the one-dimensional transport results of the neutron leakage spectrum from the reactor vessel as a source term for analysis of neutron streaming in the cavity. The purpose of comparing the spectrum from

the one-dimensional calculations and the two-dimensional calculations is to confirm the adequacy of the spectral results of the one-dimensional analysis.

Five one-dimensional cases were run and designated Case 2 through Case 6. Case 2 is the nominal case and assumed a 50 percent void fraction in the coolant in the core and a flat power distribution. Case 3 assumed a 50 percent void fraction between the core and the shroud in addition to a 50 percent coolant void fraction in the core. Case 4 was similar to Case 3 but used a more realistic power distribution. Cases 5 and 6 are the runs to produce the leakage source for the cavity calculations and, therefore, do not have the biological shield in the calculation.

Two DOT calculations were made in an R-theta model of the BF3 core and vessel. The two cases correspond to an attempt to examine the effect of the axial power distribution. The power distribution in fuel assemblies for both the top and middle of the core were modeled using data from the BF3 second cycle. The two cases are referred to as TOP and MIDDLE, respectively.

There are really two comparisons to make:

1. Case-to-case comparisons in which the effects of geometry and power distribution are examined, and
2. One-dimensional case comparisons with the DOT calculations.

The first observation in the comparisons is that there is no significant spectral difference at the outer surface of the pressure vessel as a function of azimuthal position around the surface of the vessel. This can be seen in Figures 3-1 through 3-9, which compare the flux for neutron energies above 0.1 MeV for nine azimuthal positions around the pressure vessel surface. It should be noted that the fluxes have been normalized in order to facilitate a comparison of the energy spectrum and this comparison does not infer that the magnitude of the flux does not vary with position around the circumference of the vessel.

The second observation is that differences in the leakage spectrum between Cases 2, 3, and 4 are not significant. Figures 3-10 and 3-11 show this comparison. However, for Cases 5 and 6 corresponding to Figures 3-12 and 3-13 the effect of the albedo reflection from the cavity shield is apparent.

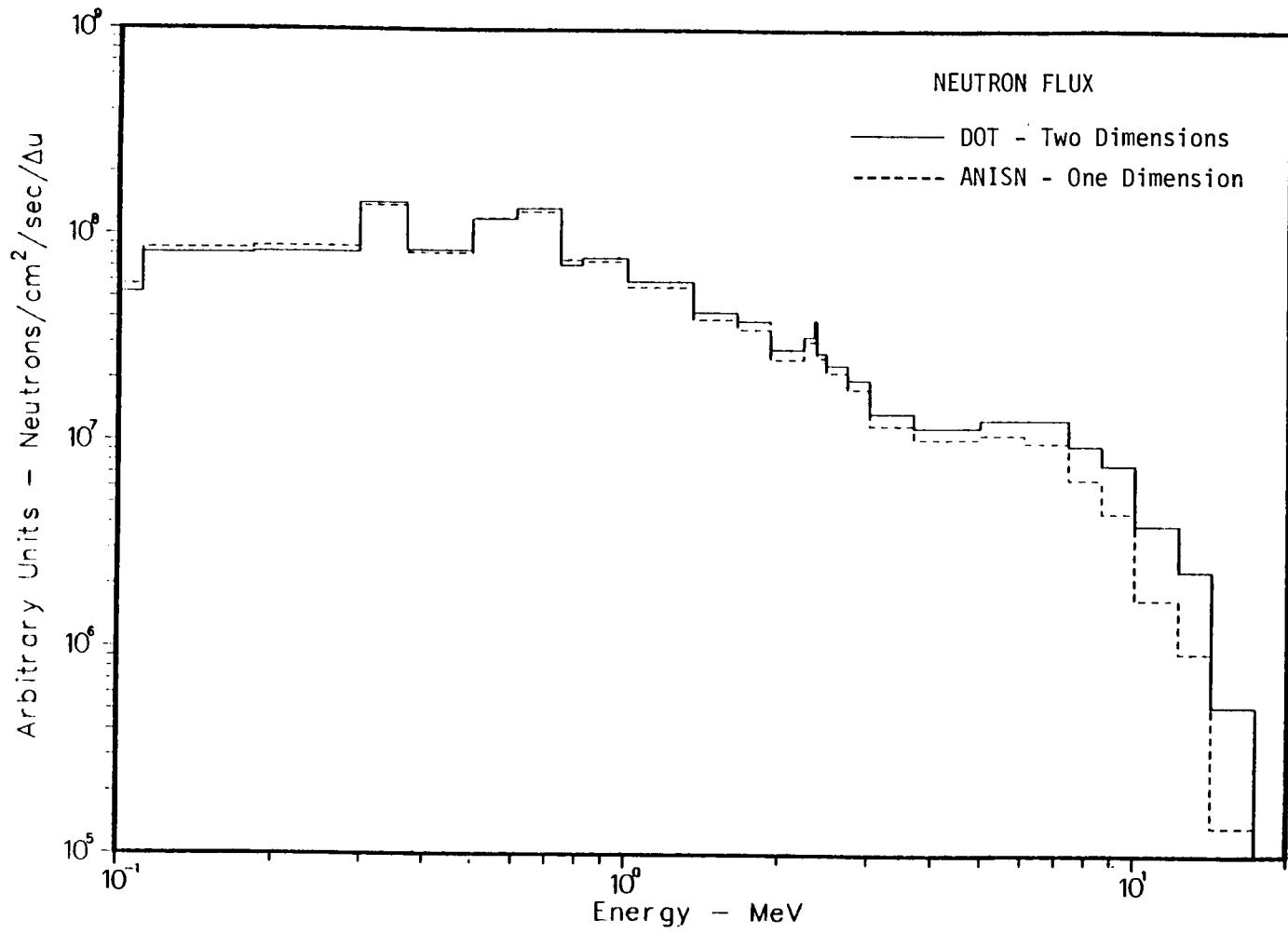


Figure 3-1. Case 2 vs Middle Case/Theta 1

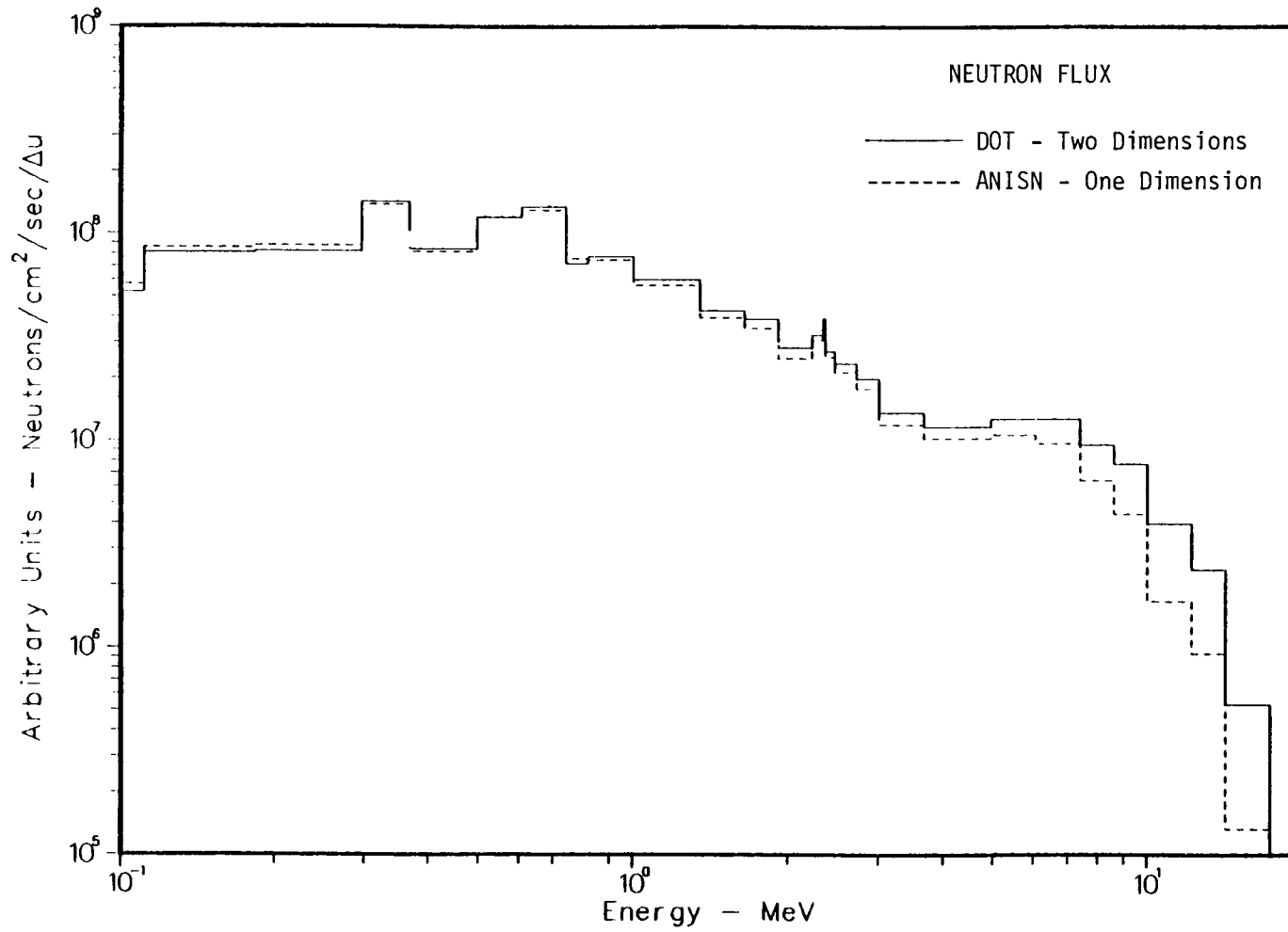


Figure 3-2. Case 2 vs Middle Case/Theta 5

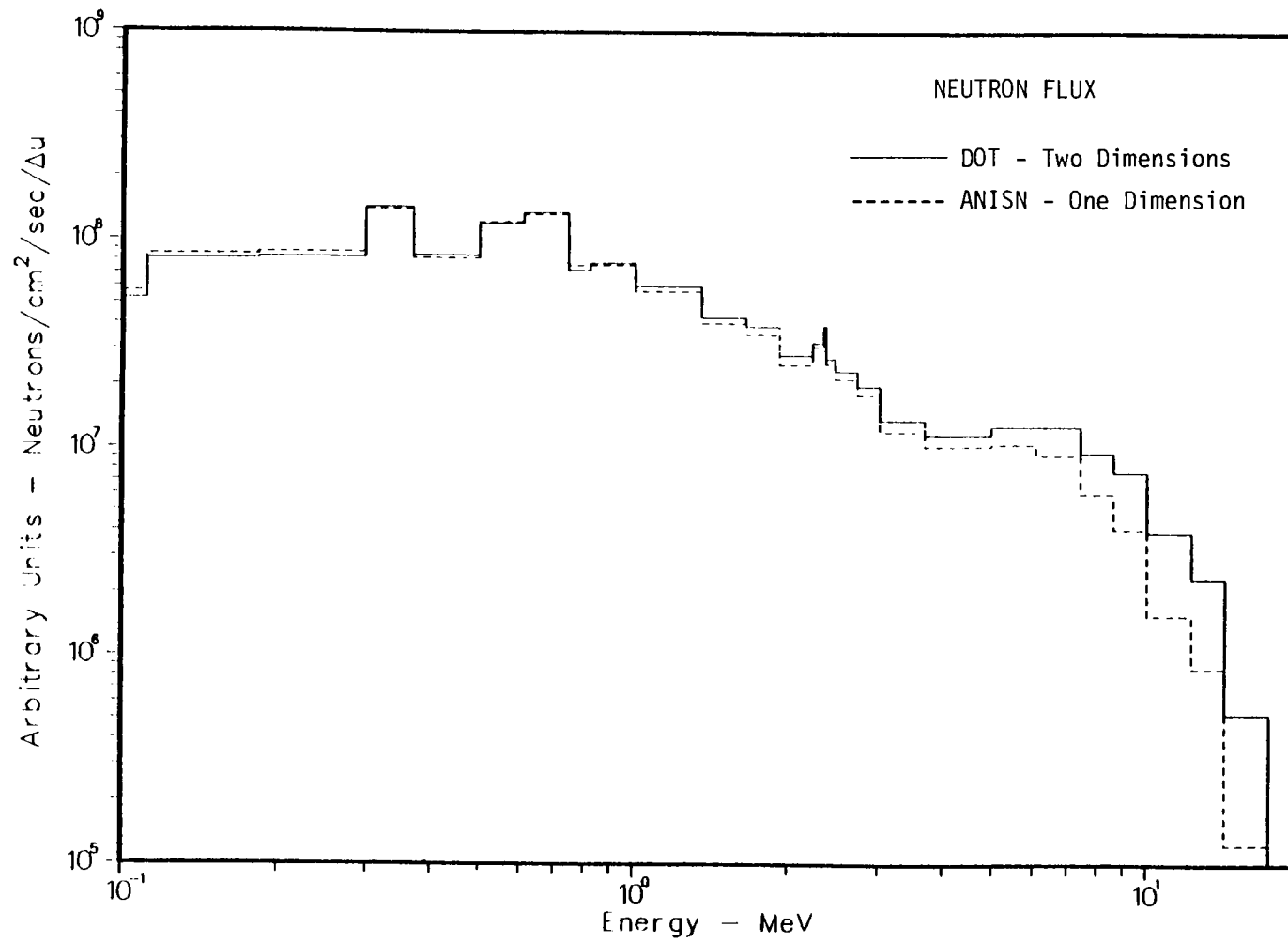


Figure 3-3. Case 2 vs Middle Case/Theta 10

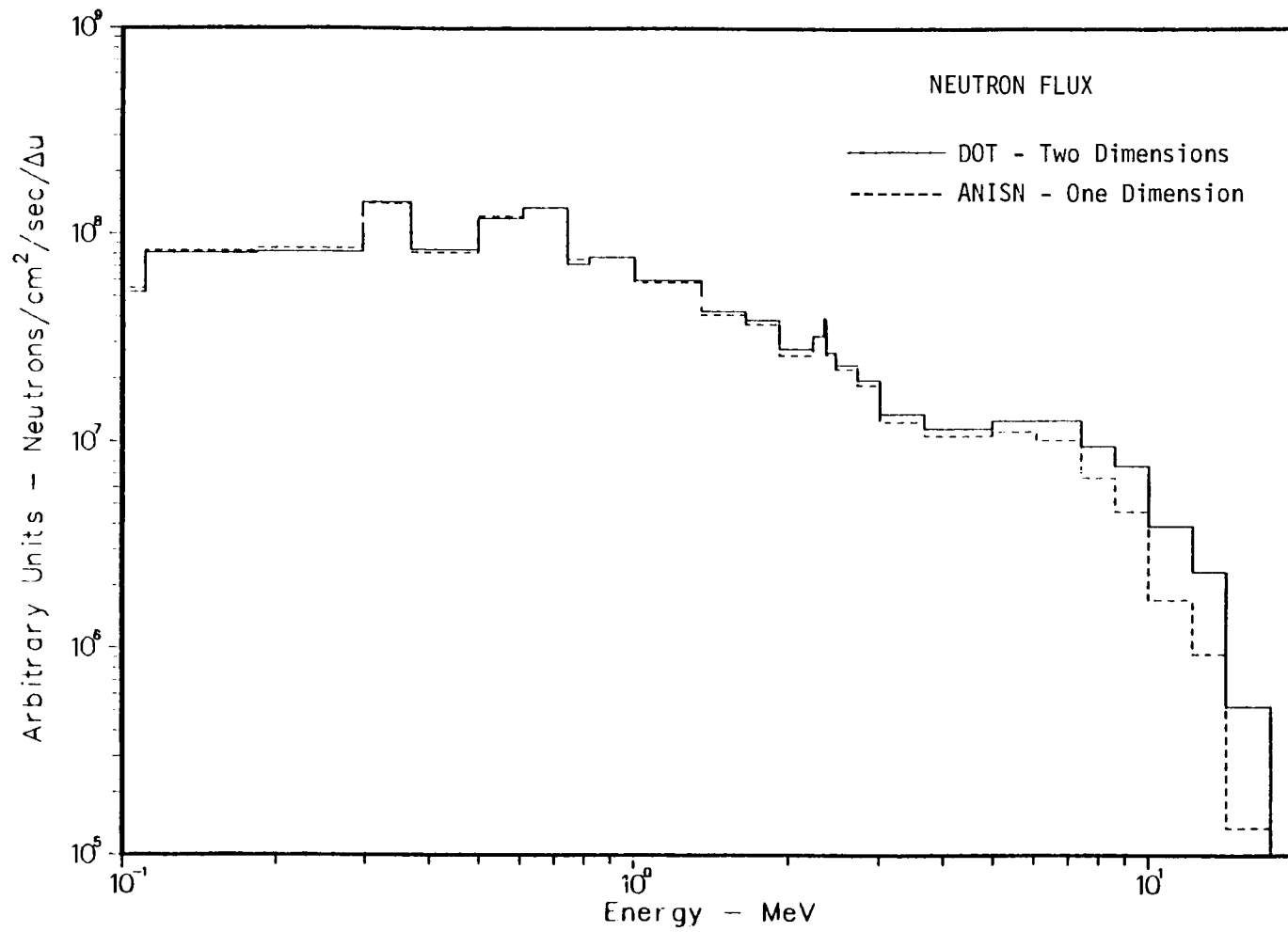


Figure 3-4. Case 2 vs Middle Case/Theta 15

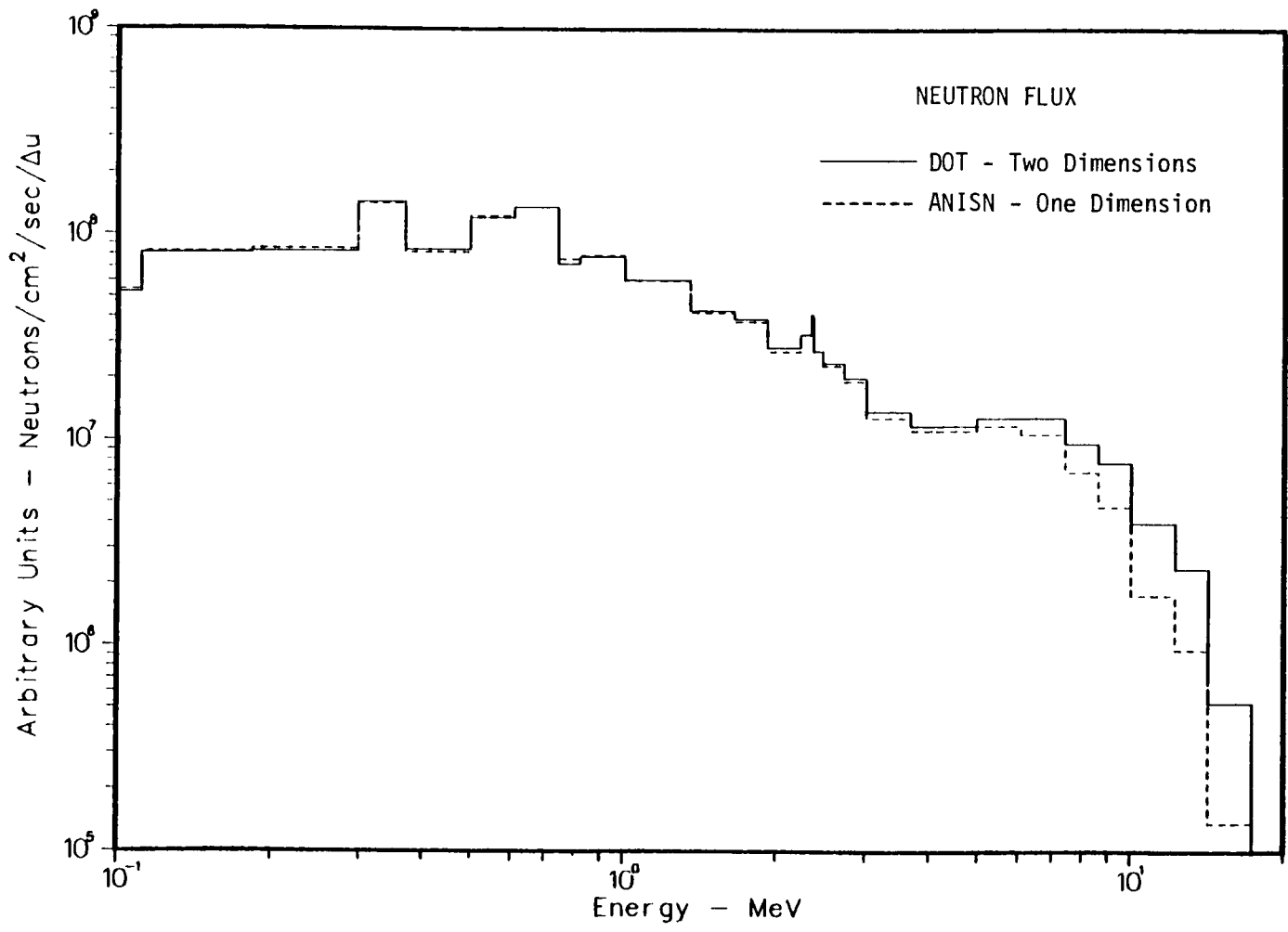


Figure 3-5. Case 2 vs Middle Case/Theta 20

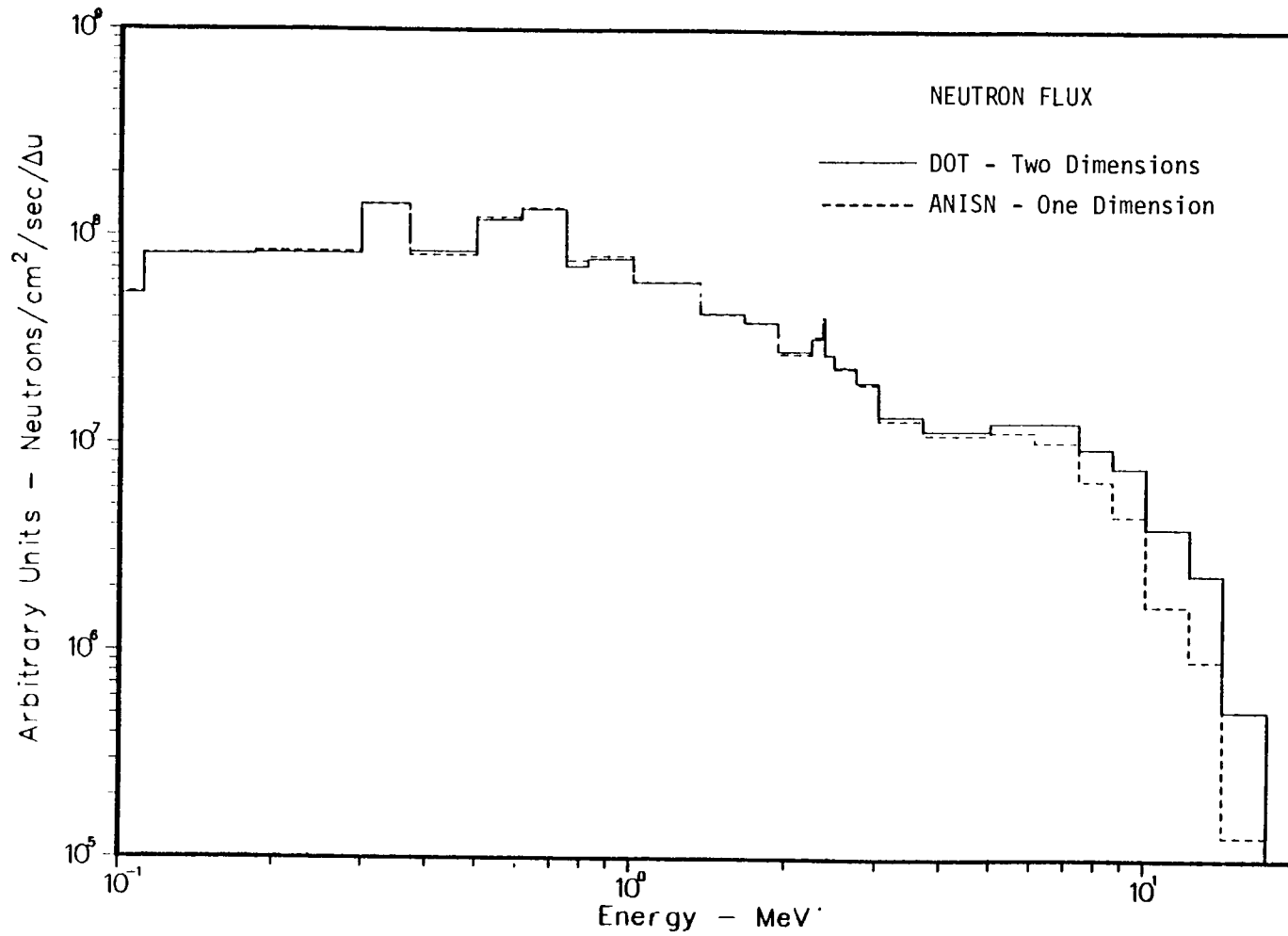


Figure 3-6. Case 2 vs Middle Case/Theta 25

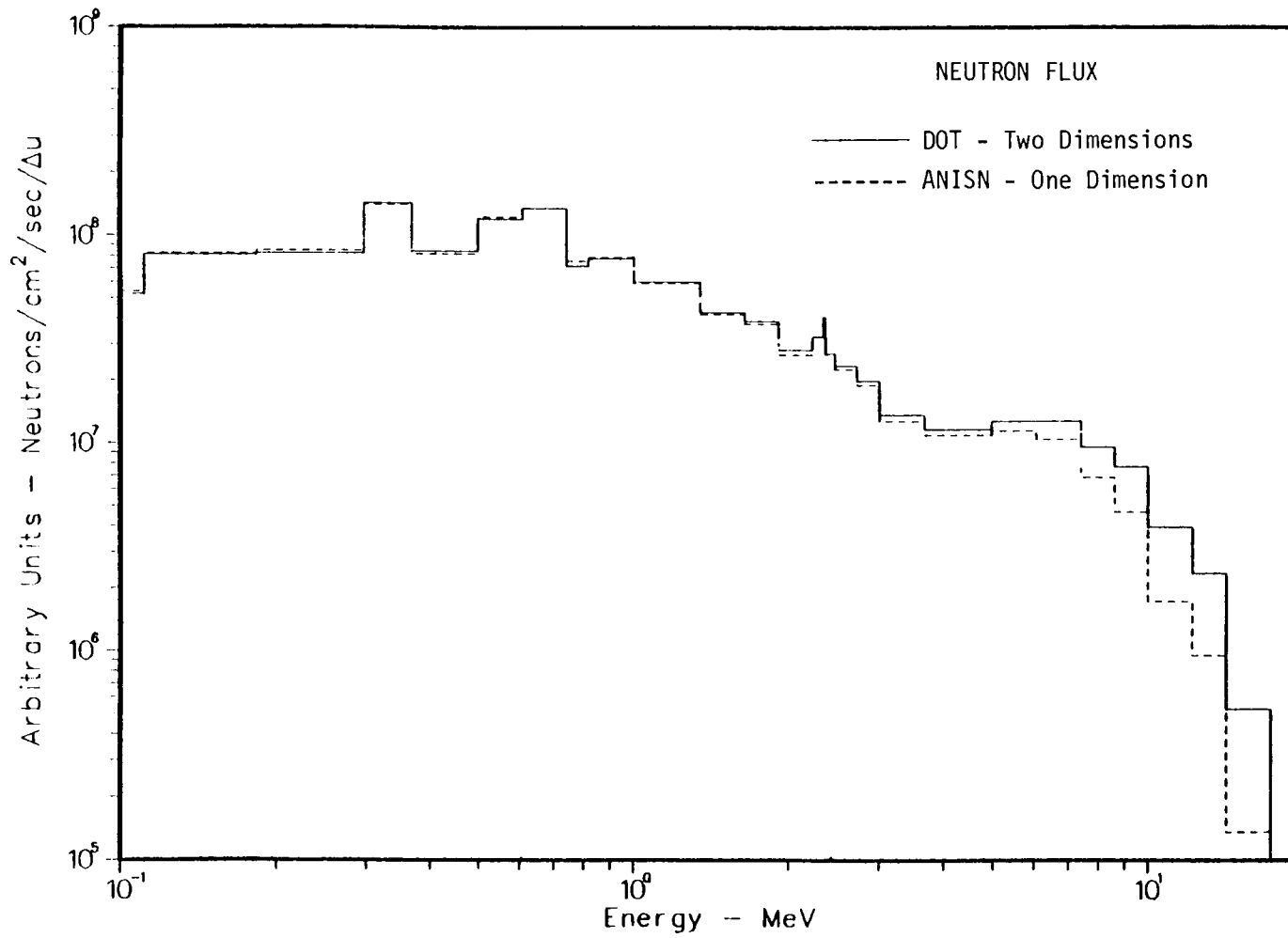


Figure 3-7. Case 2 vs Middle Case/Theta 30

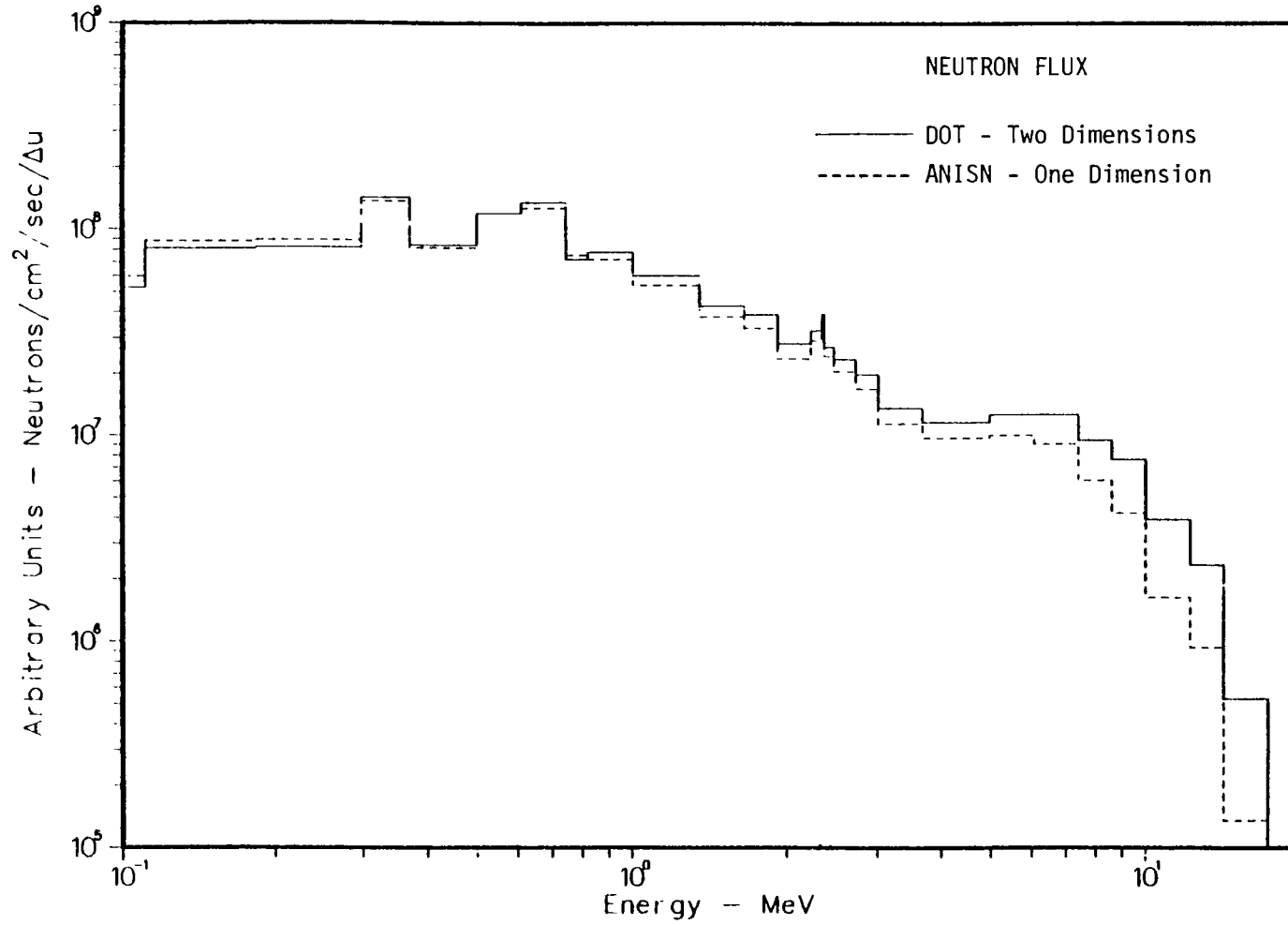


Figure 3-8. Case 2 vs Middle Case/Theta 35

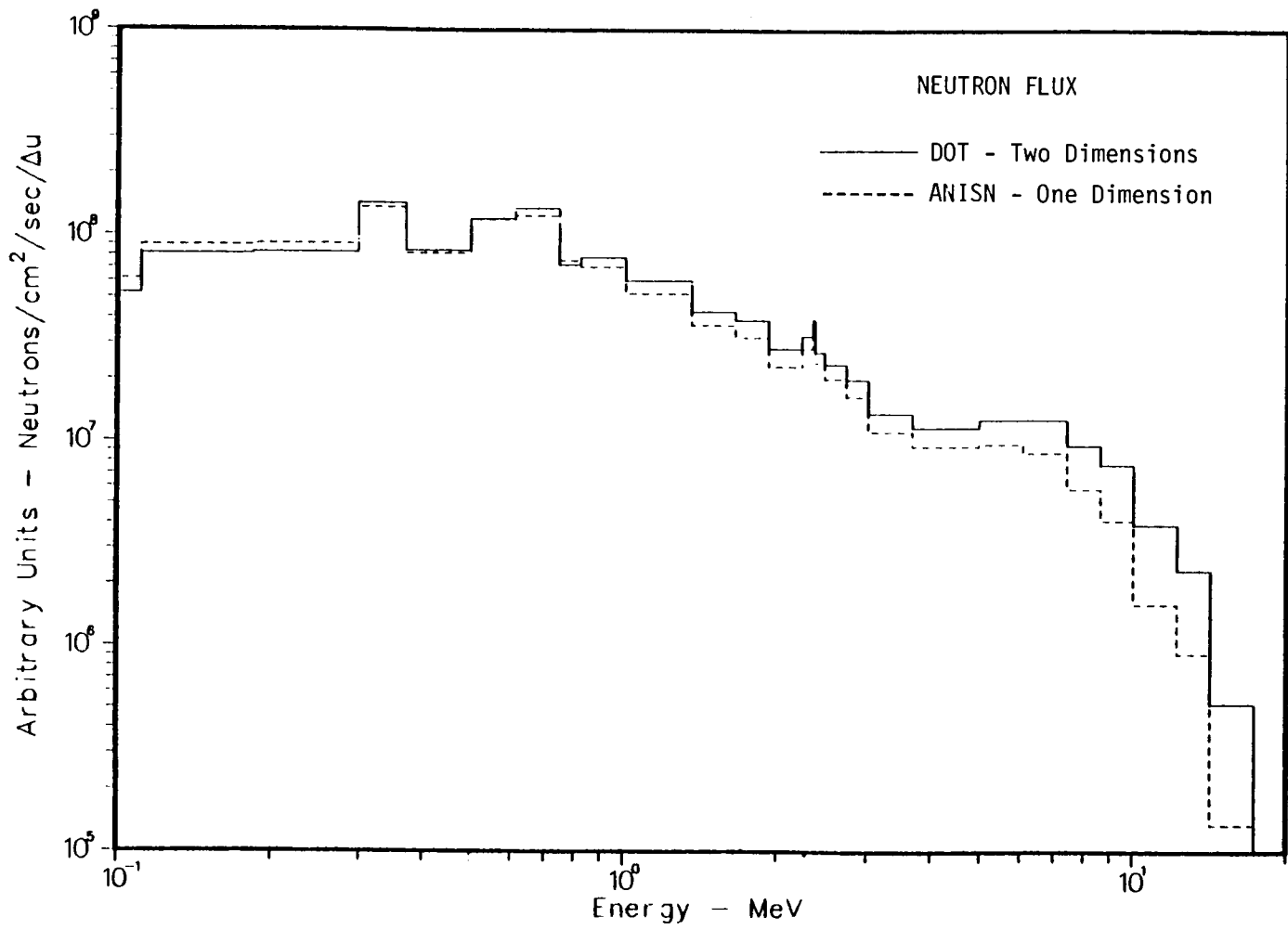


Figure 3-9. Case 2 vs Middle Case/Theta 40

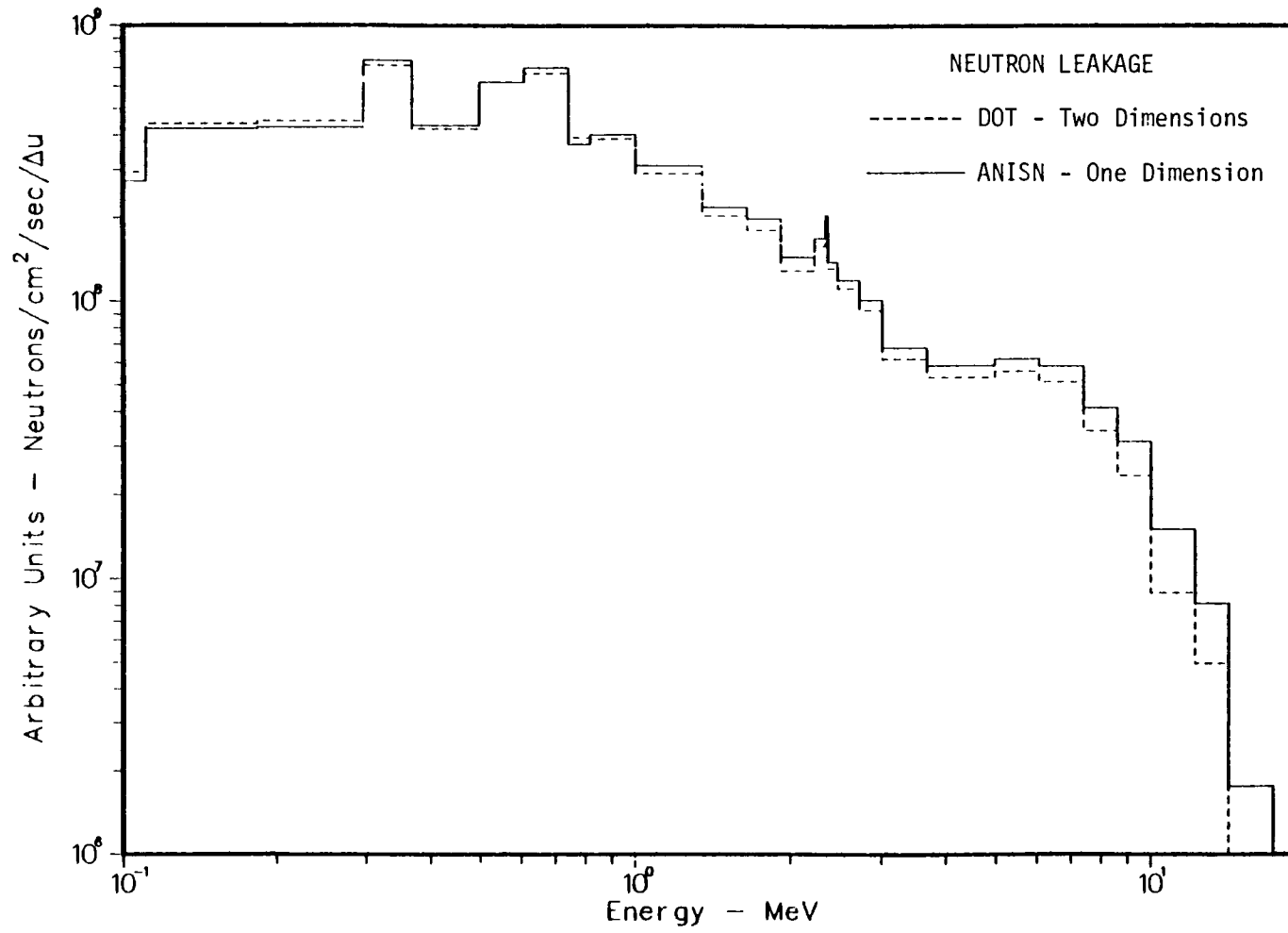


Figure 3-10. Case 2 vs Middle Case/Theta 1

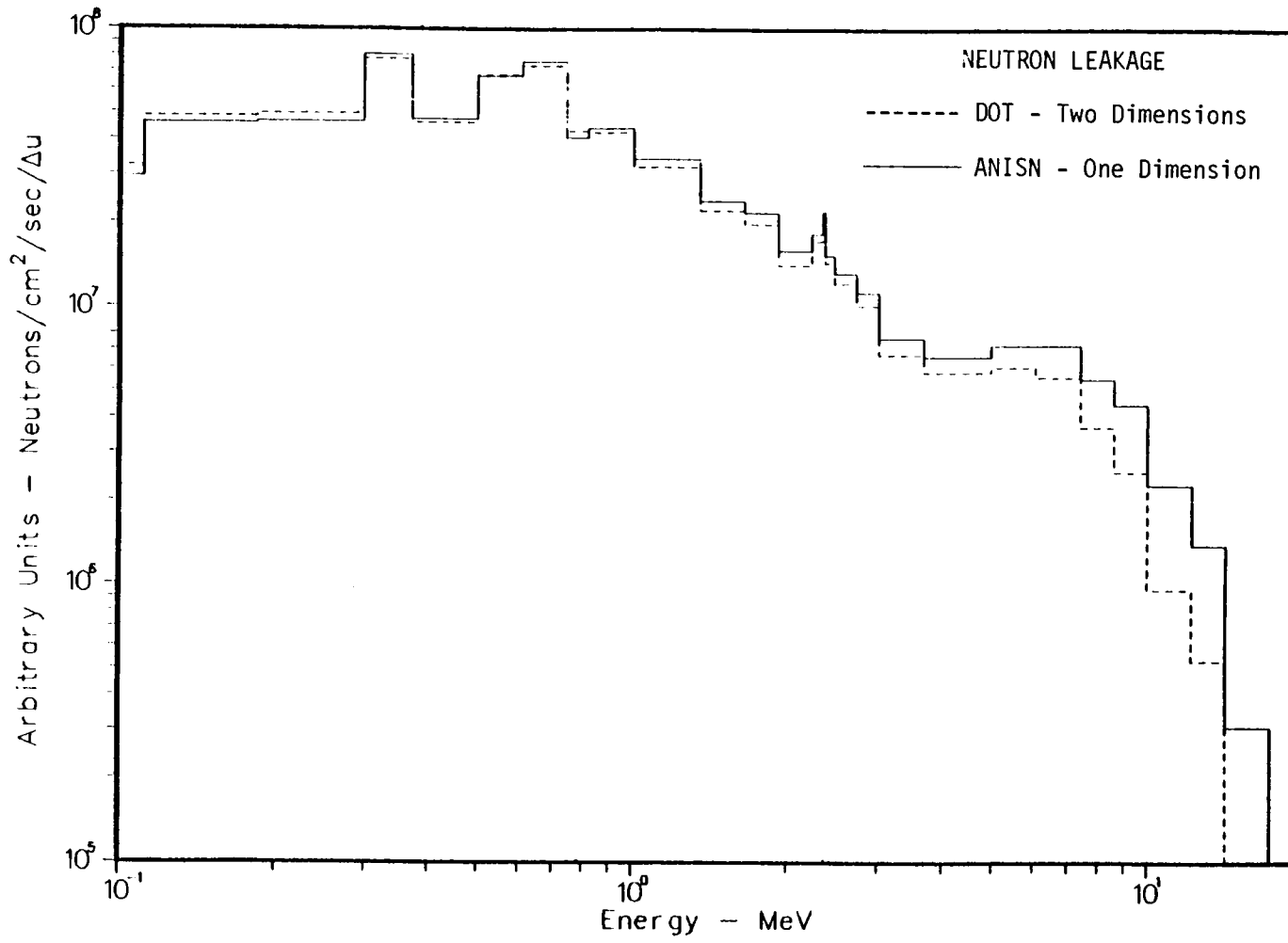


Figure 3-11. Case 4 vs Middle Case/Theta 1

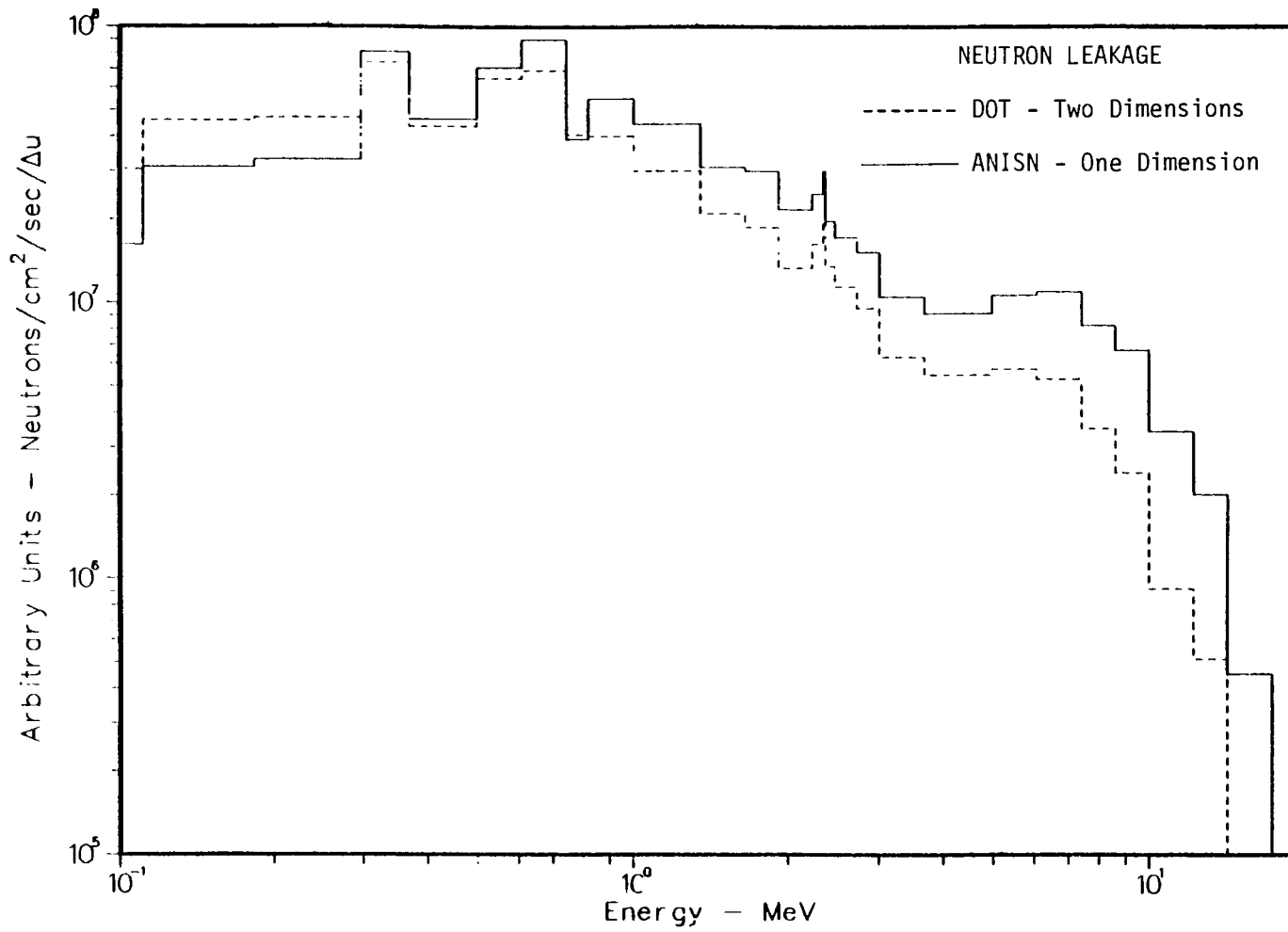


Figure 3-12. Case 5 vs Middle Case/Theta 1

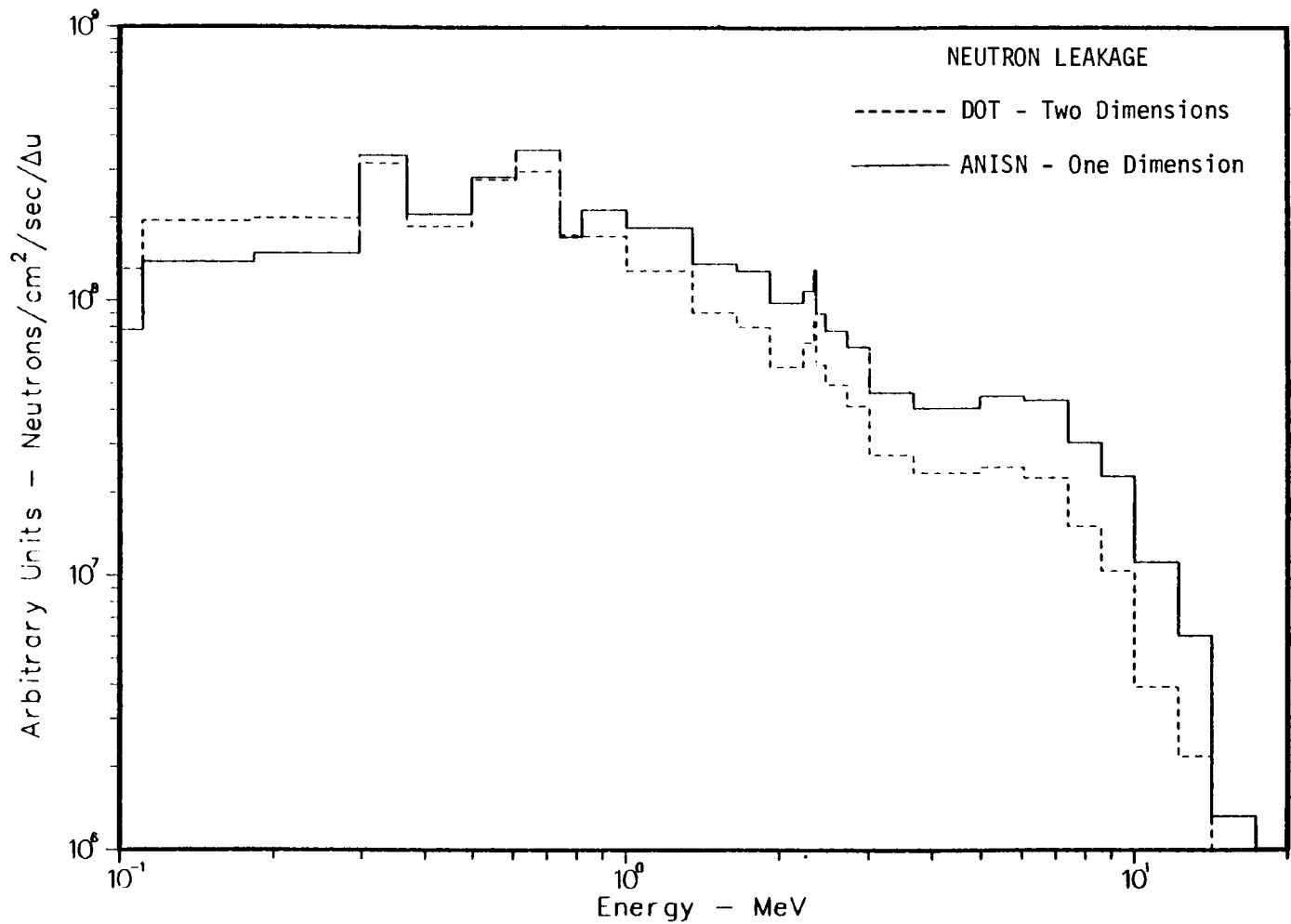


Figure 3-13. Case 6 vs Middle Case/Theta 1

The third and last observation is that the differences in the leakage spectrum between the comparisons with the top and middle DOT cases are insignificant. Figures 3-14 through 3-18 (TOP) are analogous to Figures 3-1 and 3-10 through 3-13 (MIDDLE) where the one-dimensional ANISN cases are compared individually with the DOT fluxes.

Finally, a comparison of the energy spectrum obtained from the one- and two-dimensional R-theta calculations with the energy spectrum derived from the unfolded dosimetric data is shown in Figure 3-19. It is observed that both the one- and two-dimensional results agree well with the experimental results.

#### CALCULATIONS OF THE AXIAL DISTRIBUTION OF THE NEUTRON FLUX IN THE CAVITY

A calculation of the neutron flux in the BF3 reactor cavity was performed using a somewhat standard methodology for cavity streaming analysis. The objective of the calculation was to obtain a comparison with the BF3 experiment of the axial distribution of the integral flux greater than 1 MeV and the Ni activation response.

The cavity streaming calculation was performed in a simplified geometry of the BF3 cavity (essentially a void space between a cylindrical pressure vessel with an outside radius of 334.744 cm and a cylindrical biological shield with an inside radius of 364.264 cm). Radiation transport in the pressure vessel and biological shield are approximated by surface albedo scattering in steel and concrete, respectively. The radiation source for the cavity streaming calculation was a boundary leakage source on the pressure vessel surface. The energy spectrum was obtained from the one-dimensional discrete ordinates calculations (Figure 3-19). The axial distribution of the cavity source was approximated by the axial power distribution obtained from GE for the BF3 second cycle. The azimuthal distribution of the cavity source was approximated by the pressure vessel leakage from an R-theta calculation of the neutron leakage from the pressure vessel. This R-theta calculation was previously referred to as the MIDDLE case (reference Figures 3-1 through 3-9). This azimuthal PV leakage distribution is tabulated in Table 3-1.

The results of the calculated integral flux for neutron energies greater than 1 MeV are shown in Figure 3-20 along with the unfolded results from the BF3

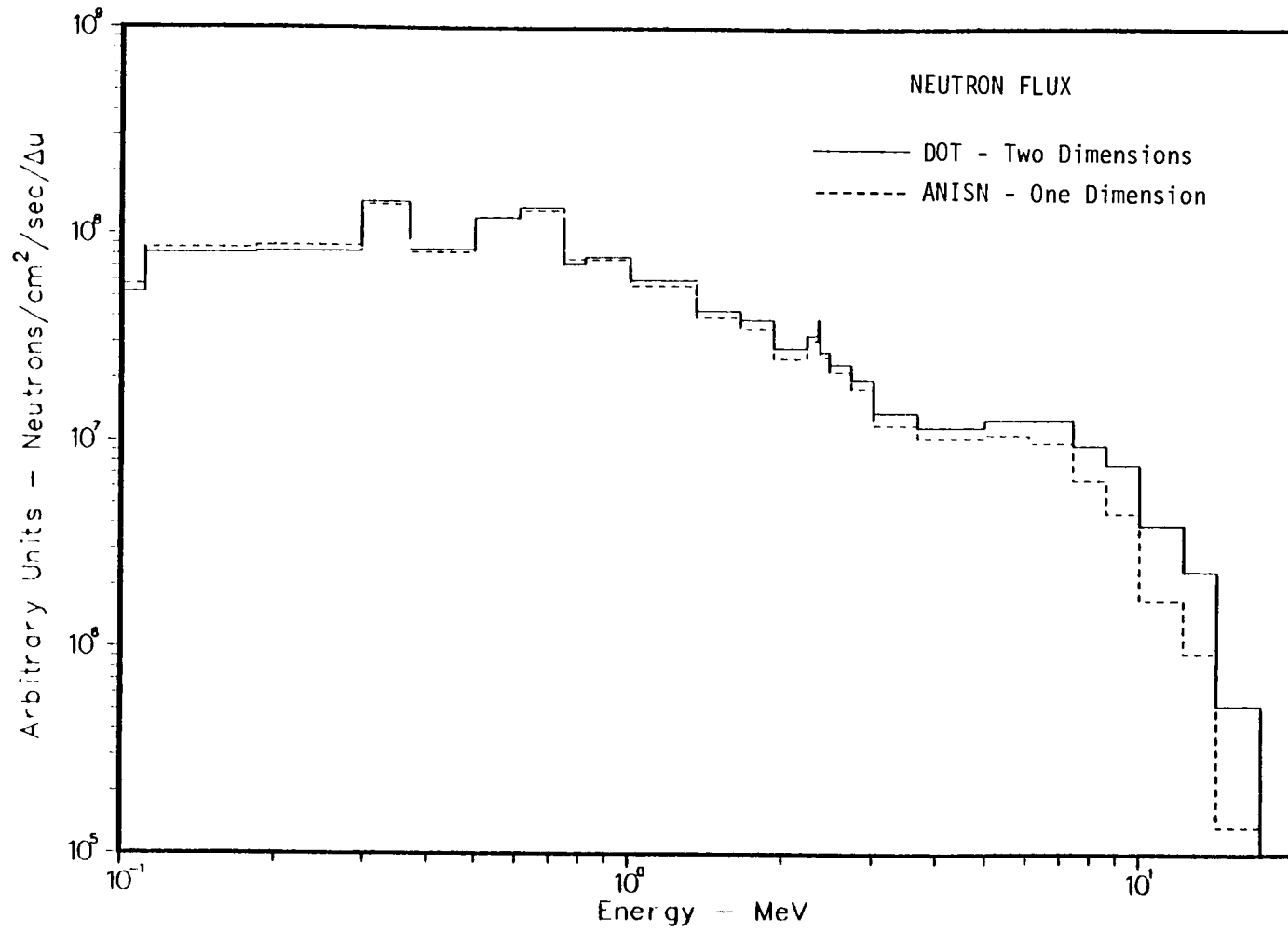


Figure 3-14. Case 2 vs Top Case/Theta 1

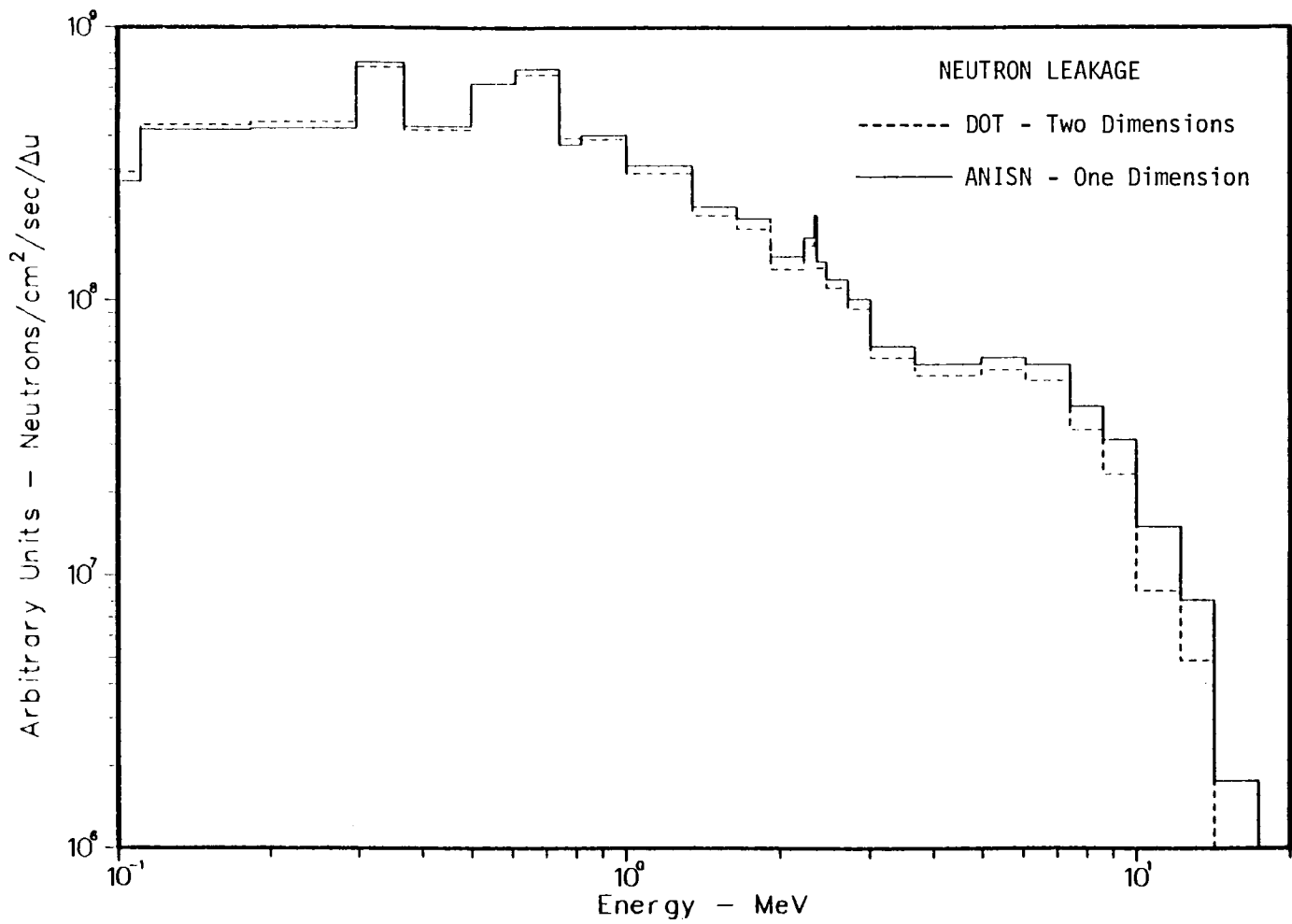


Figure 3-15. Case 3 vs Top Case/Theta 1

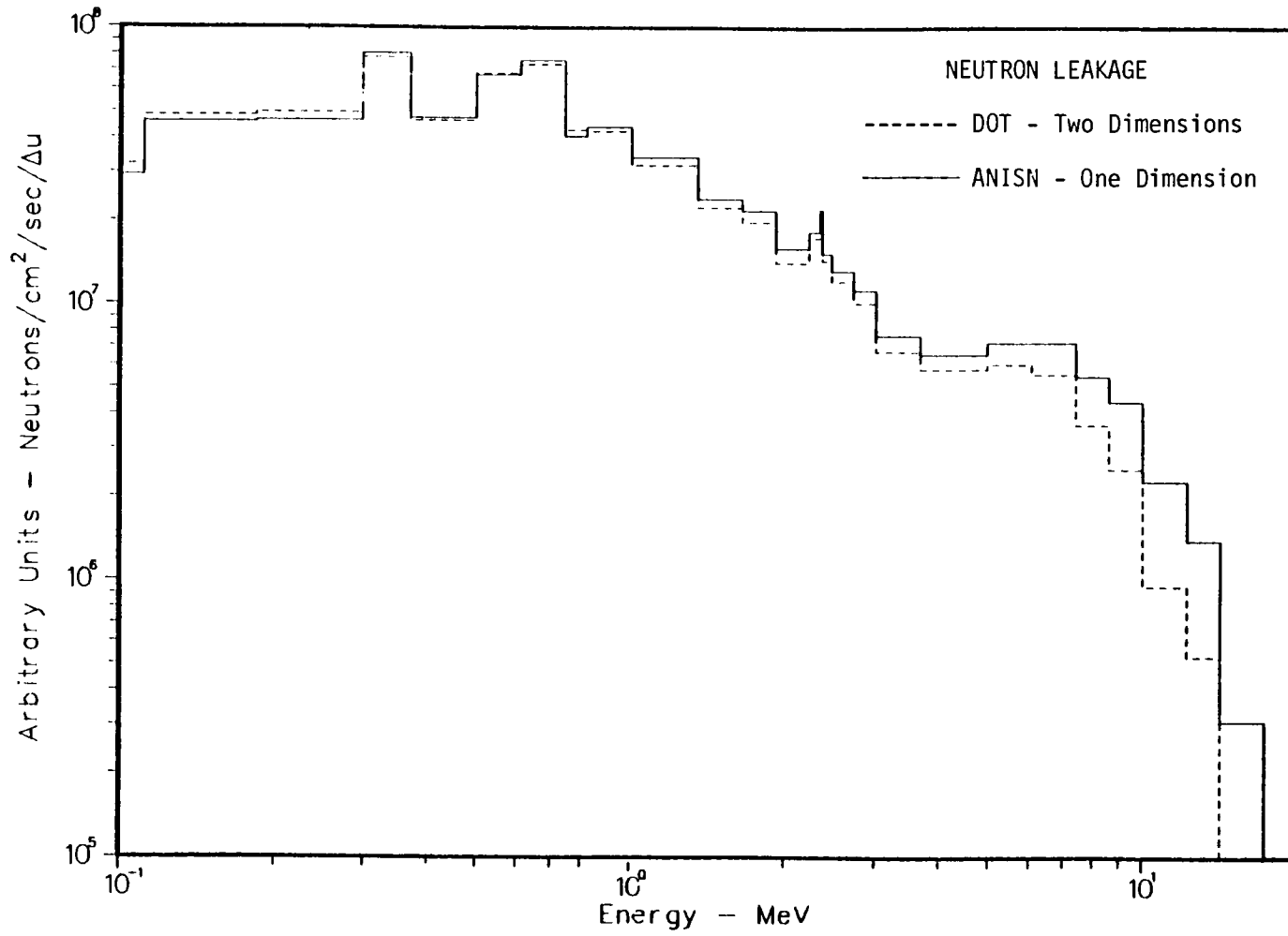


Figure 3-16. Case 4 vs Top Case/Theta 1

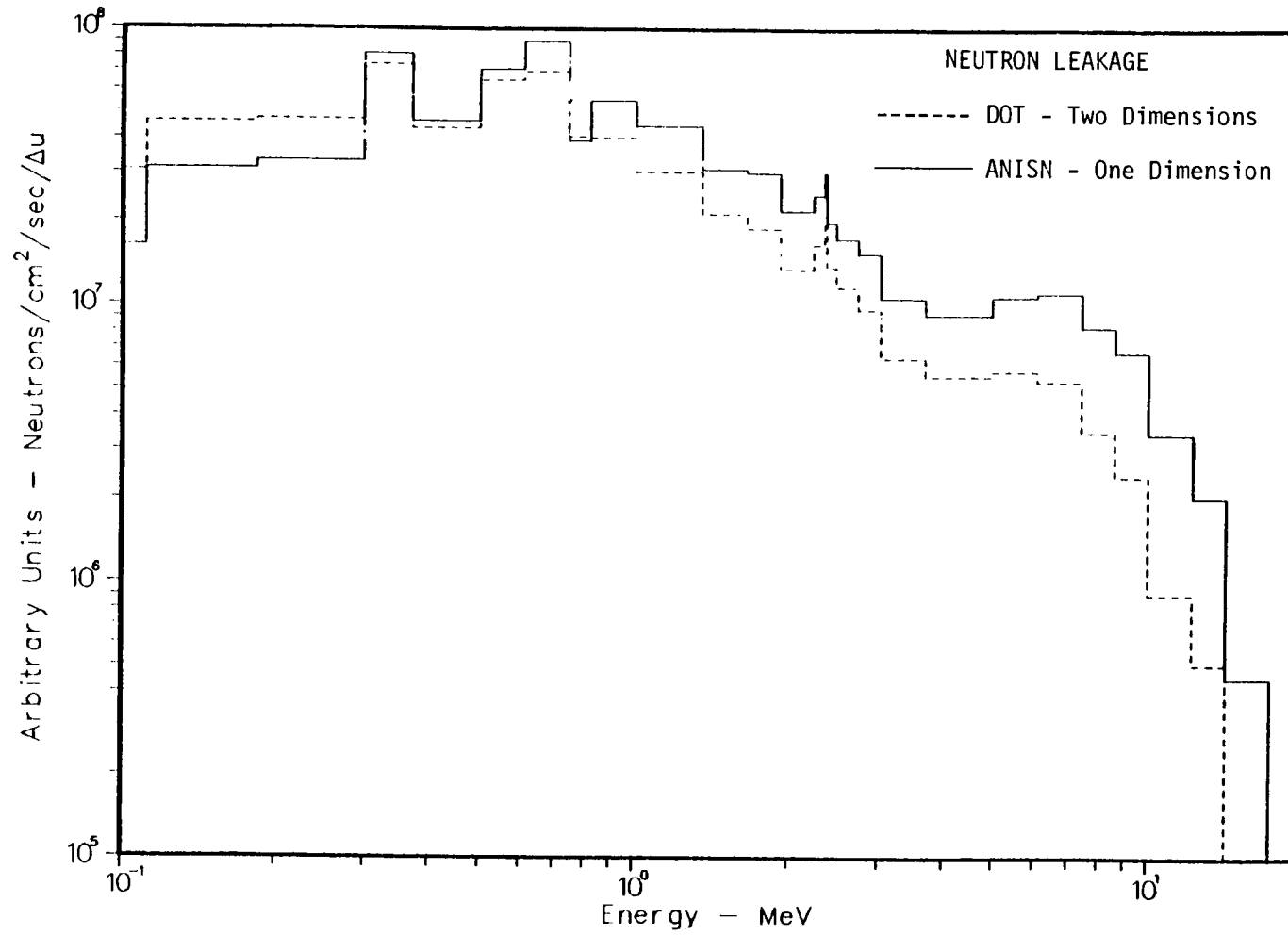


Figure 3-17. Case 5 vs Top Case/Theta 1

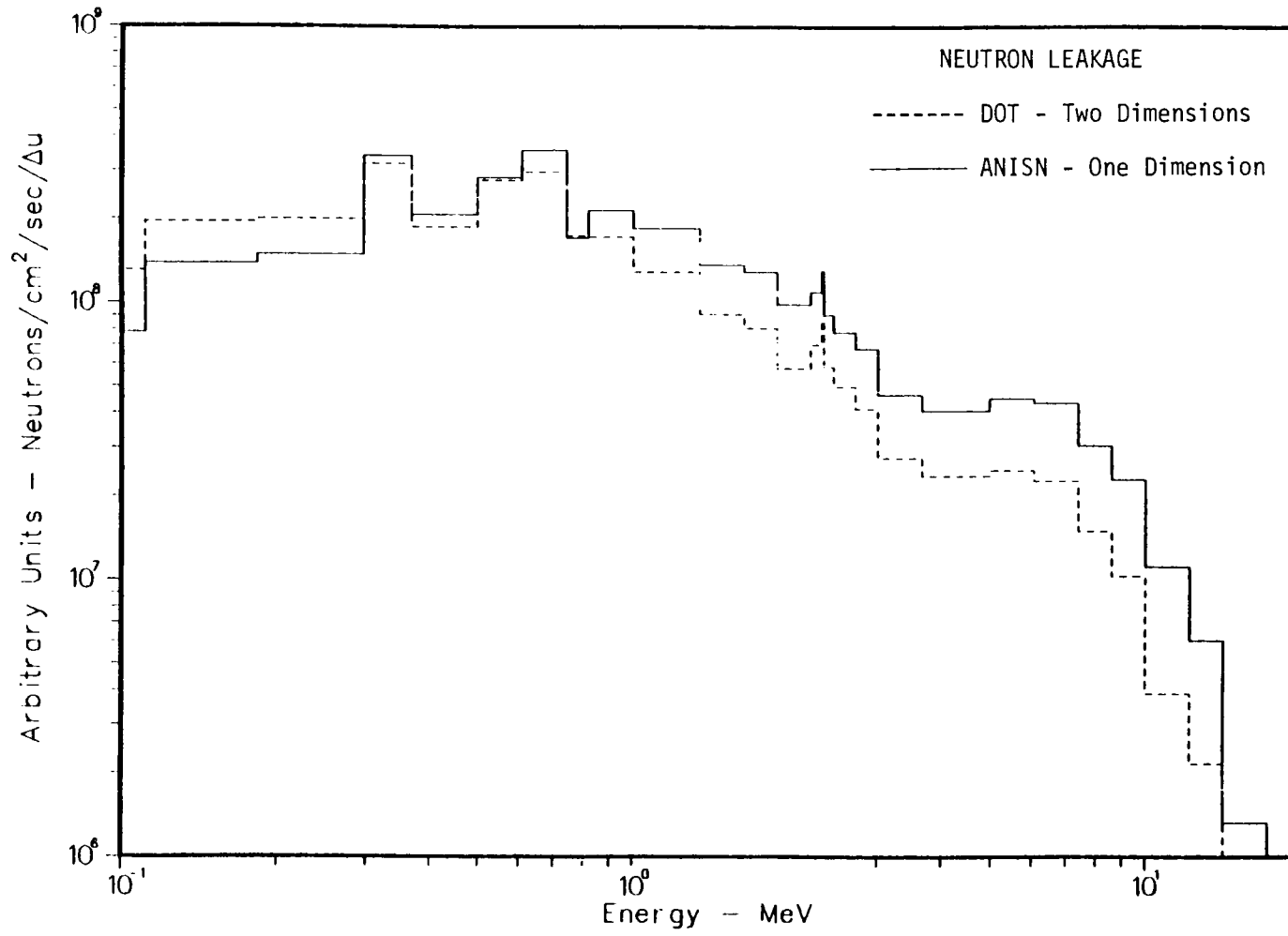


Figure 3-18. Case 6 vs Top Case/Theta 1

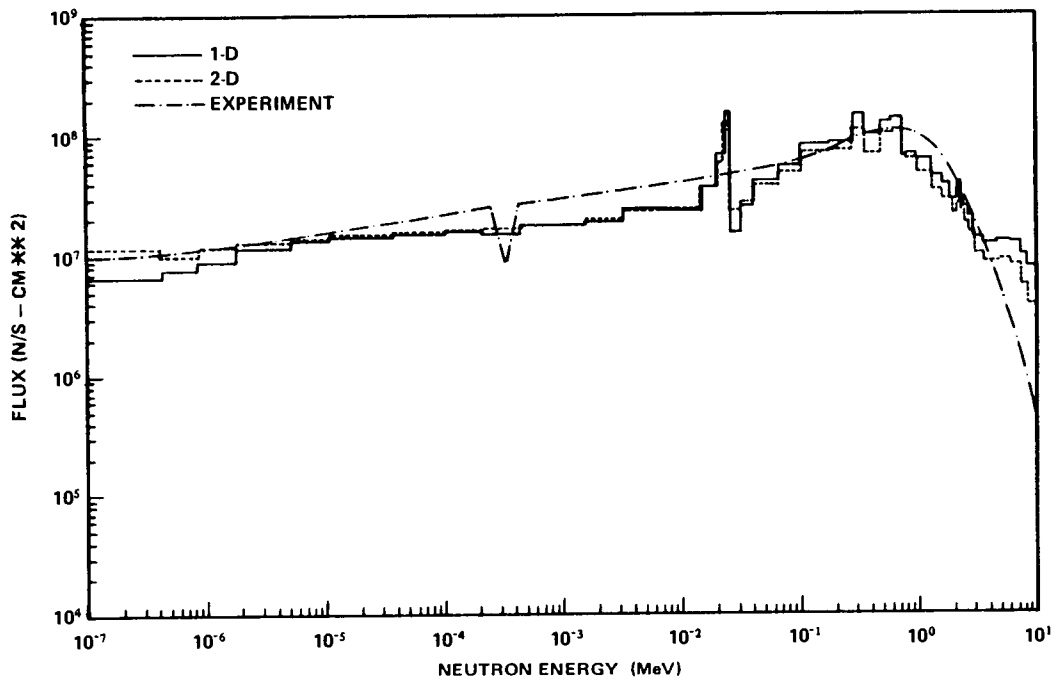


Figure 3-19. Comparison of One- and Two-Dimensional Calculated Spectrum with Unfolded Experimentally Derived Spectrum

Table 3-1

PV Leakage Azimuthal Distribution from MIDDLE Case  
Power Distribution

Theta		Relative Leakage at PV Boundary	Theta		Relative Leakage at PV Boundary
#	Radians	$J^+$	#	Radians	$J^+$
1	0.020	0.0248	21	0.412	0.0282
2	0.039	0.0247	22	0.432	0.0283
3	0.059	0.0248	23	0.452	0.0283
4	0.078	0.0249	24	0.471	0.0283
5	0.098	0.0250	25	0.491	0.0282
6	0.118	0.0251	26	0.510	0.0281
7	0.137	0.0252	27	0.530	0.0279
8	0.157	0.0254	28	0.550	0.0275
9	0.176	0.0255	29	0.569	0.0270
10	0.196	0.0257	30	0.589	0.0259
11	0.216	0.0259	31	0.609	0.0245
12	0.236	0.0262	32	0.628	0.0229
13	0.255	0.0265	33	0.648	0.0215
14	0.275	0.0268	34	0.667	0.0202
15	0.294	0.0271	35	0.687	0.0194
16	0.314	0.0274	36	0.707	0.0189
17	0.334	0.0276	37	0.726	0.0185
18	0.353	0.0278	38	0.746	0.0182
19	0.373	0.0280	40	0.785	0.0179

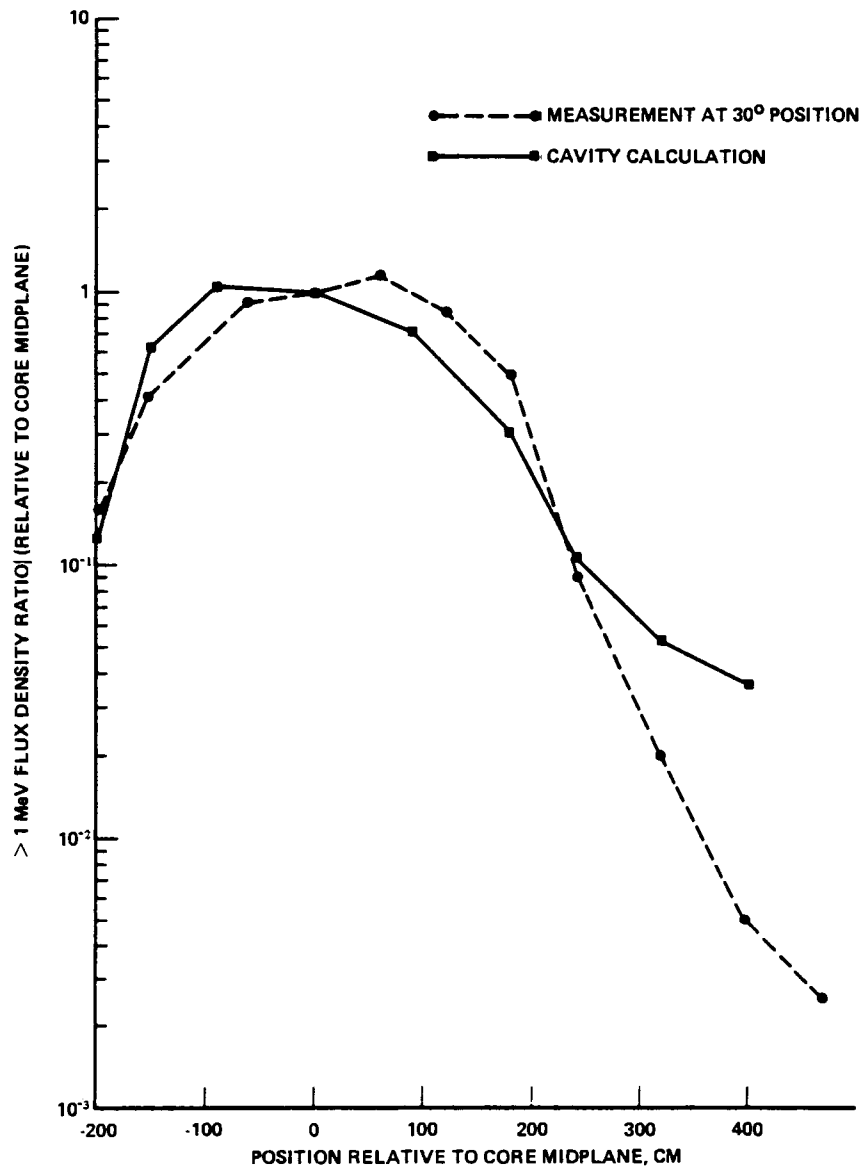


Figure 3-20. Comparison of Calculated and Measured Integral Flux > 1 MeV

dosimetric data (Reference 3, Table 2-3). Similarly, a comparison of measured and calculated Ni response ratio relative to the core midplane is given in Figure 3-21.

The comparisons of the  $>1$  MeV flux and Ni response exhibit the same characteristics that the calculation is higher than the measurement below the core midplane. Above the core midplane, the calculation is lower than the measurement. There is another cross over above the top of the core and the calculation again is higher than the measurement. The comparison of the shape of the measured and calculated curves is not very satisfactory.

One deficiency in the approach taken in constructing the cavity source term for the calculation is that the one-dimensional calculation in the pressure vessel does not allow the distribution of the void fraction in the coolant to be taken into account. Of course, this void distribution only effects calculations in a BWR. In order to consider the effect of the void distribution on the leakage from the pressure vessel, a two-dimensional R-Z calculation is necessary.

#### R-Z CALCULATION

The BWR R-Z calculation reported in Reference 1 was repeated with the addition of an axial variation in the coolant void fraction in the outer assemblies of the core. The void distribution was not entered in the central regions of the core in order to minimize the computer resource requirements for the calculation and it is known from previous analysis that the neutron leakage at the pressure vessel is predominantly affected by the outer assemblies of the core.

Figure 3-22 shows the void fraction in the coolant as a function of axial position.

The results of the R-Z calculation are compared with the measured data in Figure 3-23. The effect of the assumed void distribution is seen to be significant, and, in fact, now results in a calculated Ni response in the upper part of the core, which is higher than the measured response.

Unfortunately, there is not a readily available check of the assumed axial void distribution.

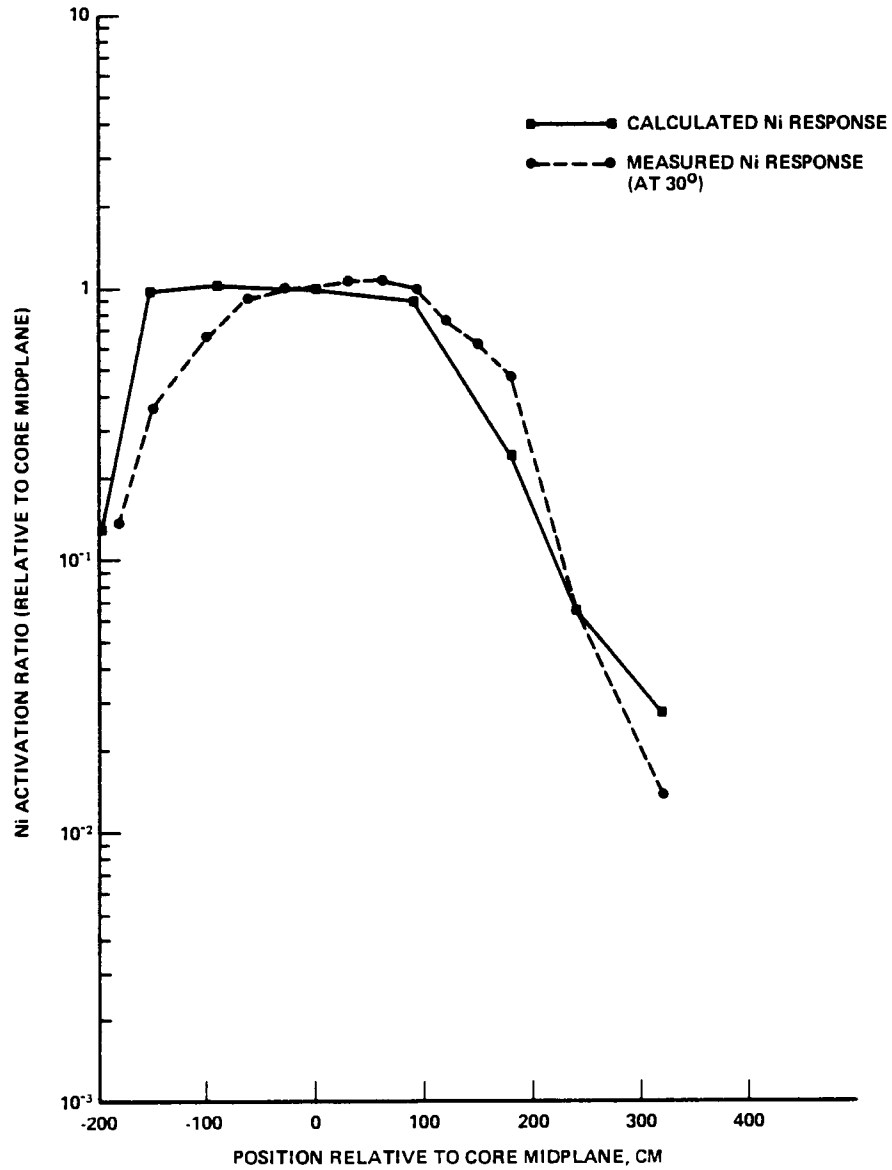


Figure 3-21. Nickel Activation Ratio (relative to core midplane) vs Distance from Core Midplane

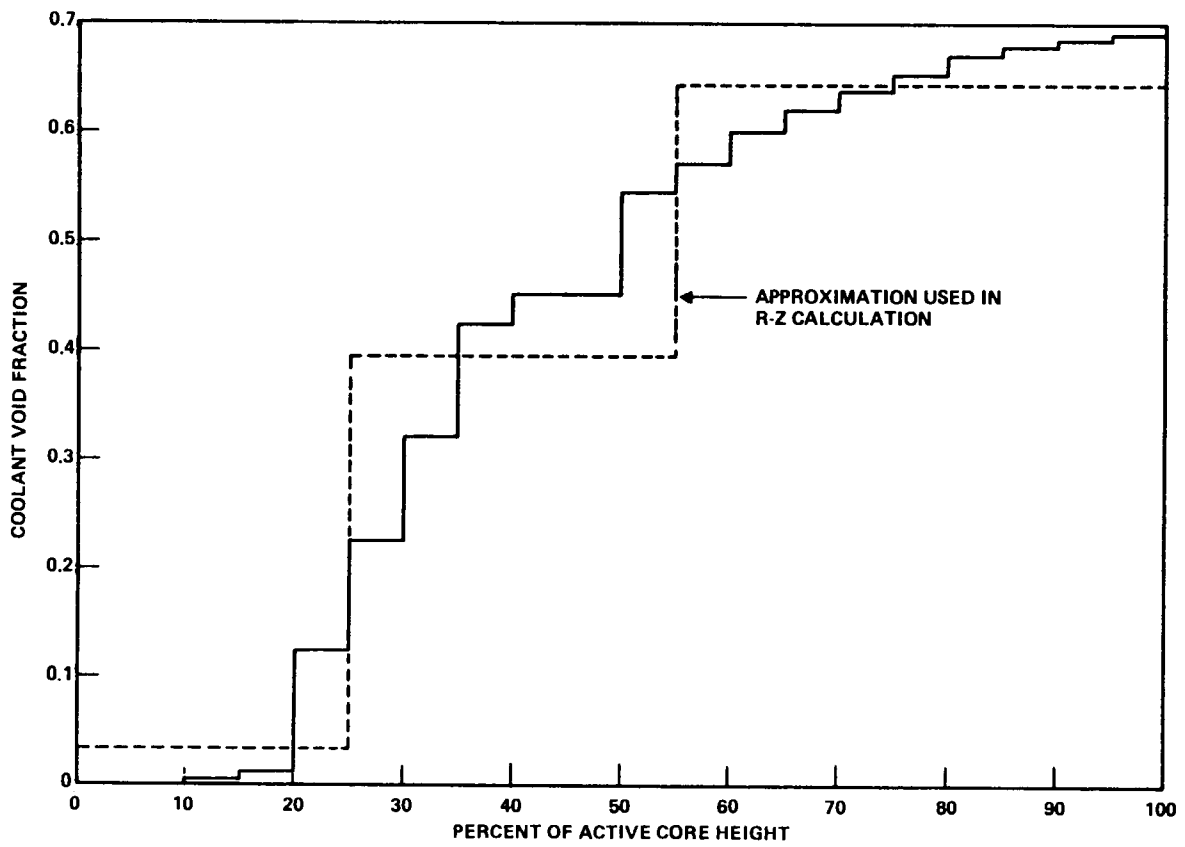


Figure 3-22. Assumed Axial Variation of Void Fraction in Core

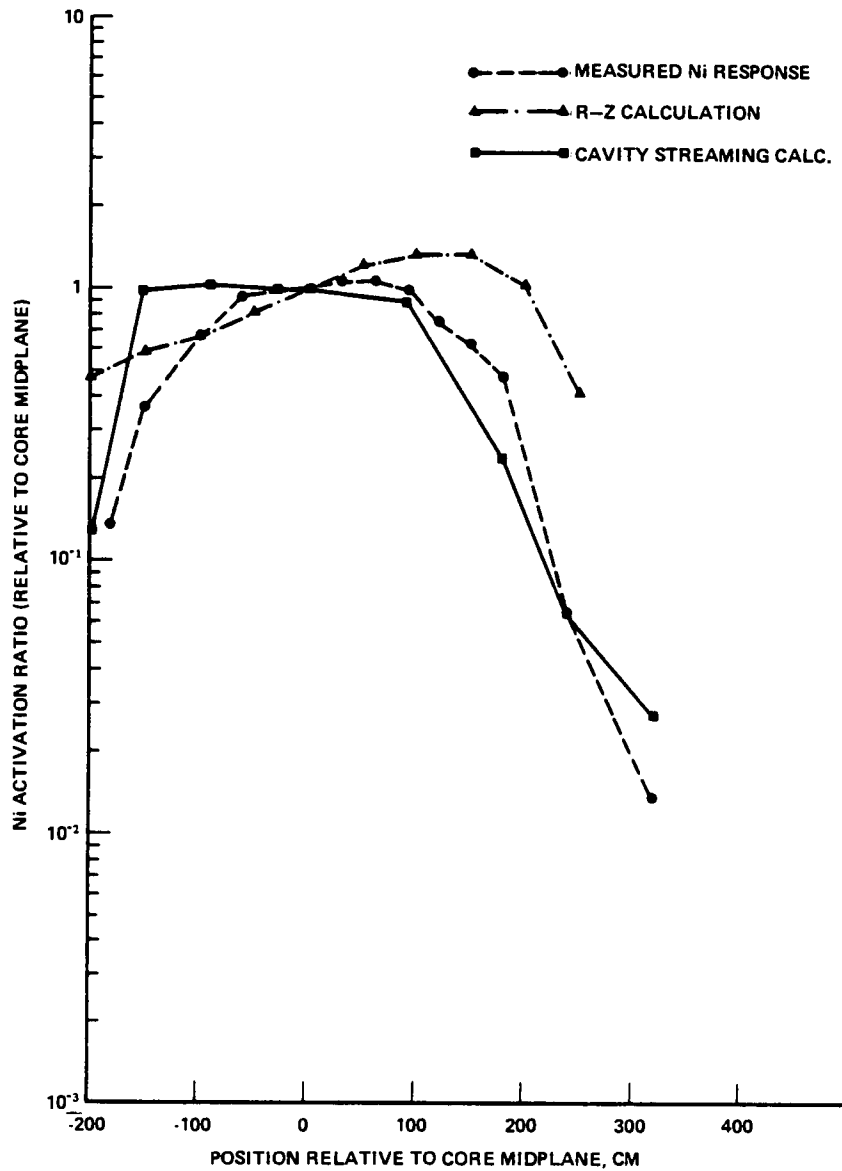


Figure 3-23. Nickel Activation Ratio (relative to core midplane): Comparison of Experiment with R-Z Calculations

The objective of using the BF3 cavity measurements as a benchmark for calculations was not completely successful in that a complete problem specification could not be obtained. The energy spectrum of the neutron fluence in the reactor cavity was calculated with good fidelity and some integrals of these spectra are compared in Table 3-2 with the GE experiment. The calculations did not successfully compare with the spatial distribution of the neutron fluence in the cavity region. The comparison is quite good in the region above and below the core midplane within the boundaries of the reactor fuel. Discrepancies begin to develop near the ends of the fuel elements. It is believed that a large part of the discrepancy is in the imprecise knowledge of the coolant void distribution at high power. This data may exist but is not generally available. The fact that the two calculational cases bracket the experimental results indicate that there exists an assumed void distribution which will match the experiment. Whether this distribution is close to the real one is another question.

Although good results have been obtained for cavity streaming problems utilizing the calculational methods and data in PWR cavities, no detailed comparisons have been made with cavity dosimetric measurements for BWRs. The apparent sensitivity of the BWR cavity results to the coolant void distribution and the lack of measured results on the void distributions during the irradiation cycle obviates, to a large extent, the utility of the BWR measurements as a calculational benchmark. If better data on void distribution becomes available it may be useful to reassess these conclusions. It should be noted that the calculations are quite good at or near the core midplane where the maximum fluence on the vessel occurs.

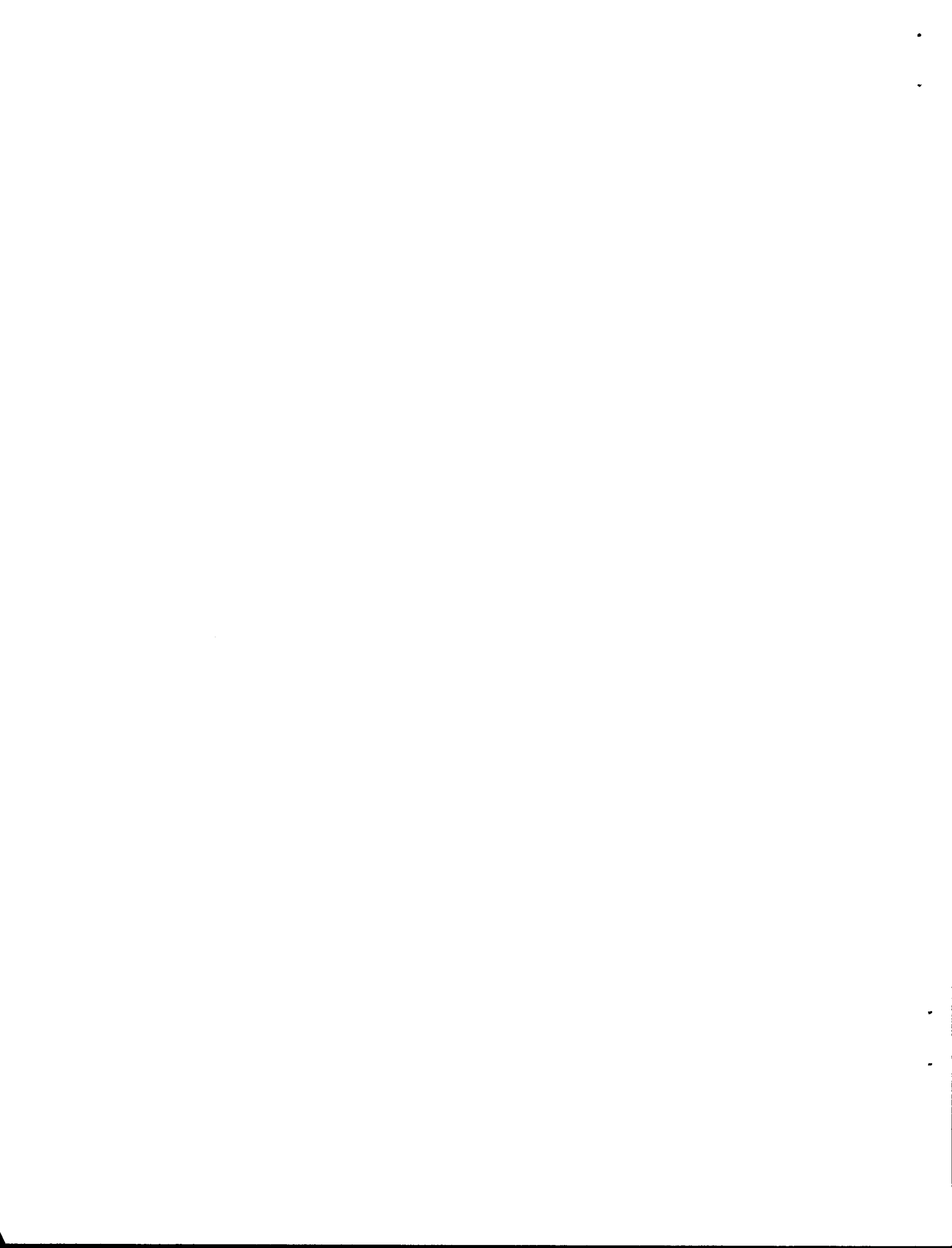
Table 3-2  
Integral Flux Comparison's  $\phi > E$

Measurement Position: Reactor Cavity Core Mid-Plane

E(MeV)	SAI	GE	Estimated Error
6	$3.5 \times 10^6$	$1.9 \times 10^6$	
4	$6.2 \times 10^6$	$4.0 \times 10^6$	
3	$8.1 \times 10^6$	$6.2 \times 10^6$	<u>+30</u>
2	$1.3 \times 10^7$	$1.1 \times 10^7$	
1	$3.1 \times 10^7$	$3.1 \times 10^7$	<u>+30</u>
0.1	$1.5 \times 10^8$	$1.2 \times 10^8$	<u>+35</u>
0.01	$2.0 \times 10^8$	$1.7 \times 10^8$	<u>+40</u>
0.001	$2.2 \times 10^8$	$2.1 \times 10^8$	<u>+45</u>

Section 4  
REFERENCES

1. T. E. Albert, M. L. Gritzner, G. L. Simmons, and E. A. Straker, "PWR and BWR Radiation Environments for Radiation Damage Studies," EPRI NP-152, September 1977.
2. G. C. Martin, "Browns Ferry Unit 3 In-Vessel Neutron Spectral Analysis," NEDO-24793, August 1980.
3. G. C. Martin, "Browns Ferry Unit 3 Cavity Neutron Spectral Analysis," EPRI NP-1997, August 1981.
4. J. MacKenzie and W. E. Selph, "Passive Neutron Dosimetry for Measurements at the McGuire Reactor," EPRI NP-2570, September 1982.



Appendix A

SAILOR — A COUPLED MULTIGROUP CROSS  
SECTION LIBRARY FOR LIGHT WATER REACTORS

## Acknowledgment

The authors thank the Radiation Shielding Information Center (RSIC) for providing facilities to perform the AMPX-II calculations and are grateful to members of the Oak Ridge National Laboratory (ORNL) staff, N. M. Greene, L. M. Petrie, and J. E. White, for advice and consultation in running AMPX-II and interpreting results. We also thank W. K. Hagan and T. E. Albert of Science Applications, Inc. (SAI) for various helpful suggestions during the course of this effort.

## Section A1 INTRODUCTION

The nuclear cross section for a material forms the essential ingredient in any radiation transport calculation. The accuracy of the cross section data used in these analyses govern, to a large extent, the ability to predict results obtained by experiments. Knowledge that the cross section data are the best available and were correctly prepared for the analysis of interest, forms an important base for reconciliation of analytical and experimental differences. This is particularly important in the nuclear reactor pressure vessel dosimetry studies. Here, the analytical prediction of the experimental result and the experimentalist determination of reportable parameters are intertwined such that one has a difficult time proceeding without the other. This is particularly true when the threshold foil technique is used and trial spectra must be provided in order to unfold the results and obtain the true spectra. Also, once the calculations are validated by measured parameters, the resulting analytic methods can be used to predict other phenomena of interest.

It is one of the goals of the Electric Power Research Institute (EPRI) pressure vessel dosimetry program to provide a verified technique which can be used to predict the neutron environments at key locations in a variety of nuclear power reactors. The cross section data that have been developed to be an integral part of this methodology are the subject of this report. Aside from this requirement, it was felt that there was a pressing need to provide a state-of-the-art library for a variety of power reactor shielding applications. To gain a better appreciation for the need for such a library of processed cross section data, it is useful to briefly outline the historical perspective from which this library has evolved.

### HISTORICAL PERSPECTIVE

The DLC-23/CASK (1) (22n,18g) library has received extensive use throughout the industry for LWR reactor shielding calculations. Note, here we use the DLC designators to identify the library as it is distributed by the Radiation Shielding Information Center (RSIC) and the 22n,18g notation to identify the

number of neutron groups-22 and the number of gamma-ray groups-18. Even though it is based on a 1970 evaluated library (ENDF/B-II) which contained no gamma-ray production (CASK used data sets from DLC-12/POPLIB [2]) and was not designed for use in LWR shielding problems, its availability as one of the first coupled libraries and the economy of its use have made it a popular choice in the community. It was the CASK library that was used for the calculations described in a previous report (3) prepared by Science Applications, Inc. (SAI) on radiation environment in power reactors.

After the release of ENDF/B-IV (4) in 1974 several, multi-group libraries were produced which had the potential for replacing CASK. However, none of these newer libraries were designed for LWR shielding applications. The DLC-31/FEWG1 (5) (37n,21g) library sponsored by the Defense Nuclear Agency (DNA) focused on air and concrete problems of interest to the weapons radiation transport community. A (27n,18g) library based on the DLC-43/CSRL (6) 218n library was developed on behalf of the Nuclear Regulatory Commission (NRC) for out-of-core criticality and shielding problems (7). An ENDF/B-IV LASL library DLC-36B/CLAW-IV (8) (30n,12g) was recently released through RSIC.

The DLC-47/BUGLE (9) (45n,16g) library was produced by collapse from DLC-41/VITAMIN-C (10) for use by ANS 6.1.2 as part of that group's efforts to develop a standard for preparing multi-group cross sections for shielding applications. BUGLE was produced by self-shielding for an infinite homogeneous concrete medium via a BONAMI run using AMPX-II (11). The spectrum used to collapse from (171n,36g) to (45n,16g) contained features of both a fusion and fission spectrum. Comparison of BUGLE results with several multi-group libraries for a concrete slab problem (12) and an LWR model (13) revealed deficiencies that limit its' usefulness as a cross-section library for use in various LWR shielding applications. In particular, it was discovered that the particular collapsing spectrum used in the generation of this library resulted in a larger within group scattering cross section at high energies than would be expected for LWR applications. The resulting effect is that the predicted spectrum at several locations of interest in BWR and PWR plants is much harder than had been indicated in previous analysis. The cross section for hydrogen in this library was perhaps the singularly most important isotope that was impacted by this increase in the in-group scattering cross section.

It was recognized that changes to the group structure, self shielding appropriate to specific geometries and compositions, proper treatment of temperature effects, and collapse with appropriate energy spectra would be required to develop a broad group library for application to specific LWR problems.

It was from this perspective that the multi-group cross section library which we have designated SAILOR (Shielded and Application Independent Libraries for Operating Reactors) was developed. In the preparation of SAILOR, there were a few ground rules that we tried to adhere to during the course of development. They were:

- The cross section library should be applicable to both boiling water and pressurized water reactors at their normal operating conditions.
- The library should make use of the most recently developed fine group libraries as a basis and would thereby take advantage of the enormous amount of work effort that had been devoted to their preparation.
- The library should have fewer than 70 groups total, i.e., both neutron and gamma-ray groups.
- The broad group library should produce equivalent results to those obtained from the reference fine group library for calculations of interest.
- Have a sufficient number of neutron groups for energies above 100 keV to allow the user of the cross sections to generate an adequate trial spectrum for threshold foil unfolding codes.
- The cross section library should be useful in providing satisfactory results for calculated quantities both inside and outside of the reactor pressure vessel.



Section A2  
APPROACH USED TO PREPARE THE CROSS SECTIONS

In the previous section, we discussed the ground rules that served as a guide for the generation of the cross sections. The basis goal was, of course, to have a cross section library that could be used for a wide range of radiation transport problems associated with Light Water Reactors (LWRs). To this end, it was decided to construct one-dimensional models of a Pressurized Water Reactor (PWR) and a Boiling Water Reactor (BWR) and to use these models as the focal point for the determination of reference spectra. These calculated spectra would then be used in making comparisons between various cross section libraries and also as the source of weighting spectra for collapsing the Vitamin-C library.

POWER REACTOR AND FUEL MODELS

The development of the SAILOR library was initiated by building upon the models that had been used to develop data presented in EPRI NP-152 (14). NP-152 described a series of calculations performed, for a PWR and BWR, to determine the radiation environments that would be useful for studies of neutron embrittlement of reactor pressure vessels. The PWR model was based on a Westinghouse four-loop power reactor with a thermal power rating of 3425 megawatts and fueled with 169 fuel assemblies. These fuel assemblies contained 264 fuel rods in a 17x17 array. The remainder of the fuel rod locations are occupied by control rod guide tubes and a single instrument tube. The BWR model was based on a General Electric BWR-6 plant with a rating of 3579 megawatts-thermal. The pressure vessel for this reactor had a 238 inch outside diameter and the 732 fuel assemblies contained 63 fuel rods in a 8x8 array with the single central rod position being used as an instrument guide tube.

Material and dimensional information for the reactor fuel assemblies was used to develop pin cell models appropriate for each reactor type. These models formed the basis for determining the resonance self-shielding parameters to be used in generating the cross sections. Table A1 summarizes the key parameters for the two types of reactor fuel that were considered appropriate for each fuel cell calculation.

Table A1

Key Parameters for BWR and PWR Pin Cells.

	<u>BWR</u>	<u>PWR</u>
Inner Radius Clad (cm)	0.53213	0.41783
Outer Radius Clad (cm)	0.6134	0.47498
Outer Radius Cell (cm)	0.9174	0.71079
Region-Temperature (Kelvin)		
Pellet	921	921
Clad	672	672
Moderator	583	551
Pellet Nuclear Density*		
U-235	4.959-4	6.325-4
U-238	2.177-2	2.166-2
Oxygen	4.455-2	4.465-2
Moderator Density*		
Hydrogen	2.475-2	4.714-2
Oxygen	1.238-2	2.357-2
Boron-10	0	4.200-6
Zircalloy-4 Density*		
Chromium	7.64-5	
Iron	1.45-4	
Nickel	8.77-4	
Zirconium	4.27-2	

\*Nuclear densities are in atoms/barn-cm

For the PWR and BWR, a one-dimensional cylindrical geometry was developed. These models were patterned after those given in NP-152. One-dimensional models were used to represent conditions at the reactor mid-plane and served as the basis for determining the neutron and gamma-ray spectra at various radial locations. The reactor models consisted of a central fuel region surrounded by various steel, water, air, and concrete regions. For the BWR, the model consisted of seven concentric regions which are: reactor core, water region, core barrel, downcomer, pressure vessel, reactor cavity, and concrete shield. The PWR model consists of eight regions which are: reactor core, flow baffle, water region, core barrel, downcomer, pressure vessel, reactor cavity, and reactor shield. The downcomer region contains coolant only for the PWR and coolant plus jet pumps in the BWR. Table A2 gives the appropriate dimensions for each of these models. Note that we have cylindricalized the reactor core by preserving the total fuel cross-sectional area. The appropriate nuclear densities for the materials used in the models are given in Table A3.

Several power distributions were used for these studies. They included the power distributions that were used in the NP-152 study and a flat power distribution. It was demonstrated in these studies, that the shape of the neutron and gamma-ray spectra is relatively insensitive to the reactor core power distribution, but the absolute value of the predicted spectra was determined by the shape of the power distribution. For the purpose of collapsing cross section data, it was felt that the power distributions which were used represented those of interest for power reactor applications.

#### APPLICATION OF AMPX-II TO GENERATE SAILOR

The models for the reactors and reactor fuel were defined in the previous section and it would seem that a rather straightforward application of the various modules contained in the AMPX system would result in a workable cross section library. The AMPX system is a collection of modular computer codes that can be used to generate a coupled neutron and gamma-ray cross section library in a variety of formats beginning with basic data in the ENDF/B format. This procedure is only straightforward after one has acquired some experience. The entire scheme used in preparing the cross sections is shown pictorially in Figure A1. What we have not shown in the various starts, restarts, backtracking, and computer code problems that took place during this effort. We

Table A2  
 Radial Dimensions in Centimeters for One  
 Dimensional Reactor Models.

	<u>PWR</u>	<u>BWR</u>
Core-OR*	168.51	235.15
Flow Baffle-OR	171.40	not applicable
Core Barrel-IR**	187.96	253.73
Core Barrel-OR	193.68	258.83
Pressure Vessel-IR	219.71	302.26
Pressure Vessel-OR	241.62	317.50
Primary Shield	260.0	347.22

\*OR - outer radius  
 \*\*IR - inner radius

Table A3

Nuclear Densities\* Used in One Dimensional Problems.

Homogeneous Cores

	BWR	PWR
Hydrogen	2.050-2	2.768-2
Oxygen	1.025-2	1.384-2
Zirconium	6.469-3	4.257-3
Iron	2.045-3	1.346-3
U-235	7.513-5	1.903-4
U-238	3.298-3	6.515-3
Fuel Oxygen	6.749-3	1.343-2
Boron-10	0	2.466-6

Coolant

	<sup>4.950-2</sup> BWR	PWR
Hydrogen	<del>4.960-2</del>	4.714-2
Oxygen	2.475-2	2.357-2
Boron-10	0	4.200-6

Steels and Zircalloy

	SS-304	AS33-B	Zirc-4
Carbon	2.37-4	9.81-4	0
Silicon	8.93-4	3.71-4	0
Chromium	1.74-2	1.27-4	7.64-5
Manganese	1.52-3	1.12-3	0
Iron	5.83-2	8.19-2	1.48-4
Nickel	8.55-3	4.44-4	8.77-4
Zirconium	0	0	4.27-2

Concrete Type-04

Hydrogen	7.77-3
Carbon	1.15-4
Oxygen	4.38-2
Sodium	1.05-3
Magnesium	1.48-4
Aluminum	2.39-3
Silicon	1.58-2
Potassium	6.93-4
Calcium	2.29-3
Iron	3.13-4

\*Units are Atoms/barn-cm

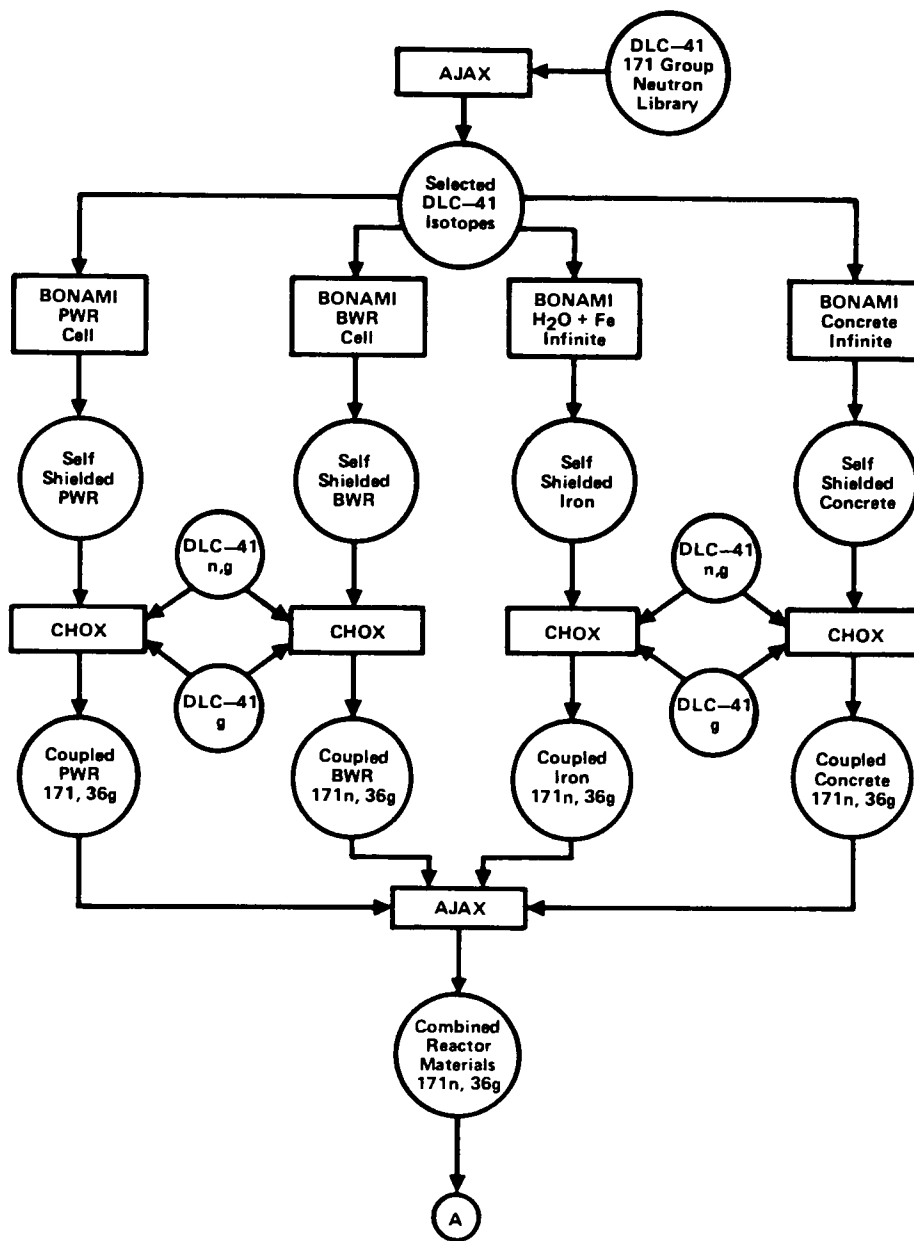


Figure A1. SAILOR Cross Section Generating Procedure Using AMPX-II

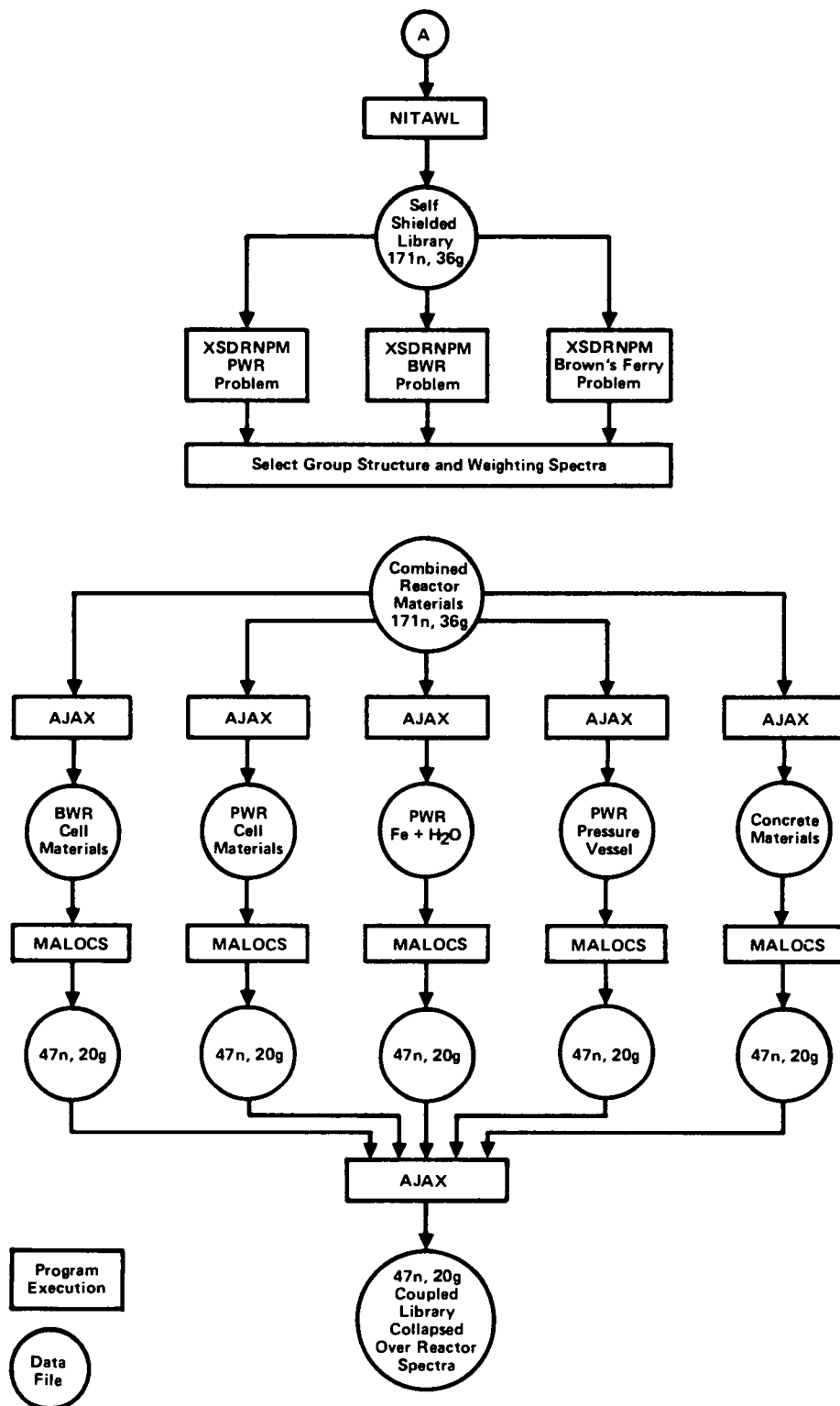


Figure A1. SAILOR Cross Section Generating Procedure Using AMPX-II (Continued)

have also indicated on this figure a reference to data sets that were generated at each step. Appendix B contains a listing of each of the AMPX job streams that were used to produce the cross sections in the final form. We used the "standard" IBM procedure that is distributed with the AMPX-II package to execute each job.

The process began by extracting from the VITAMIN-C (DLC-41) library the appropriate neutron microscopic cross sections for BWR fuel, PWR fuel, and concrete/steel and placing them on three separate disk files using the AJAX module. This procedure was used to avoid creating excess copies of the DLC-41 library and reducing the amount of input/output that is required. These three data sets were then used as input to self-shielding calculations.

The neutron cross sections on DLC-41 must be self shielded using the BONAMI module. Four separate self-shielding calculations were performed. One each for the BWR and PWR fuel cells, using the geometry and materials appropriate for the lattice. Another calculation was performed for an infinite medium of concrete. The final calculation was performed for a steel/water mixture appropriate for the core barrel/pressure vessel regions. The main feature of this final run was to include the effects of the different material in the resulting iron self-shielding calculation. The four files produced by these calculations represented the 171 group neutron cross section data that have been self shielded for reactor type, concrete, and steel/water mixtures.

Next it was necessary to form a coupled library consisting of 171 neutron groups and 36 gamma-ray groups and combine them into a single library. This was done by executing the CHOX module four times, using the DLC-41 secondary gamma-ray production library and the DLC-41 36 group gamma-ray library. The resulting data set contained all of the nuclides produced by the four BONAMI runs in the form of an AMPX master interface. In order to run the transport calculations with XSDRNPM (using the one dimensional reactor models), the AMPX master interface produced by CHOX had to be converted into an AMPX working interface by using the NITAWL module.

The output from NITAWL was a coupled library of microscopic cross sections that could be used in the one dimensional calculations. At this point, we could have elected to mix these cross sections into the various materials required for

input to XSDRNPM, but elected rather to keep the microscopic form. Several one dimensional calculations were made with XSDRNPM and the resulting neutron and gamma-ray fluxes were saved on tape for later processing.

This processing involved the plotting of the neutron and gamma-ray spectra obtained at various locations in the one-dimensional problems. These spectra were inter-compared and representative spectra at five locations were selected for use in preparing the collapsed cross sections.

It was at this stage that the major effort in the process used to generate the cross section library was expended. This effort involved using the neutron and gamma-ray spectra obtained at the reference points in the BWR and PWR calculations to collapse the 171n,36g data into a new group structure. These reference neutron and gamma-ray spectra are given in Tables A4 and A5. When this collapse was performed using MALOCS and a new set of cross sections produced, then the XSDRNPM calculations for the reactor models were carried out using these new data. An extensive set of comparisons were made, including spectra comparisons and integral parameter comparisons. Our goal here was to be able to reproduce key parameters obtained by using the 171n,36g library in similar calculations made with the collapsed library. To say the least, this was not an easy task and consumed several starts and restarts. A few comparison plots of the spectral comparisons are shown in Figures A2 through A7 with the 47 group results shown as dashed lines. We also had another model based on the Brown's Ferry BWR which was used as an alternative point of comparison. In the final analysis, a group structure was determined which contained 47 neutron groups and 20 gamma-ray groups and satisfied all of the requirements that were identified as our initial goals. The resulting neutron and gamma-ray group structures for the SAILOR library is given in Tables A6 and A7, along with the group numbers from the 171n,36g library that were used to form the new group structure.

Upon completion of this portion of the effort, a series of MALOCS runs were made to perform the necessary collapsing of the cross sections into the new group structure. Also the required portion of the calculational sequence was repeated for the plutonium isotopes that might be formed in a PWR core midway through a burnup cycle. These additional isotopes were included in the library. Upon completion of this calculation, an AXMIX run was made to prepare various

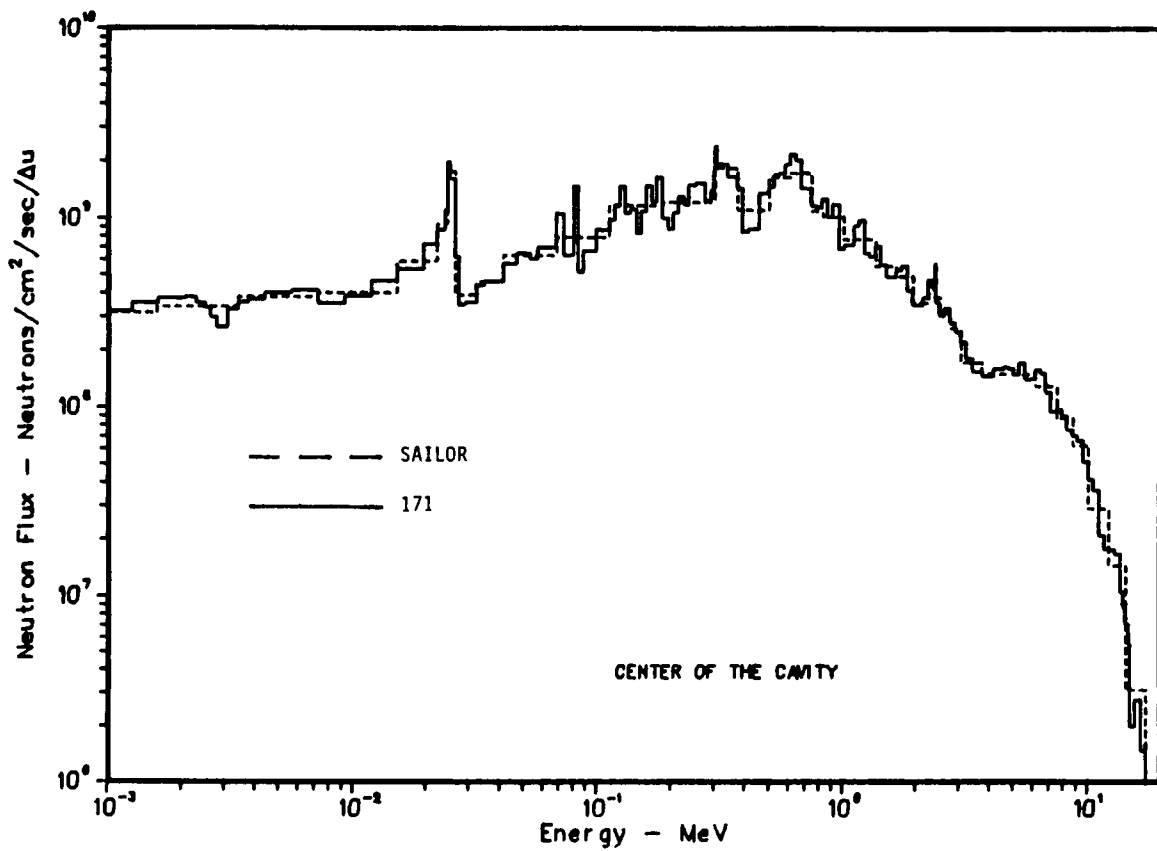


Figure A2. Neutron Spectra at the Cavity Center of a BWR

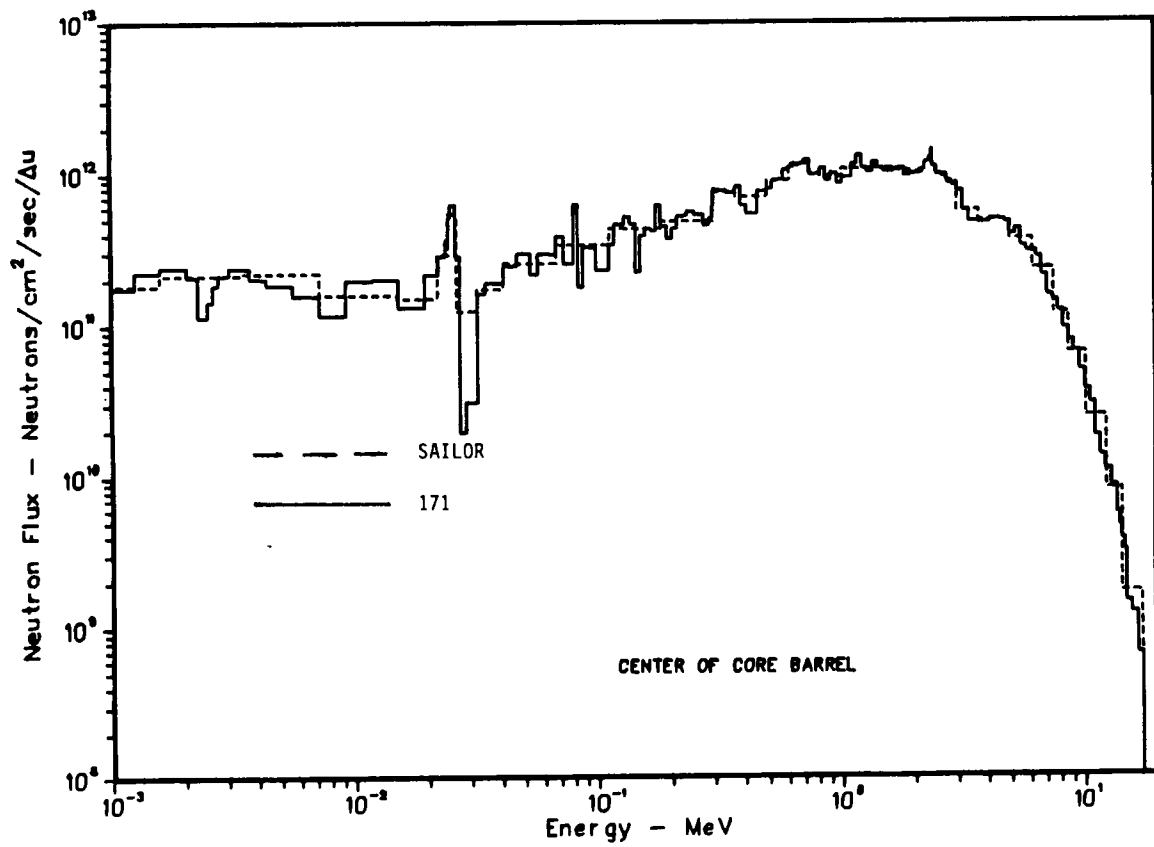


Figure A3. Neutron Spectra at the Center of the Core Barrel of a BWR

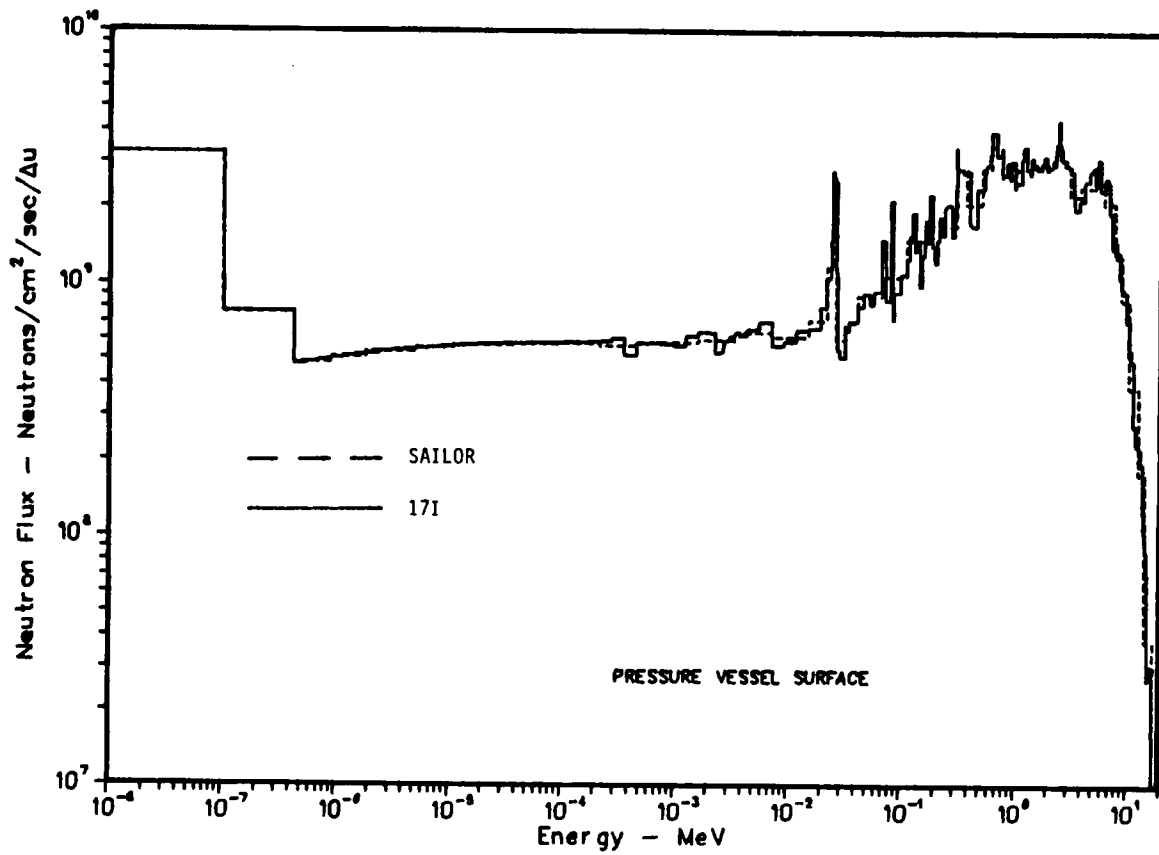


Figure A4. Neutron Spectra at a BWR Pressure Vessel Inner Surface

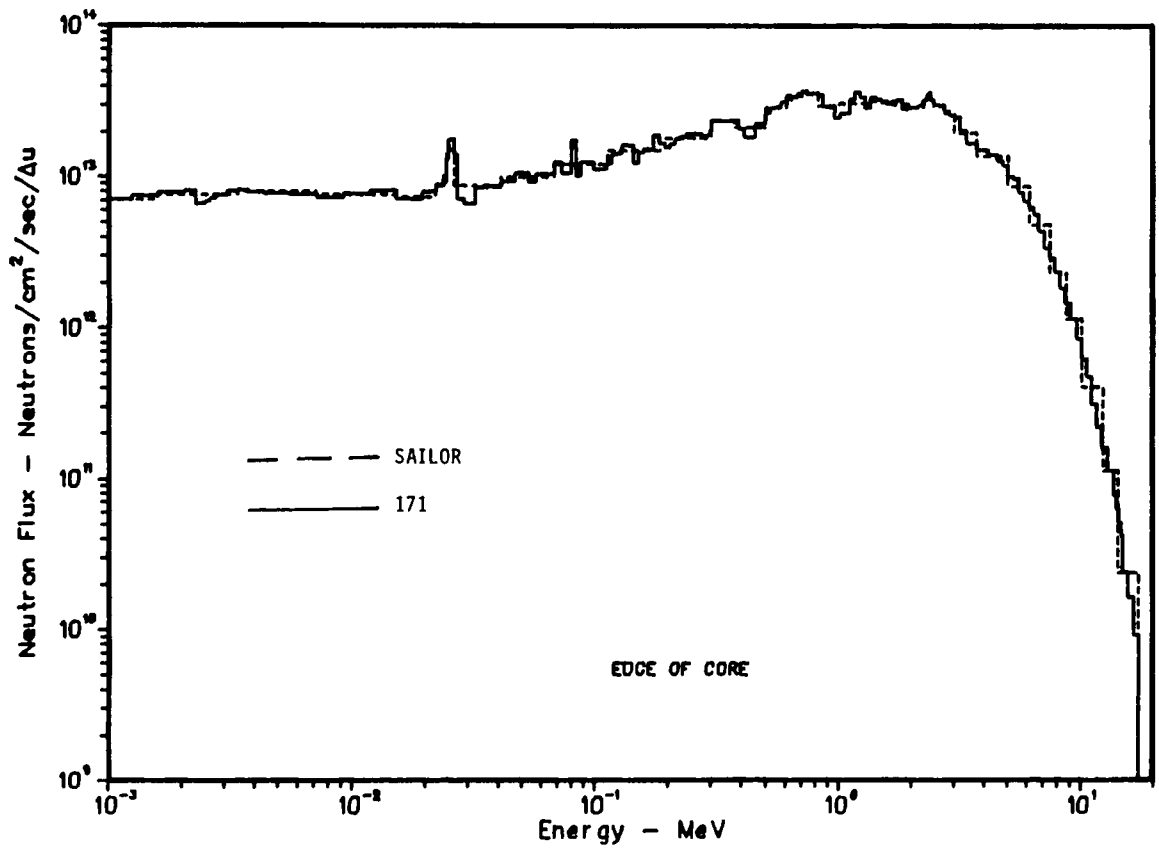


Figure A5. Neutron Spectra at Core Edge of a PWR

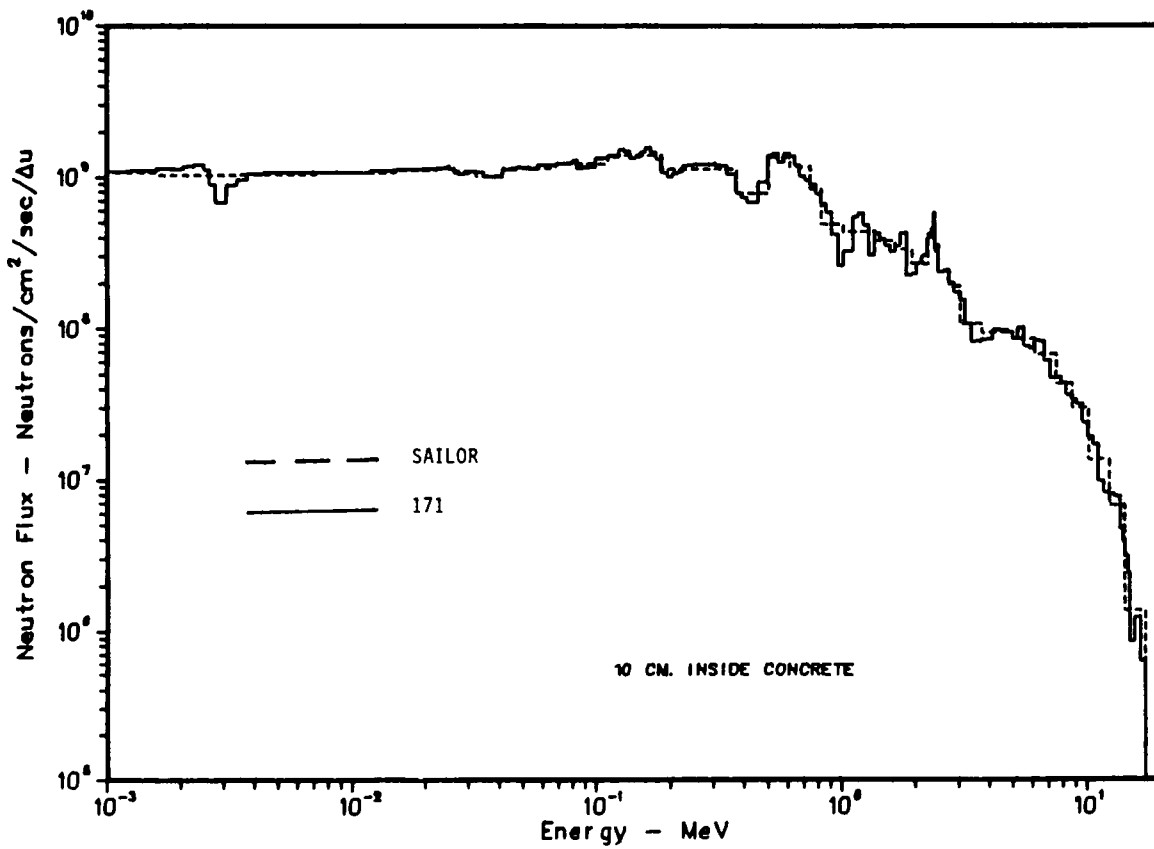


Figure A6. Neutron Spectra Inside a PWR Concrete Shield

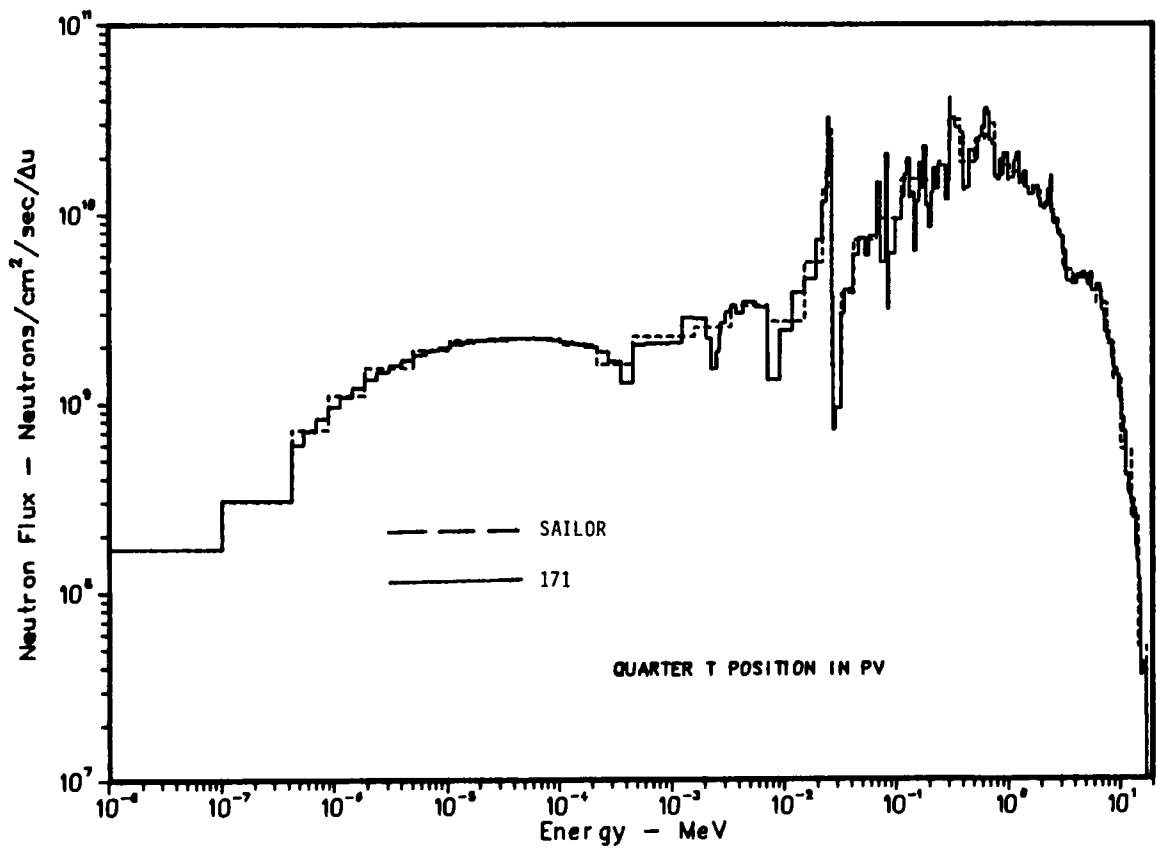


Figure A7. Neutron Spectra at the 1/4 T Position of a PWR Pressure Vessel

Table A4

## Neutron Weighting Spectra

Group	Energy*	BWR Core	PWR Core	Downcomer	1/4T in PV	Concrete
1	1.7333E+01	6.063E+08	9.049E+08	8.433E+06	1.078E+06	3.087E+04
2	1.6487E+01	1.072E+09	1.604E+09	1.567E+07	2.040E+06	5.980E+04
3	1.5683E+01	1.600E+09	2.363E+09	1.630E+07	1.757E+06	4.163E+04
4	1.4918E+01	1.371E+09	2.053E+09	1.950E+07	2.298E+06	5.856E+04
5	1.4550E+01	1.658E+09	2.477E+09	2.322E+07	2.868E+06	7.631E+04
6	1.4191E+01	2.062E+09	3.073E+09	2.813E+07	3.519E+06	9.475E+04
7	1.3840E+01	2.553E+09	3.802E+09	3.421E+07	4.252E+06	1.152E+05
8	1.3499E+01	7.319E+09	1.095E+10	1.047E+08	1.331E+07	3.766E+05
9	1.2840E+01	1.050E+10	1.561E+10	1.289E+08	1.490E+07	3.942E+05
10	1.2214E+01	1.473E+10	2.170E+10	1.537E+08	1.618E+07	4.010E+05
11	1.1618E+01	2.086E+10	3.056E+10	2.006E+08	2.019E+07	4.779E+05
12	1.1052E+01	3.128E+10	4.619E+10	3.309E+08	3.432E+07	8.293E+05
13	1.0513E+01	4.161E+10	6.105E+10	3.996E+08	4.050E+07	9.341E+05
14	1.0000E+01	5.650E+10	8.288E+10	5.244E+08	5.169E+07	1.173E+06
15	9.5123E+00	7.612E+10	1.117E+11	6.969E+08	6.752E+07	1.540E+06
16	9.0484E+00	9.640E+10	1.404E+11	7.969E+08	7.415E+07	1.655E+06
17	8.6071E+00	1.220E+11	1.769E+11	9.312E+08	8.308E+07	1.771E+06
18	8.1873E+00	1.574E+11	2.286E+11	1.181E+09	1.024E+08	2.138E+06
19	7.7880E+00	1.933E+11	2.801E+11	1.364E+09	1.149E+08	2.327E+06
20	7.4082E+00	2.278E+11	3.278E+11	1.420E+09	1.158E+08	2.289E+06
21	7.0469E+00	2.925E+11	4.224E+11	1.885E+09	1.506E+08	2.992E+06
22	6.7032E+00	1.120E+11	1.616E+11	7.154E+08	5.647E+07	1.156E+06
23	6.5924E+00	2.522E+11	3.648E+11	1.627E+09	1.279E+08	2.664E+06
24	6.3763E+00	4.256E+11	6.125E+11	2.610E+09	2.057E+08	4.091E+06
25	6.0653E+00	4.705E+11	6.703E+11	2.502E+09	1.912E+08	3.628E+06
26	5.7695E+00	5.418E+11	7.692E+11	2.672E+09	1.914E+08	3.770E+06
27	5.4881E+00	6.664E+11	9.500E+11	3.428E+09	2.374E+08	4.957E+06
28	5.2205E+00	6.962E+11	9.811E+11	3.002E+09	2.051E+08	4.161E+06
29	4.9659E+00	8.185E+11	1.156E+12	3.570E+09	2.300E+08	4.642E+06
30	4.7237E+00	8.722E+11	1.225E+12	3.578E+09	2.406E+08	4.766E+06
31	4.4933E+00	1.947E+12	2.717E+12	7.089E+09	4.611E+08	9.520E+06
32	4.0657E+00	2.117E+12	2.915E+12	6.351E+09	4.158E+08	8.331E+06
33	3.6788E+00	2.345E+12	3.199E+12	6.263E+09	4.319E+08	7.996E+06
34	3.3287E+00	1.435E+12	1.954E+12	3.771E+09	2.428E+08	5.291E+06
35	3.1664E+00	1.756E+12	2.394E+12	5.059E+09	3.109E+08	7.570E+06
36	3.0119E+00	1.774E+12	2.406E+12	5.264E+09	3.664E+08	8.570E+06
37	2.8650E+00	1.872E+12	2.530E+12	5.485E+09	3.990E+08	9.821E+06
38	2.7253E+00	2.053E+12	2.766E+12	5.977E+09	4.568E+08	1.190E+07
39	2.5924E+00	2.074E+12	2.776E+12	5.826E+09	4.340E+08	1.154E+07
40	2.4660E+00	1.454E+12	1.947E+12	4.357E+09	3.313E+08	1.064E+07
41	2.3852E+00	3.963E+11	5.350E+11	1.405E+09	1.130E+08	3.581E+06
42	2.3653E+00	4.070E+11	5.496E+11	1.564E+09	1.282E+08	4.720E+06
43	2.3457E+00	7.956E+11	1.061E+12	2.575E+09	1.918E+08	7.369E+06
44	2.3069E+00	1.406E+12	1.865E+12	4.476E+09	4.352E+08	1.290E+07
45	2.2313E+00	1.924E+12	2.543E+12	5.664E+09	5.558E+08	1.480E+07
46	2.1225E+00	1.868E+12	2.461E+12	5.257E+09	5.124E+08	1.317E+07
47	2.0190E+00	1.837E+12	2.414E+12	5.159E+09	5.320E+08	1.118E+07
48	1.9205E+00	1.793E+12	2.349E+12	4.888E+09	5.848E+08	1.097E+07
49	1.8268E+00	2.157E+12	2.819E+12	6.119E+09	6.806E+08	2.096E+07

Table A4  
Neutron Weighting Spectra  
(Continued)

Group	Energy*	BWR Core	PWR Core	Downcomer	1/4T in PV	Concrete
50	1.7377E+00	2.066E+12	2.677E+12	5.605E+09	6.621E+08	1.716E+07
51	1.6530E+00	1.996E+12	2.575E+12	5.201E+09	6.193E+08	1.581E+07
52	1.5724E+00	2.049E+12	2.636E+12	5.286E+09	6.166E+08	1.736E+07
53	1.4957E+00	2.141E+12	2.747E+12	5.379E+09	6.685E+08	1.935E+07
54	1.4227E+00	2.111E+12	2.687E+12	5.381E+09	8.117E+08	2.120E+07
55	1.3534E+00	1.768E+12	2.249E+12	4.231E+09	7.434E+08	1.509E+07
56	1.2873E+00	2.268E+12	2.864E+12	5.489E+09	6.981E+08	2.379E+07
57	1.2246E+00	2.300E+12	2.880E+12	5.692E+09	1.021E+09	2.843E+07
58	1.1648E+00	2.083E+12	2.603E+12	5.071E+09	9.272E+08	2.686E+07
59	1.1080E+00	3.370E+12	4.198E+12	7.757E+09	1.503E+09	3.193E+07
60	1.0026E+00	1.328E+12	1.657E+12	2.982E+09	6.073E+08	1.068E+07
61	9.6164E-01	2.248E+12	2.785E+12	5.122E+09	1.182E+09	2.413E+07
62	9.0718E-01	2.158E+12	2.625E+12	4.668E+09	7.785E+08	2.867E+07
63	8.6294E-01	2.498E+12	3.002E+12	5.198E+09	9.469E+08	3.265E+07
64	8.2085E-01	2.740E+12	3.253E+12	5.351E+09	7.345E+08	3.838E+07
65	7.8082E-01	2.596E+12	3.054E+12	4.987E+09	7.667E+08	4.423E+07
66	7.4274E-01	2.432E+12	2.854E+12	4.851E+09	1.139E+09	4.739E+07
67	7.0651E-01	2.362E+12	2.754E+12	4.721E+09	1.201E+09	4.999E+07
68	6.7206E-01	2.315E+12	2.696E+12	4.665E+09	1.667E+09	5.929E+07
69	6.3928E-01	2.241E+12	2.608E+12	4.576E+09	1.766E+09	6.843E+07
70	6.0810E-01	2.175E+12	2.523E+12	4.491E+09	1.408E+09	7.119E+07
71	5.7844E-01	2.120E+12	2.452E+12	4.342E+09	1.252E+09	6.178E+07
72	5.5023E-01	2.058E+12	2.375E+12	4.212E+09	1.172E+09	7.108E+07
73	5.2340E-01	1.956E+12	2.252E+12	3.997E+09	9.487E+08	6.856E+07
74	4.9787E-01	3.003E+12	3.516E+12	6.338E+09	2.116E+09	9.044E+07
75	4.5049E-01	2.649E+12	3.126E+12	5.789E+09	1.334E+09	6.633E+07
76	4.0762E-01	1.458E+12	1.720E+12	3.201E+09	6.491E+08	3.598E+07
77	3.8774E-01	1.492E+12	1.764E+12	3.236E+09	1.317E+09	3.883E+07
78	3.6883E-01	3.418E+12	3.961E+12	6.923E+09	2.797E+09	1.035E+08
79	3.3373E-01	3.334E+12	3.834E+12	6.658E+09	3.147E+09	1.183E+08
80	3.0197E-01	3.736E+11	4.286E+11	7.449E+08	4.618E+08	1.415E+07
81	2.9850E-01	1.398E+11	1.602E+11	2.797E+08	1.454E+08	5.373E+06
82	2.9720E-01	2.886E+11	3.298E+11	5.775E+08	2.204E+08	1.096E+07
83	2.9452E-01	7.948E+11	9.042E+11	1.577E+09	3.919E+08	2.974E+07
84	2.8725E-01	1.556E+12	1.765E+12	3.087E+09	5.772E+08	6.016E+07
85	2.7324E-01	2.963E+12	3.384E+12	5.946E+09	1.756E+09	1.200E+08
86	2.4724E-01	1.417E+12	1.615E+12	2.869E+09	9.232E+08	5.957E+07
87	2.3518E-01	1.371E+12	1.559E+12	2.800E+09	6.579E+08	5.884E+07
88	2.2371E-01	1.332E+12	1.522E+12	2.740E+09	8.504E+08	5.323E+07
89	2.1280E-01	1.297E+12	1.478E+12	2.679E+09	6.254E+08	5.154E+07
90	2.0242E-01	1.260E+12	1.433E+12	2.621E+09	4.156E+08	4.937E+07
91	1.9255E-01	1.227E+12	1.405E+12	2.569E+09	5.390E+08	5.262E+07
92	1.8316E-01	1.197E+12	1.381E+12	2.527E+09	1.111E+09	6.499E+07
93	1.7422E-01	1.165E+12	1.331E+12	2.468E+09	6.604E+08	7.287E+07
94	1.6573E-01	1.139E+12	1.310E+12	2.425E+09	9.067E+08	7.761E+07
95	1.5764E-01	1.109E+12	1.269E+12	2.374E+09	5.639E+08	7.178E+07
96	1.4996E-01	1.085E+12	1.237E+12	2.330E+09	3.104E+08	6.718E+07
97	1.4264E-01	1.061E+12	1.227E+12	2.291E+09	6.295E+08	6.599E+07
98	1.3569E-01	1.039E+12	1.197E+12	2.258E+09	5.916E+08	7.358E+07

Table A4

Neutron Weighting Spectra  
(Continued)

Group	Energy*	BWR Core	PWR Core	Downcomer	1/4T in PV	Concrete
99	1.2907E-01	1.018E+12	1.176E+12	2.221E+09	9.603E+08	7.573E+07
100	1.2277E-01	9.953E+11	1.147E+12	2.181E+09	7.821E+08	6.729E+07
101	1.1679E-01	9.777E+11	1.124E+12	2.143E+09	6.016E+08	6.846E+07
102	1.1109E-01	2.361E+12	2.717E+12	5.193E+09	1.137E+09	1.636E+08
103	9.8037E-02	2.258E+12	2.599E+12	5.016E+09	7.523E+08	1.431E+08
104	8.6517E-02	8.329E+11	9.464E+11	1.856E+09	1.458E+08	5.354E+07
105	8.2500E-02	6.401E+11	7.579E+11	1.458E+09	7.515E+08	4.718E+07
106	7.9500E-02	1.674E+12	1.927E+12	3.759E+09	5.371E+08	1.205E+08
107	7.2000E-02	1.092E+12	1.273E+12	2.481E+09	9.452E+08	7.979E+07
108	6.7379E-02	2.775E+12	3.210E+12	6.332E+09	1.308E+09	2.052E+08
109	5.6562E-02	1.152E+12	1.330E+12	2.633E+09	4.391E+08	8.345E+07
110	5.2475E-02	1.870E+12	2.171E+12	4.323E+09	9.115E+08	1.423E+08
111	4.6309E-02	1.816E+12	2.104E+12	4.219E+09	7.373E+08	1.377E+08
112	4.0868E-02	2.459E+12	2.850E+12	5.749E+09	6.763E+08	1.718E+08
113	3.4307E-02	1.028E+12	1.190E+12	2.421E+09	2.180E+08	7.974E+07
114	3.1828E-02	1.487E+12	1.684E+12	3.502E+09	1.012E+08	1.188E+08
115	2.8500E-02	7.175E+11	8.137E+11	1.703E+09	3.836E+07	5.540E+07
116	2.7000E-02	4.691E+11	5.917E+11	1.145E+09	1.271E+08	3.832E+07
117	2.6058E-02	6.546E+11	7.954E+11	1.630E+09	1.174E+09	5.587E+07
118	2.4788E-02	3.255E+11	3.849E+11	8.107E+08	7.882E+08	2.905E+07
119	2.4176E-02	3.242E+11	3.793E+11	7.964E+08	4.190E+08	2.838E+07
120	2.3579E-02	9.651E+11	1.127E+12	2.350E+09	8.408E+08	8.391E+07
121	2.1875E-02	1.585E+12	1.851E+12	3.836E+09	8.865E+08	1.391E+08
122	1.9305E-02	3.095E+12	3.615E+12	7.525E+09	1.111E+09	2.736E+08
123	1.5034E-02	3.011E+12	3.533E+12	7.502E+09	9.354E+08	2.694E+08
124	1.1709E-02	2.943E+12	3.457E+12	7.436E+09	5.923E+08	2.619E+08
125	9.1188E-03	2.888E+12	3.391E+12	7.350E+09	3.231E+08	2.639E+08
126	7.1017E-03	2.849E+12	3.365E+12	7.364E+09	7.897E+08	2.607E+08
127	5.5308E-03	2.807E+12	3.318E+12	7.373E+09	8.408E+08	2.614E+08
128	4.3074E-03	1.661E+12	1.969E+12	4.431E+09	4.403E+08	1.534E+08
129	3.7074E-03	1.101E+12	1.312E+12	2.966E+09	3.182E+08	9.319E+07
130	3.3546E-03	1.090E+12	1.298E+12	2.966E+09	2.979E+08	8.646E+07
131	3.0354E-03	1.062E+12	1.281E+12	2.961E+09	2.599E+08	6.604E+07
132	2.7465E-03	5.415E+11	6.415E+11	1.476E+09	1.125E+08	4.381E+07
133	2.6126E-03	5.655E+11	6.602E+11	1.472E+09	9.156E+07	5.486E+07
134	2.4852E-03	1.058E+12	1.267E+12	2.946E+09	1.480E+08	1.190E+08
135	2.2487E-03	1.094E+12	1.301E+12	2.982E+09	2.146E+08	1.159E+08
136	2.0347E-03	2.640E+12	3.169E+12	7.484E+09	6.880E+08	2.775E+08
137	1.5846E-03	2.632E+12	3.154E+12	7.495E+09	6.946E+08	2.686E+08
138	1.2341E-03	2.628E+12	3.150E+12	7.494E+09	5.075E+08	2.645E+08
139	9.6112E-04	2.579E+12	3.108E+12	7.556E+09	5.031E+08	2.633E+08
140	7.4852E-04	2.548E+12	3.079E+12	7.603E+09	5.051E+08	2.625E+08
141	5.8295E-04	2.518E+12	3.054E+12	7.647E+09	4.968E+08	2.619E+08
142	4.5400E-04	2.496E+12	3.031E+12	7.649E+09	3.119E+08	2.610E+08
143	3.5358E-04	2.486E+12	3.028E+12	7.757E+09	4.061E+08	2.605E+08
144	2.7536E-04	2.423E+12	2.972E+12	7.810E+09	4.571E+08	2.598E+08
145	2.1445E-04	2.415E+12	2.962E+12	7.853E+09	4.829E+08	2.590E+08
146	1.6702E-04	2.378E+12	2.930E+12	7.900E+09	5.015E+08	2.583E+08
147	1.3007E-04	2.178E+12	2.731E+12	7.944E+09	5.168E+08	2.574E+08

Table A4  
Neutron Weighting Spectra  
(Continued)

Group	Energy*	BWR Core	PWR Core	Downcomer	1/4T in PV	Concrete
148	1.0130E-04	2.375E+12	2.925E+12	7.990E+09	5.264E+08	2.565E+08
149	7.8893E-05	2.262E+12	2.811E+12	8.037E+09	5.348E+08	2.556E+08
150	6.1442E-05	2.256E+12	2.808E+12	8.084E+09	5.390E+08	2.545E+08
151	4.7851E-05	2.131E+12	2.694E+12	8.131E+09	5.399E+08	2.536E+08
152	3.7267E-05	2.075E+12	2.599E+12	7.973E+09	5.245E+08	2.460E+08
153	2.9203E-05	2.190E+12	2.760E+12	8.425E+09	5.456E+08	2.573E+08
154	2.2603E-05	1.816E+12	2.344E+12	8.266E+09	5.241E+08	2.498E+08
155	1.7603E-05	2.024E+12	2.578E+12	8.307E+09	5.126E+08	2.484E+08
156	1.3710E-05	1.997E+12	2.543E+12	8.352E+09	4.984E+08	2.471E+08
157	1.0677E-05	1.938E+12	2.483E+12	8.392E+09	4.810E+08	2.455E+08
158	8.3153E-06	1.472E+12	1.964E+12	8.432E+09	4.608E+08	2.440E+08
159	6.4760E-06	1.565E+12	2.104E+12	8.471E+09	4.380E+08	2.424E+08
160	5.0435E-06	1.749E+12	2.295E+12	8.508E+09	4.125E+08	2.406E+08
161	3.9279E-06	1.751E+12	2.292E+12	8.544E+09	3.856E+08	2.388E+08
162	3.0590E-06	1.791E+12	2.342E+12	8.723E+09	3.622E+08	2.410E+08
163	2.3724E-06	1.717E+12	2.249E+12	8.466E+09	3.210E+08	2.309E+08
164	1.8554E-06	1.741E+12	2.282E+12	8.641E+09	2.953E+08	2.328E+08
165	1.4450E-06	1.707E+12	2.243E+12	8.668E+09	2.639E+08	2.305E+08
166	1.1254E-06	1.670E+12	2.201E+12	8.696E+09	2.329E+08	2.282E+08
167	8.7642E-07	1.661E+12	2.191E+12	8.717E+09	2.027E+08	2.257E+08
168	6.8256E-07	1.636E+12	2.162E+12	8.737E+09	1.738E+08	2.231E+08
169	5.3158E-07	1.597E+12	2.116E+12	8.754E+09	1.471E+08	2.202E+08
170	4.1399E-07	1.350E+13	1.852E+13	1.042E+11	4.221E+08	1.823E+09
171	1.0000E-07	1.842E+13	2.685E+13	1.210E+12	3.805E+08	1.005E+10
172	1.0000E-11					

\*Upper energy of group (MeV)

Table A5

## Gamma Ray Weighting Spectra

Group	Energy*	BWR Core	PWR Core	Downcomer	1/4T in PV	Concrete
1	1.4000E+01	4.509E+02	2.372E+02	6.553E+04	7.358E+03	3.202E+03
2	1.2000E+01	6.746E+06	1.174E+07	1.841E+07	2.022E+06	1.070E+06
3	1.0000E+01	5.562E+09	3.854E+10	9.219E+10	9.507E+09	9.371E+07
4	8.0000E+00	1.809E+10	4.007E+11	1.346E+11	1.418E+10	2.946E+08
5	7.5000E+00	3.696E+10	1.058E+11	4.555E+10	5.442E+09	1.057E+08
6	7.0000E+00	6.978E+10	1.278E+11	2.815E+10	3.840E+09	5.911E+07
7	6.5000E+00	2.138E+11	4.012E+11	4.262E+10	5.459E+09	2.392E+08
8	6.0000E+00	2.862E+11	5.900E+11	4.921E+10	6.283E+09	1.499E+08
9	5.5000E+00	4.154E+11	7.308E+11	3.550E+10	5.254E+09	1.269E+08
10	5.0000E+00	5.413E+11	9.633E+11	3.961E+10	5.895E+09	3.148E+08
11	4.5000E+00	1.539E+12	2.579E+12	5.593E+10	7.754E+09	2.072E+08
12	4.0000E+00	2.281E+12	3.794E+12	6.080E+10	8.801E+09	4.167E+08
13	3.5000E+00	3.392E+12	5.718E+12	8.510E+10	1.144E+10	2.497E+08
14	3.0000E+00	6.087E+12	1.014E+13	1.082E+11	1.438E+10	3.045E+08
15	2.5000E+00	1.153E+13	1.918E+13	5.596E+11	3.174E+10	6.558E+08
16	2.0000E+00	1.043E+13	1.715E+13	1.920E+11	2.203E+10	4.094E+08
17	1.6600E+00	5.807E+12	9.696E+12	1.021E+11	1.176E+10	1.851E+08
18	1.5000E+00	7.239E+12	1.222E+13	1.207E+11	1.406E+10	1.876E+08
19	1.3300E+00	1.715E+13	2.910E+13	2.888E+11	3.373E+10	4.548E+08
20	1.0000E+00	1.263E+13	2.171E+13	2.532E+11	2.925E+10	3.683E+08
21	8.0000E-01	7.103E+12	1.210E+13	1.461E+11	1.638E+10	2.311E+08
22	7.0000E-01	7.703E+12	1.304E+13	1.733E+11	1.911E+10	2.510E+08
23	6.0000E-01	6.725E+12	1.128E+13	1.840E+11	2.010E+10	2.704E+08
24	5.1200E-01	3.912E+12	6.597E+12	9.930E+10	2.324E+10	2.581E+08
25	5.1000E-01	4.722E+12	8.455E+12	3.868E+11	2.204E+10	3.077E+08
26	4.5000E-01	3.485E+12	5.900E+12	2.046E+11	2.064E+10	2.768E+08
27	4.0000E-01	5.862E+12	1.004E+13	5.406E+11	5.279E+10	7.490E+08
28	3.0000E-01	3.890E+12	6.682E+12	9.284E+11	8.197E+10	1.333E+09
29	2.0000E-01	7.829E+11	1.332E+12	7.443E+11	5.305E+10	1.077E+09
30	1.5000E-01	3.030E+11	4.955E+11	1.097E+12	4.458E+10	1.674E+09
31	1.0000E-01	9.872E+10	1.243E+11	7.214E+11	7.919E+09	9.085E+08
32	7.5000E-02	2.231E+10	2.287E+10	4.828E+11	8.636E+08	4.746E+08
33	6.0000E-02	8.672E+09	9.512E+09	4.486E+11	5.932E+07	1.848E+08
34	4.5000E-02	2.194E+10	1.207E+10	2.100E+11	3.169E+06	1.952E+07
35	3.0000E-02	5.560E+08	8.811E+08	1.767E+10	6.234E+05	5.421E+05
36	2.0000E-02	2.107E+08	6.318E+08	1.767E+08	1.278E+05	5.835E+04
37	1.0000E-02					

\*Upper energy of group (MeV)

Table A6

Neutron Groups for SAILOR and Their Components from  
171 Group Structure

Group	Energy	Groups from 171 Group Structure									
1	1.733E+01	1	2	3	4	5					
2	1.419E+01	6	7	8	9						
3	1.221E+01	10	11	12	13						
4	1.000E+01	14	15	16							
5	8.607E+00	17	18	19							
6	7.408E+00	20	21	22	23	24					
7	6.065E+00	25	26	27	28						
8	4.966E+00	29	30	31	32						
9	3.679E+00	33	34	35							
10	3.012E+00	36	37								
11	2.725E+00	38	39								
12	2.466E+00	40	41								
13	2.365E+00	42									
14	2.346E+00	43	44								
15	2.231E+00	45	46	47							
16	1.920E+00	48	49	50							
17	1.653E+00	51	52	53	54						
18	1.353E+00	55	56	57	58	59					
19	1.003E+00	60	61	62	63						
20	8.208E-01	64	65								
21	7.427E-01	66	67	68	69						
22	6.081E-01	70	71	72	73						
23	4.979E-01	74	75	76	77						
24	3.688E-01	78	79	80	81						
25	2.972E-01	82	83	84	85	86	87	88	89	90	91
26	1.832E-01	92	93	94	95	96	97	98	99	100	101
27	1.111E-01	102	103	104	105	106	107				
28	6.738E-02	108	109	110	111						
29	4.087E-02	112	113								
30	3.183E-02	114	115	116							
31	2.606E-02	117	118								
32	2.418E-02	119	120								
33	2.188E-02	121	122								
34	1.503E-02	123	124	125							
35	7.102E-03	126	127	128	129						
36	3.355E-03	130	131	132	133	134	135	136			
37	1.585E-03	137	138	139	140	141					
38	4.540E-04	142	143	144							
39	2.144E-04	145	146	147							
40	1.013E-04	148	149	150	151						
41	3.727E-05	152	153	154	155	156					
42	1.068E-05	157	158	159							
43	5.043E-06	160	161	162	163						
44	1.855E-06	164	165	166							
45	8.764E-07	167	168	169							
46	4.140E-07	170									
47	1.000E-07	171									
	1.000E-11										

Table A7

Gamma Ray for SAILOR and Their Components from  
36 Group Structure

Group	Energy	Groups from 36 Group Structure			
1	14.000	1	2		
2	10.000	3			
3	8.000	4	5		
4	7.000	6	7		
5	6.000	8	9		
6	5.000	10	11		
7	4.000	12	13		
8	3.000	14	15		
9	2.000	16	17		
10	1.500	18	19		
11	1.000	20			
12	0.800	21			
13	0.700	22			
14	0.600	23	24	25	26
15	0.400	27	28		
16	0.200	29	30		
17	0.100	31	32		
18	0.060	33	34		
19	0.030	35			
20	0.020	36			
	0.010				

commonly used materials by making mixtures of cross sections. The densities used for these mixtures are given in Table A8. The resulting cross section library called SAILOR contains 58 materials with a  $P_3$  scattering approximation and 2 materials (ID's 1 and 2) which contain response functions in the 47n,20g group structure. The identification of each "material" is given in Table A9, along with the appropriate ANISN cross section ID for the  $P_0$  component of the cross section. The two response cross sections, were obtained by collapsing the SAND-II cross section library over a flat spectrum and the spectrum at a 1/4 T position in a PWR pressure vessel. The type of neutron response and its position in the cross section table is given in Table A10. The listing of the response cross sections for the uniform (flat) neutron spectra is contained in Table A11.

It is felt that this library should be adequate for most practical problems that are encountered for light water reactors and should be of particular use for pressure vessel dosimetry and vessel fluence analysis. The data contained in Appendix B should also serve as a reference for repeating this cross section generation process if and when it is worth repeating with new data.

Table A8

SAILOR P<sub>0</sub> Cross Sections ID's for ANISN

ID	Description
1	ENDF/B-IV DOSIMETRY FILE FLAT WEIGHTING
2	ENDF/B-IV DOSIMETRY FILE 1/4 T PRESS. VESS.
3	HYDROGEN PWR CORE P3 47N/20G SAILWR LIB
7	BORON-10 PWR CORE P3 47N/20G SAILWR LIB
11	OXYGEN PWR CORE P3 47N/20G SAILWR LIB
15	CHROMIUM PWR CORE P3 47N/20G SAILWR LIB
19	IRON PWR CORE P3 47N/20G SAILWR LIB
23	NICKEL PWR CORE P3 47N/20G SAILWR LIB
27	ZIRCONIUM PWR CORE P3 47N/20G SAILWR LIB
31	U-235 PWR CORE P3 47N/20G SAILWR LIB
35	U-238 PWR CORE P3 47N/20G SAILWR LIB
39	OXYGEN PWR CORE P3 47N/20G SAILWR LIB
43	U-235 BWR CORE P3 47N/20G SAILWR LIB
47	U-238 BWR CORE P3 47N/20G SAILWR LIB
51	OXYGEN BWR CORE P3 47N/20G SAILWR LIB
55	HYDROGEN PWR DOWNCOMER P3 47N/20G SAILWR LIB
59	OXYGEN PWR DOWNCOMER P3 47N/20G SAILWR LIB
63	CHROMIUM PWR DOWNCOMER P3 47N/20G SAILWR LIB
67	MN-55 PWR DOWNCOMER P3 47N/20G SAILWR LIB
71	IRON PWR DOWNCOMER P3 47N/20G SAILWR LIB
75	NICKEL PWR DOWNCOMER P3 47N/20G SAILWR LIB
79	CARBON PWR DOWNCOMER P3 47N/20G SAILWR LIB
83	HYDROGEN CONCRETE WTG. P3 47N/20G SAILWR LIB
87	CARBON CONCRETE WTG. P3 47N/20G SAILWR LIB
91	OXYGEN CONCRETE WTG. P3 47N/20G SAILWR LIB
95	SODIUM CONCRETE WTG. P3 47N/20G SAILWR LIB
99	MAGNESIUM CONCRETE WTG. P3 47N/20G SAILWR LIB
103	ALUMINUM CONCRETE WTG. P3 47N/20G SAILWR LIB
107	SILICON CONCRETE WTG. P3 47N/20G SAILWR LIB
111	POTASSIUM CONCRETE WTG. P3 47N/20G SAILWR LIB
115	CALCIUM CONCRETE WTG. P3 47N/20G SAILWR LIB
119	IRON CONCRETE WTG. P3 47N/20G SAILWR LIB
123	CHROMIUM 1/4 T IN P. V. P3 47N/20G SAILWR LIB
127	MN-55 1/4 T IN P. V. P3 47N/20G SAILWR LIB
131	IRON 1/4 T IN P. V. P3 47N/20G SAILWR LIB
135	NICKEL 1/4 T IN P. V. P3 47N/20G SAILWR LIB
139	CARBON 1/4 T IN P. V. P3 47N/20G SAILWR LIB

Table A9

SAILOR P<sub>0</sub> Cross Section ID's for ANISN:  
Mixtures and Plutonium Isotopes

ID	Description
143	U-235 PWR MOX FUEL P3 47N/20G SAILWR LIB
147	U-236 PWR MOX FUEL P3 47N/20G SAILWR LIB
151	U-238 PWR MOX FUEL P3 47N/20G SAILWR LIB
155	PU-239 PWR MOX FUEL P3 47N/20G SAILWR LIB
159	PU-240 PWR MOX FUEL P3 47N/20G SAILWR LIB
163	PU-241 PWR MOX FUEL P3 47N/20G SAILWR LIB
167	PU-242 PWR MOX FUEL P3 47N/20G SAILWR LIB
171	NP-237 PWR MOX FUEL P3 47N/20G SAILWR LIB
175	OXYGEN PWR MOX FUEL P3 47N/20G SAILWR LIB
179	WATER AT 1.0 G/CC P3 47N/20G
183	STAINLESS STEEL 304 AT 7.94 G/CC P3 47N/20G
187	A-533-B LOW CARBON STEEL AT 7.38 G/ P3 47N/20G
191	A-508 CL2 STEEL P3 47N/20G
195	ANSI STANDARD CONCRETE TYPE04 @2.31 P3 47N/20G
199	ZIRCALOY-4 AT 6.56 G/CC P3 47N/20G
203	U02 .711 W/O U-235 10.412 G/CC BWR P3 47N/20G
207	U02 1.76 W/O U-235 10.412 G/CC BWR P3 47N/20G
211	U02 2.10 W/O U-235 10.412 G/CC BWR P3 47N/20G
215	U02 2.23 W/O U-235 10.412 G/CC BWR P3 47N/20G
219	U02 2.60 W/O U-235 10.412 G/CC PWR P3 47N/20G
223	U02 3.00 W/O U-235 10.412 G/CC PWR P3 47N/20G
227	U02 3.30 W/O U-235 10.412 G/CC PWR P3 47N/20G
231	U02 92.5 W/O U-235 10.412 G/CC PWR P3 47N/20G

Table A10

## Neutron Response by Position in Materials 1 and 2

Position	Neutron Response
1	Group Maximum Energy (MeV)
2	Fission Spectrum
3	Li-6 (n,alpha)
4	B-10 (n,alpha)
5	Th-232 (n,fission)
6	U-235 (n,fission)
7	U-238 (n,fission)
8	Np-237 (n,fission)
9	Pu-239 (n,fission)
10	Al-27 (n,p)
11	Al-27 (n,alpha)
12	S-32 (n,p)
13	Ti-46 (n,p)
14	Ti-47 (n,p)
15	Ti-47 (n,n'p)
16	Ti-48 (n,p)
17	Ti-48 (n,n'p)
18	Mn-55 (n,2n)
19	Fe-54 (n,p)
20	Fe-56 (n,p)
21	Co-59 (n,2n)
22	Co-59 (n,alpha)
23	Ni-58 (n,p)
24	Ni-58 (n,2n)
25	Ni-60 (n,p)
26	Cu-63 (n,alpha)
27	Cu-65 (n,2n)
28	In-115 (n,nn')
29	I-127 (n,2n)
30	Sc-45 (n,g)
31	Na-24 (n,g)
32	Fe-58 (n,g)
33	Co-59 (n,g)
34	Cu-63 (n,g)
35	In-115 (n,g)
36	Au-197 (n,g)
37	Th-232 (n,g)
38	U-238 (n,g)
39	Square Root (E)
40	Constant
41	U-234 (n,fission)
42	U-236 (n,fission)
43	Pu-240 (n,fission)
44	Pu-241 (n,fission)
45	Pu-242 (n,fission)

Table A11

## Neutron Response Cross Sections Based on Uniform Weighting

Energy (MeV)	Fission Spectrum	Li-6 n,alpha	B-10 n,alpha	Th-232 n,fiss	U-235 n,fiss
1.733E+01	8.369E-05	4.399E-01	5.875E-01	4.203E-01	2.213E+00
1.419E+01	2.899E-04	4.588E-01	5.764E-01	3.354E-01	2.035E+00
1.221E+01	1.456E-03	5.018E-01	5.275E-01	2.853E-01	1.740E+00
1.000E+01	3.046E-03	5.660E-01	4.811E-01	2.947E-01	1.793E+00
8.607E+00	6.349E-03	6.176E-01	4.645E-01	3.266E-01	1.748E+00
7.408E+00	1.699E-02	6.563E-01	4.832E-01	2.773E-01	1.427E+00
6.065E+00	3.101E-02	6.715E-01	6.080E-01	1.403E-01	1.089E+00
4.966E+00	7.889E-02	6.533E-01	5.053E-01	1.437E-01	1.126E+00
3.679E+00	7.327E-02	5.431E-01	3.354E-01	1.344E-01	1.205E+00
3.012E+00	4.146E-02	4.032E-01	3.901E-01	1.240E-01	1.245E+00
2.725E+00	4.376E-02	3.331E-01	3.630E-01	1.126E-01	1.269E+00
2.466E+00	1.875E-02	3.033E-01	3.377E-01	1.132E-01	1.278E+00
2.365E+00	3.769E-03	2.990E-01	3.429E-01	1.150E-01	1.279E+00
2.346E+00	2.281E-02	2.950E-01	3.582E-01	1.166E-01	1.279E+00
2.231E+00	6.922E-02	2.726E-01	4.895E-01	1.134E-01	1.276E+00
1.920E+00	6.862E-02	2.638E-01	5.213E-01	8.902E-02	1.266E+00
1.653E+00	8.712E-02	2.542E-01	2.929E-01	7.381E-02	1.253E+00
1.353E+00	1.151E-01	2.468E-01	2.057E-01	5.966E-03	1.251E+00
1.003E+00	6.405E-02	2.576E-01	2.341E-01	0	1.180E+00
8.208E-01	2.811E-02	2.729E-01	3.042E-01	0	1.132E+00
7.427E-01	4.874E-02	2.974E-01	4.259E-01	0	1.140E+00
6.081E-01	3.960E-02	3.537E-01	6.568E-01	0	1.159E+00
4.979E-01	4.481E-02	5.494E-01	8.543E-01	0	1.206E+00
3.688E-01	2.352E-02	1.240E+00	9.880E-01	0	1.250E+00
2.972E-01	3.400E-02	2.435E+00	1.221E+00	0	1.317E+00
1.832E-01	1.804E-02	9.752E-01	1.655E+00	0	1.474E+00
1.111E-01	8.900E-03	6.859E-01	2.119E+00	0	1.657E+00
6.738E-02	4.317E-03	7.428E-01	2.639E+00	0	1.850E+00
4.087E-02	1.225E-03	8.512E-01	3.164E+00	0	1.988E+00
3.183E-02	7.019E-04	9.354E-01	3.529E+00	0	2.113E+00
2.606E-02	2.139E-04	9.823E-01	3.729E+00	0	2.184E+00
2.418E-02	2.508E-04	1.017E+00	3.870E+00	0	2.187E+00
2.188E-02	6.690E-04	1.122E+00	4.310E+00	0	2.295E+00
1.503E-02	6.016E-04	1.494E+00	5.829E+00	0	2.877E+00
7.102E-03	1.962E-04	2.231E+00	8.826E+00	0	4.256E+00
3.355E-03	6.382E-05	3.015E+00	1.201E+01	0	5.509E+00
1.585E-03	2.600E-05	5.208E+00	2.094E+01	0	1.037E+01
4.540E-04	3.183E-06	8.500E+00	3.434E+01	0	1.671E+01
2.144E-04	1.033E-06	1.237E+01	5.015E+01	0	2.128E+01
1.013E-04	3.858E-07	1.926E+01	7.826E+01	0	3.475E+01
3.727E-05	5.849E-08	3.399E+01	1.384E+02	0	5.075E+01
1.068E-05	3.537E-08	5.550E+01	2.262E+02	0	5.017E+01
5.043E-06	1.148E-08	8.641E+01	3.523E+02	0	1.656E+01
1.855E-06	4.289E-09	1.331E+02	5.430E+02	0	4.400E+01
8.764E-07	8.320E-10	1.932E+02	7.880E+02	0	7.178E+01
4.140E-07	2.700E-10	3.335E+02	1.361E+03	0	1.844E+02
1.000E-07	1.294E-10	4.191E+03	1.711E+04	0	2.753E+03

Table A11

Neutron Response Cross Sections Based on Uniform Weighting  
(Continued)

Energy (MeV)	U-238 n,fiss	Np-237 n,fiss	Pu-239 n,fiss	Al-27 n,p	Al-27 n,alpha
1.733E+01	1.275E+00	2.535E+00	2.601E+00	6.663E-02	1.045E-01
1.419E+01	1.086E+00	2.320E+00	2.426E+00	8.246E-02	1.264E-01
1.221E+01	9.844E-01	2.334E+00	2.311E+00	9.865E-02	1.080E-01
1.000E+01	9.864E-01	2.329E+00	2.374E+00	1.004E-01	7.634E-02
8.607E+00	9.891E-01	2.248E+00	2.324E+00	8.525E-02	4.135E-02
7.408E+00	8.574E-01	1.965E+00	2.020E+00	6.103E-02	1.055E-02
6.065E+00	5.849E-01	1.520E+00	1.698E+00	3.513E-02	3.921E-04
4.966E+00	5.615E-01	1.538E+00	1.740E+00	1.409E-02	5.073E-07
3.679E+00	5.475E-01	1.638E+00	1.830E+00	3.885E-03	3.526E-21
3.012E+00	5.463E-01	1.680E+00	1.874E+00	7.350E-04	0
2.725E+00	5.527E-01	1.697E+00	1.910E+00	1.115E-04	0
2.466E+00	5.521E-01	1.695E+00	1.942E+00	9.307E-06	0
2.365E+00	5.512E-01	1.694E+00	1.949E+00	3.684E-06	0
2.346E+00	5.504E-01	1.693E+00	1.952E+00	2.541E-06	0
2.231E+00	5.390E-01	1.677E+00	1.958E+00	5.517E-08	0
1.920E+00	4.685E-01	1.645E+00	1.937E+00	3.385E-16	0
1.653E+00	2.706E-01	1.604E+00	1.883E+00	0	0
1.353E+00	4.502E-02	1.543E+00	1.784E+00	0	0
1.003E+00	1.102E-02	1.389E+00	1.699E+00	0	0
8.208E-01	2.881E-03	1.205E+00	1.689E+00	0	0
7.427E-01	1.397E-03	9.845E-01	1.641E+00	0	0
6.081E-01	5.378E-04	6.437E-01	1.594E+00	0	0
4.979E-01	1.502E-04	2.642E-01	1.568E+00	0	0
3.688E-01	8.333E-05	8.800E-02	1.532E+00	0	0
2.972E-01	6.168E-05	3.552E-02	1.495E+00	0	0
1.832E-01	4.668E-05	2.043E-02	1.533E+00	0	0
1.111E-01	4.015E-05	1.542E-02	1.587E+00	0	0
6.738E-02	4.000E-05	1.228E-02	1.605E+00	0	0
4.087E-02	6.176E-05	1.088E-02	1.610E+00	0	0
3.183E-02	8.610E-05	1.023E-02	1.632E+00	0	0
2.606E-02	8.700E-05	1.002E-02	1.655E+00	0	0
2.418E-02	8.700E-05	9.906E-03	1.677E+00	0	0
2.188E-02	8.700E-05	9.723E-03	1.715E+00	0	0
1.503E-02	5.650E-05	1.004E-02	1.936E+00	0	0
7.102E-03	4.860E-11	6.506E-03	2.527E+00	0	0
3.355E-03	7.439E-10	8.716E-03	3.423E+00	0	0
1.585E-03	4.199E-04	2.303E-02	7.449E+00	0	0
4.540E-04	1.464E-08	3.701E-02	1.228E+01	0	0
2.144E-04	1.044E-08	6.129E-02	1.893E+01	0	0
1.013E-04	1.243E-08	9.027E-02	4.635E+01	0	0
3.727E-05	1.955E-08	2.296E-02	7.784E+01	0	0
1.068E-05	3.086E-08	1.014E-02	4.791E+01	0	0
5.043E-06	4.770E-08	4.011E-03	1.164E+01	0	0
1.855E-06	7.171E-08	9.350E-03	2.857E+01	0	0
8.764E-07	5.067E-08	1.407E-02	1.474E+02	0	0
4.140E-07	1.881E-08	4.328E-03	1.152E+03	0	0
1.000E-07	1.182E-09	8.332E-02	3.570E+03	0	0

Table A11

Neutron Response Cross Sections Based on Uniform Weighting  
(Continued)

Energy (MeV)	S-32 n,p	Ti-46 n,p	Ti-47 n,p	Ti-47 n,n'p	Ti-48 n,p
1.733E+01	1.882E-01	2.363E-01	1.005E-01	7.795E-02	6.124E-02
1.419E+01	2.876E-01	2.724E-01	1.204E-01	6.693E-03	6.003E-02
1.221E+01	3.778E-01	2.688E-01	1.284E-01	4.683E-06	3.472E-02
1.000E+01	3.488E-01	2.354E-01	1.287E-01	0	1.456E-02
8.607E+00	3.246E-01	1.985E-01	1.229E-01	0	6.563E-03
7.408E+00	3.148E-01	1.486E-01	1.060E-01	0	2.859E-03
6.065E+00	2.657E-01	9.465E-02	8.675E-02	0	5.391E-04
4.966E+00	2.584E-01	3.969E-02	7.071E-02	0	2.756E-05
3.679E+00	1.784E-01	3.058E-03	4.670E-02	0	5.208E-07
3.012E+00	1.091E-01	2.856E-04	3.340E-02	0	0
2.725E+00	7.731E-02	1.711E-04	3.141E-02	0	0
2.466E+00	8.576E-02	1.356E-04	3.257E-02	0	0
2.365E+00	8.963E-02	1.286E-04	3.222E-02	0	0
2.346E+00	8.208E-02	1.224E-04	3.156E-02	0	0
2.231E+00	3.046E-02	8.010E-05	2.325E-02	0	0
1.920E+00	4.291E-03	2.727E-05	1.003E-02	0	0
1.653E+00	6.031E-04	7.104E-07	3.830E-03	0	0
1.353E+00	6.902E-05	0	2.165E-03	0	0
1.003E+00	1.794E-06	0	5.806E-05	0	0
8.208E-01	0	0	3.764E-06	0	0
7.427E-01	0	0	3.797E-07	0	0
6.081E-01	0	0	3.803E-10	0	0
4.979E-01	0	0	0	0	0
3.688E-01	0	0	0	0	0
2.972E-01	0	0	0	0	0
1.832E-01	0	0	0	0	0
1.111E-01	0	0	0	0	0
6.738E-02	0	0	0	0	0
4.087E-02	0	0	0	0	0
3.183E-02	0	0	0	0	0
2.606E-02	0	0	0	0	0
2.418E-02	0	0	0	0	0
2.188E-02	0	0	0	0	0
1.503E-02	0	0	0	0	0
7.102E-03	0	0	0	0	0
3.355E-03	0	0	0	0	0
1.585E-03	0	0	0	0	0
4.540E-04	0	0	0	0	0
2.144E-04	0	0	0	0	0
1.013E-04	0	0	0	0	0
3.727E-05	0	0	0	0	0
1.068E-05	0	0	0	0	0
5.043E-06	0	0	0	0	0
1.855E-06	0	0	0	0	0
8.764E-07	0	0	0	0	0
4.140E-07	0	0	0	0	0
1.000E-07	0	0	0	0	0

Table A11

Neutron Response Cross Sections Based on Uniform Weighting  
(Continued)

Energy (MeV)	Ti-48 n,n'p	Mn-55 n,2n	Fe-54 n,p	Fe-56 n,p	Co-59 n,2n
1.733E+01	2.354E-02	8.517E-01	2.686E-01	9.160E-02	7.212E-01
1.419E+01	7.134E-03	6.761E-01	4.137E-01	1.118E-01	5.422E-01
1.221E+01	2.400E-04	1.540E-01	5.276E-01	8.818E-02	9.345E-02
1.000E+01	0	0	5.781E-01	6.063E-02	0
8.607E+00	0	0	5.888E-01	4.378E-02	0
7.408E+00	0	0	5.590E-01	2.447E-02	0
6.065E+00	0	0	4.697E-01	6.291E-03	0
4.966E+00	0	0	3.199E-01	2.644E-04	0
3.679E+00	0	0	1.762E-01	3.756E-07	0
3.012E+00	0	0	1.155E-01	1.076E-08	0
2.725E+00	0	0	7.755E-02	0	0
2.466E+00	0	0	5.111E-02	0	0
2.365E+00	0	0	4.756E-02	0	0
2.346E+00	0	0	4.484E-02	0	0
2.231E+00	0	0	2.008E-02	0	0
1.920E+00	0	0	4.771E-03	0	0
1.653E+00	0	0	6.335E-04	0	0
1.353E+00	0	0	1.311E-05	0	0
1.003E+00	0	0	0	0	0
8.208E-01	0	0	0	0	0
7.427E-01	0	0	0	0	0
6.081E-01	0	0	0	0	0
4.979E-01	0	0	0	0	0
3.688E-01	0	0	0	0	0
2.972E-01	0	0	0	0	0
1.832E-01	0	0	0	0	0
1.111E-01	0	0	0	0	0
6.738E-02	0	0	0	0	0
4.087E-02	0	0	0	0	0
3.183E-02	0	0	0	0	0
2.606E-02	0	0	0	0	0
2.418E-02	0	0	0	0	0
2.188E-02	0	0	0	0	0
1.503E-02	0	0	0	0	0
7.102E-03	0	0	0	0	0
3.355E-03	0	0	0	0	0
1.585E-03	0	0	0	0	0
4.540E-04	0	0	0	0	0
2.144E-04	0	0	0	0	0
1.013E-04	0	0	0	0	0
3.727E-05	0	0	0	0	0
1.068E-05	0	0	0	0	0
5.043E-06	0	0	0	0	0
1.855E-06	0	0	0	0	0
8.764E-07	0	0	0	0	0
4.140E-07	0	0	0	0	0
1.000E-07	0	0	0	0	0

Table A11

Neutron Response Cross Sections Based on Uniform Weighting  
(Continued)

Energy (MeV)	Co-59 n,alpha	Ni-58 n,p	Ni-58 n,2n	Ni-60 n,p	Cu-63 n,alpha
1.733E+01	2.612E-02	2.962E-01	4.017E-02	1.035E-01	2.966E-02
1.419E+01	2.809E-02	4.416E-01	1.239E-02	1.358E-01	3.831E-02
1.221E+01	1.979E-02	6.103E-01	0	1.590E-01	4.354E-02
1.000E+01	1.310E-02	6.588E-01	0	1.424E-01	3.313E-02
8.607E+00	7.471E-03	6.553E-01	0	9.607E-02	1.717E-02
7.408E+00	2.655E-03	6.285E-01	0	5.221E-02	7.834E-03
6.065E+00	4.562E-04	5.365E-01	0	1.668E-02	5.635E-04
4.966E+00	0	3.917E-01	0	1.766E-03	0
3.679E+00	0	2.287E-01	0	4.230E-04	0
3.012E+00	0	1.658E-01	0	2.270E-04	0
2.725E+00	0	1.131E-01	0	9.538E-05	0
2.466E+00	0	9.308E-02	0	1.244E-05	0
2.365E+00	0	9.232E-02	0	5.584E-07	0
2.346E+00	0	8.614E-02	0	3.635E-07	0
2.231E+00	0	4.661E-02	0	0	0
1.920E+00	0	2.660E-02	0	0	0
1.653E+00	0	1.337E-02	0	0	0
1.353E+00	0	4.438E-03	0	0	0
1.003E+00	0	5.023E-04	0	0	0
8.208E-01	0	1.729E-04	0	0	0
7.427E-01	0	4.914E-05	0	0	0
6.081E-01	0	7.673E-06	0	0	0
4.979E-01	0	8.903E-07	0	0	0
3.688E-01	0	4.070E-08	0	0	0
2.972E-01	0	1.832E-15	0	0	0
1.832E-01	0	0	0	0	0
1.111E-01	0	0	0	0	0
6.738E-02	0	0	0	0	0
4.087E-02	0	0	0	0	0
3.183E-02	0	0	0	0	0
2.606E-02	0	0	0	0	0
2.418E-02	0	0	0	0	0
2.188E-02	0	0	0	0	0
1.503E-02	0	0	0	0	0
7.102E-03	0	0	0	0	0
3.355E-03	0	0	0	0	0
1.585E-03	0	0	0	0	0
4.540E-04	0	0	0	0	0
2.144E-04	0	0	0	0	0
1.013E-04	0	0	0	0	0
3.727E-05	0	0	0	0	0
1.068E-05	0	0	0	0	0
5.043E-06	0	0	0	0	0
1.855E-06	0	0	0	0	0
8.764E-07	0	0	0	0	0
4.140E-07	0	0	0	0	0
1.000E-07	0	0	0	0	0

Table A11

Neutron Response Cross Sections Based on Uniform Weighting  
(Continued)

Energy (MeV)	Cu-65 n,2n	In-115 n,nn'	I-127 n,2n	Sc-45 n,g	Na-24 n,g
1.733E+01	1.014E+00	5.884E-02	1.687E+00	1.815E-03	2.288E-04
1.419E+01	7.863E-01	8.549E-02	1.517E+00	1.748E-03	2.023E-04
1.221E+01	2.064E-01	1.944E-01	8.292E-01	1.653E-03	1.798E-04
1.000E+01	0	2.685E-01	7.477E-02	1.568E-03	1.740E-04
8.607E+00	0	2.874E-01	0	1.506E-03	1.701E-04
7.408E+00	0	3.052E-01	0	1.481E-03	1.668E-04
6.065E+00	0	3.160E-01	0	1.490E-03	1.634E-04
4.966E+00	0	3.197E-01	0	1.535E-03	1.608E-04
3.679E+00	0	3.137E-01	0	1.691E-03	1.686E-04
3.012E+00	0	3.072E-01	0	1.837E-03	1.746E-04
2.725E+00	0	2.965E-01	0	1.996E-03	1.794E-04
2.466E+00	0	2.867E-01	0	2.150E-03	1.831E-04
2.365E+00	0	2.848E-01	0	2.184E-03	1.839E-04
2.346E+00	0	2.830E-01	0	2.225E-03	1.846E-04
2.231E+00	0	2.655E-01	0	2.555E-03	1.900E-04
1.920E+00	0	2.259E-01	0	3.113E-03	1.978E-04
1.653E+00	0	1.636E-01	0	3.899E-03	2.071E-04
1.353E+00	0	9.837E-02	0	5.233E-03	2.198E-04
1.003E+00	0	4.068E-02	0	7.124E-03	2.407E-04
8.208E-01	0	2.191E-02	0	8.064E-03	2.896E-04
7.427E-01	0	1.270E-02	0	9.061E-03	3.411E-04
6.081E-01	0	5.995E-03	0	1.042E-02	3.223E-04
4.979E-01	0	1.828E-03	0	1.218E-02	2.755E-04
3.688E-01	0	1.184E-04	0	1.381E-02	5.641E-04
2.972E-01	0	0	0	1.561E-02	7.323E-04
1.832E-01	0	0	0	1.910E-02	1.511E-03
1.111E-01	0	0	0	2.351E-02	5.263E-04
6.738E-02	0	0	0	3.207E-02	4.031E-03
4.087E-02	0	0	0	4.383E-02	4.635E-03
3.183E-02	0	0	0	6.238E-02	2.263E-04
2.606E-02	0	0	0	1.280E-01	2.247E-04
2.418E-02	0	0	0	2.976E-02	2.257E-04
2.188E-02	0	0	0	8.451E-02	2.367E-04
1.503E-02	0	0	0	1.553E-01	8.296E-04
7.102E-03	0	0	0	1.542E-01	1.304E-02
3.355E-03	0	0	0	6.813E-02	1.476E-01
1.585E-03	0	0	0	1.014E-01	9.102E-03
4.540E-04	0	0	0	7.847E-02	8.078E-03
2.144E-04	0	0	0	1.536E-01	8.978E-03
1.013E-04	0	0	0	3.672E-01	1.152E-02
3.727E-05	0	0	0	8.356E-01	1.938E-02
1.068E-05	0	0	0	1.483E+00	3.154E-02
5.043E-06	0	0	0	2.379E+00	4.910E-02
1.855E-06	0	0	0	3.712E+00	7.564E-02
8.764E-07	0	0	0	5.404E+00	1.097E-01
4.140E-07	0	0	0	9.349E+00	1.894E-01
1.000E-07	0	0	0	1.176E+02	2.381E+00

Table A11

Neutron Response Cross Sections Based on Uniform Weighting  
(Continued)

Energy (MeV)	Fe-58 n,g	Co-59 n,g	Cu-63 n,g	In-115 n,g	Au-197 n,g
1.733E+01	1.168E-02	1.500E-03	2.547E-03	1.973E-03	9.686E-03
1.419E+01	5.839E-03	1.533E-03	2.838E-03	2.028E-03	1.029E-02
1.221E+01	1.799E-03	1.646E-03	3.263E-03	1.860E-03	1.113E-02
1.000E+01	8.985E-04	1.754E-03	3.736E-03	2.286E-03	1.196E-02
8.607E+00	9.323E-04	1.851E-03	4.146E-03	3.464E-03	1.271E-02
7.408E+00	1.000E-03	1.948E-03	4.566E-03	6.067E-03	1.368E-02
6.065E+00	1.150E-03	2.126E-03	4.871E-03	1.280E-02	1.483E-02
4.966E+00	1.229E-03	2.410E-03	5.125E-03	2.624E-02	1.677E-02
3.679E+00	1.225E-03	2.884E-03	5.596E-03	5.688E-02	2.384E-02
3.012E+00	1.224E-03	3.105E-03	5.971E-03	7.606E-02	3.155E-02
2.725E+00	1.223E-03	3.261E-03	6.264E-03	8.769E-02	3.855E-02
2.466E+00	1.222E-03	3.455E-03	6.489E-03	9.749E-02	4.443E-02
2.365E+00	1.222E-03	3.510E-03	6.534E-03	9.953E-02	4.566E-02
2.346E+00	1.222E-03	3.559E-03	6.577E-03	1.014E-01	4.679E-02
2.231E+00	1.221E-03	3.914E-03	6.896E-03	1.155E-01	5.455E-02
1.920E+00	1.232E-03	4.754E-03	7.464E-03	1.371E-01	6.418E-02
1.653E+00	1.249E-03	6.211E-03	8.334E-03	1.584E-01	7.251E-02
1.353E+00	1.272E-03	7.661E-03	9.760E-03	1.760E-01	7.973E-02
1.003E+00	1.701E-03	8.354E-03	1.110E-02	1.946E-01	8.845E-02
8.208E-01	2.664E-03	8.375E-03	1.129E-02	1.954E-01	9.684E-02
7.427E-01	2.611E-03	8.038E-03	1.295E-02	1.887E-01	1.084E-01
6.081E-01	2.542E-03	8.488E-03	1.739E-02	1.832E-01	1.290E-01
4.979E-01	2.590E-03	1.037E-02	2.310E-02	1.807E-01	1.595E-01
3.688E-01	2.715E-03	1.209E-02	2.574E-02	1.854E-01	1.964E-01
2.972E-01	2.871E-03	1.396E-02	2.518E-02	2.001E-01	2.340E-01
1.832E-01	3.573E-03	1.916E-02	2.348E-02	2.493E-01	2.807E-01
1.111E-01	4.729E-03	1.376E-02	3.363E-02	3.370E-01	3.377E-01
6.738E-02	6.060E-03	1.295E-02	4.951E-02	4.507E-01	4.394E-01
4.087E-02	7.297E-03	2.333E-02	6.114E-02	5.592E-01	5.362E-01
3.183E-02	5.037E-04	3.326E-02	8.096E-02	6.289E-01	6.084E-01
2.606E-02	5.064E-04	4.495E-02	1.032E-01	6.628E-01	6.488E-01
2.418E-02	5.121E-04	2.885E-02	8.352E-02	6.854E-01	6.771E-01
2.188E-02	7.915E-03	2.845E-02	1.101E-01	7.484E-01	7.725E-01
1.503E-02	2.052E-02	6.791E-02	2.124E-01	9.333E-01	1.220E+00
7.102E-03	2.177E-02	1.760E-01	1.864E-01	1.212E+00	2.201E+00
3.355E-03	5.357E-04	4.830E-02	7.977E-01	1.485E+00	3.444E+00
1.585E-03	9.039E-04	2.702E-02	2.134E+00	2.500E+00	1.059E+01
4.540E-04	1.407E+00	2.563E-01	4.509E-02	6.197E+00	1.521E+01
2.144E-04	7.801E-03	7.682E+01	4.923E-02	6.460E+00	1.169E+01
1.013E-04	1.509E-02	2.899E+00	7.956E-02	9.429E+00	3.701E+01
3.727E-05	3.689E-02	1.761E+00	1.535E-01	8.478E+00	8.601E-01
1.068E-05	6.713E-02	2.399E+00	2.552E-01	5.765E+01	2.988E+02
5.043E-06	1.066E-01	3.546E+00	4.048E-01	7.924E+01	1.233E+03
1.855E-06	1.661E-01	5.352E+00	6.315E-01	4.024E+03	2.495E+01
8.764E-07	2.426E-01	7.705E+00	9.211E-01	1.021E+02	2.581E+01
4.140E-07	4.188E-01	1.324E+01	1.593E+00	7.857E+01	3.772E+01
1.000E-07	5.257E+00	1.660E+02	2.003E+01	7.210E+02	4.370E+02

Table A11

Neutron Response Cross Sections Based on Uniform Weighting  
(Continued)

Energy (MeV)	Th-232 n,g	U-238 n,g	Square Root(E)	Constant	U-234 n,fiss
1.733E+01	4.710E-03	8.230E-04	3.000E-02	1.000E+00	1.990E+00
1.419E+01	5.587E-03	1.109E-03	3.228E-02	1.000E+00	1.866E+00
1.221E+01	6.889E-03	1.637E-03	3.546E-02	1.000E+00	1.805E+00
1.000E+01	8.430E-03	2.347E-03	3.870E-02	1.000E+00	1.955E+00
8.607E+00	1.004E-02	3.196E-03	4.171E-02	1.000E+00	1.958E+00
7.408E+00	1.248E-02	4.629E-03	4.561E-02	1.000E+00	1.647E+00
6.065E+00	1.614E-02	6.954E-03	5.033E-02	1.000E+00	1.327E+00
4.966E+00	2.175E-02	1.119E-02	5.635E-02	1.000E+00	1.295E+00
3.679E+00	3.203E-02	2.018E-02	6.515E-02	1.000E+00	1.390E+00
3.012E+00	3.872E-02	2.638E-02	6.965E-02	1.000E+00	1.404E+00
2.725E+00	4.486E-02	3.233E-02	7.332E-02	1.000E+00	1.422E+00
2.466E+00	5.018E-02	3.735E-02	7.626E-02	1.000E+00	1.447E+00
2.365E+00	5.134E-02	3.839E-02	7.688E-02	1.000E+00	1.453E+00
2.346E+00	5.248E-02	3.943E-02	7.747E-02	1.000E+00	1.459E+00
2.231E+00	6.137E-02	4.781E-02	8.182E-02	1.000E+00	1.492E+00
1.920E+00	7.607E-02	6.131E-02	8.837E-02	1.000E+00	1.461E+00
1.653E+00	9.517E-02	8.008E-02	9.644E-02	1.000E+00	1.312E+00
1.353E+00	1.258E-01	1.045E-01	1.081E-01	1.000E+00	1.174E+00
1.003E+00	1.611E-01	1.214E-01	1.238E-01	1.000E+00	1.167E+00
8.208E-01	1.720E-01	1.216E-01	1.335E-01	1.000E+00	1.213E+00
7.427E-01	1.778E-01	1.167E-01	1.438E-01	1.000E+00	9.628E-01
6.081E-01	1.797E-01	1.107E-01	1.588E-01	1.000E+00	6.124E-01
4.979E-01	1.790E-01	1.078E-01	1.820E-01	1.000E+00	3.293E-01
3.688E-01	1.782E-01	1.126E-01	2.074E-01	1.000E+00	1.643E-01
2.972E-01	1.831E-01	1.284E-01	2.406E-01	1.000E+00	7.507E-02
1.832E-01	2.182E-01	1.623E-01	3.124E-01	1.000E+00	3.228E-02
1.111E-01	2.947E-01	2.113E-01	4.063E-01	1.000E+00	2.239E-02
6.738E-02	3.893E-01	3.311E-01	5.167E-01	1.000E+00	1.828E-02
4.087E-02	4.328E-01	4.089E-01	6.272E-01	1.000E+00	1.608E-02
3.183E-02	4.860E-01	4.547E-01	7.029E-01	1.000E+00	1.464E-02
2.606E-02	5.137E-01	4.809E-01	7.438E-01	1.000E+00	1.402E-02
2.418E-02	5.321E-01	4.970E-01	7.727E-01	1.000E+00	1.366E-02
2.188E-02	5.839E-01	5.474E-01	8.621E-01	1.000E+00	1.277E-02
1.503E-02	7.447E-01	7.010E-01	1.166E+00	1.000E+00	1.051E-02
7.102E-03	1.080E+00	1.060E+00	1.757E+00	1.000E+00	7.915E-03
3.355E-03	1.612E+00	1.470E+00	2.378E+00	1.000E+00	3.946E-03
1.585E-03	3.021E+00	2.852E+00	4.113E+00	1.000E+00	4.660E-05
4.540E-04	8.436E+00	4.646E+00	6.710E+00	1.000E+00	0
2.144E-04	1.481E+01	1.875E+01	9.764E+00	1.000E+00	0
1.013E-04	1.772E+01	3.019E+01	1.520E+01	1.000E+00	0
3.727E-05	3.222E+01	7.328E+01	2.681E+01	1.000E+00	0
1.068E-05	1.353E-01	1.732E+02	4.376E+01	1.000E+00	0
5.043E-06	3.064E-01	7.103E-01	6.812E+01	1.000E+00	0
1.855E-06	7.039E-01	5.023E-01	1.050E+02	1.000E+00	0
8.764E-07	1.247E+00	6.211E-01	1.523E+02	1.000E+00	0
4.140E-07	2.458E+00	9.914E-01	2.628E+02	1.000E+00	0
1.000E-07	3.327E+01	1.199E+01	3.304E+03	1.000E+00	0

Table A11

Neutron Response Cross Sections Based on Uniform Weighting  
(Continued)

Energy (MeV)	U-236 n,fiss	Pu-240 n,fiss	Pu-241 n,fiss	Pu-242 n,fiss
1.733E+01	1.634E+00	2.253E+00	2.609E+00	1.932E+00
1.419E+01	1.660E+00	2.206E+00	2.427E+00	1.875E+00
1.221E+01	1.745E+00	2.057E+00	2.241E+00	1.883E+00
1.000E+01	1.824E+00	2.083E+00	2.285E+00	1.936E+00
8.607E+00	1.719E+00	1.877E+00	2.215E+00	1.970E+00
7.408E+00	1.261E+00	1.523E+00	1.906E+00	1.976E+00
6.065E+00	8.579E-01	1.489E+00	1.529E+00	1.829E+00
4.966E+00	8.584E-01	1.566E+00	1.513E+00	1.746E+00
3.679E+00	8.491E-01	1.667E+00	1.556E+00	1.705E+00
3.012E+00	8.467E-01	1.679E+00	1.610E+00	1.634E+00
2.725E+00	8.699E-01	1.593E+00	1.665E+00	1.523E+00
2.466E+00	8.789E-01	1.583E+00	1.698E+00	1.458E+00
2.365E+00	8.785E-01	1.593E+00	1.703E+00	1.448E+00
2.346E+00	8.761E-01	1.602E+00	1.706E+00	1.439E+00
2.231E+00	8.416E-01	1.646E+00	1.730E+00	1.391E+00
1.920E+00	7.579E-01	1.639E+00	1.764E+00	1.324E+00
1.653E+00	6.889E-01	1.666E+00	1.740E+00	1.366E+00
1.353E+00	5.686E-01	1.677E+00	1.669E+00	1.495E+00
1.003E+00	2.789E-01	1.313E+00	1.519E+00	1.166E+00
8.208E-01	1.136E-01	1.071E+00	1.476E+00	8.417E-01
7.427E-01	2.577E-02	8.542E-01	1.497E+00	5.900E-01
6.081E-01	2.739E-04	5.730E-01	1.504E+00	3.318E-01
4.979E-01	0	2.389E-01	1.545E+00	1.536E-01
3.688E-01	0	1.431E-01	1.629E+00	8.315E-02
2.972E-01	0	1.062E-01	1.738E+00	5.204E-02
1.832E-01	0	8.027E-02	1.987E+00	3.200E-02
1.111E-01	0	6.102E-02	2.211E+00	2.950E-02
6.738E-02	0	6.492E-02	2.443E+00	3.758E-02
4.087E-02	0	8.358E-02	2.524E+00	4.396E-02
3.183E-02	0	8.460E-02	2.622E+00	4.749E-02
2.606E-02	0	8.433E-02	2.673E+00	4.928E-02
2.418E-02	0	8.397E-02	2.704E+00	5.051E-02
2.188E-02	0	8.217E-02	2.832E+00	5.451E-02
1.503E-02	0	7.115E-02	3.520E+00	3.554E-02
7.102E-03	0	1.289E-01	5.515E+00	0
3.355E-03	0	2.685E-01	7.485E+00	0
1.585E-03	0	2.609E-01	1.259E+01	0
4.540E-04	0	2.188E-01	2.346E+01	0
2.144E-04	0	3.237E-01	3.061E+01	0
1.013E-04	0	4.683E-01	4.249E+01	0
3.727E-05	0	1.005E-01	1.083E+02	0
1.068E-05	0	7.037E-04	2.458E+02	0
5.043E-06	0	3.196E-03	9.555E+01	0
1.855E-06	0	2.038E+00	2.921E+01	0
8.764E-07	0	8.252E-02	5.491E+01	0
4.140E-07	0	3.061E-02	8.186E+02	0
1.000E-07	0	2.484E-01	4.471E+03	0



Section A3  
COMPARISONS WITH OTHER CROSS SECTION SETS

Several cross section sets that have been used for pressure vessel fluence calculations were described in the Introduction of this report. It is useful to provide some comparisons of calculations of neutron spectra obtained using the SAILOR library with similar calculations using the older cross section libraries. In particular, both the DNA (37n,21g) and CASK (22n,18g) cross section libraries were selected as points of comparison. These libraries were selected primarily because of their use in previous studies of fluence calculation and photofission effects on foil threshold dosimetry.

In making these comparisons, we have performed calculations using the reference models that were described previously. Also, the power distributions and material densities used in these calculations were identical to those in the SAILOR cross section preparation activity. The single exceptions to this consistency of parameters is the zirconium in the fuel. For the DNA library, which does not have cross section data for zirconium, we substituted a small amount of iron for the zirconium. It has been our experience that this approximation makes little difference in the neutron spectrum prediction for the situation analyzed.

The comparisons are presented for the PWR case and it is noted that a similar analysis has been made for the BWR and the results are comparable. The data were presented for eight locations, which represent a range of spectra changes both in intensity and shape. These results are given in Figures A8 through A15.

Starting at the center of the reactor core, we note that SAILOR predicts higher values for spectral components than does either the 22 or 37 group cross set. This trend continues down into the thermal range, with the SAILOR library producing a harder spectrum. This trend is most reflective of the treatment used in resonance self-shielding in SAILOR, where none existed in the CASK or DNA library. The SAILOR library and CASK library calculated intensities are in quite good agreement out to the pressure vessel surface, where the CASK results are higher. Note, however, that the spectral shapes calculated by both cross

section sets are in good agreement. Thus, we would conclude that predicted values obtained using SAILOR, at the pressure vessel and beyond would have a generally lower intensity than those obtained from CASK. This trend is primarily due to the lack of adequate energy group resolution of important minima in the CASK library.

For the DNA library, the trend is to be lower than the SAILOR results yet to predict spectral shapes that are equivalent. This trend is likely due to the lack of resonance self shielding for the DNA library.

Using these results, the user of SAILOR should be able to estimate the differences that would be expected between SAILOR and the CASK or DNA library. It is felt, however, that the SAILOR library should provide a state-of-the-art cross section library for application to light water reactor radiation transport calculations. In fact, the BUGLE-80 library (15), which was derived from VITAMIN-C using the concrete spectrum (see Table A4), has the same group structure as has been designated as conforming to ANS 6.1.2 proposed Standard (16) for cross sections for radiation protection calculations at nuclear power plants.

The SAILOR library is available from RSIC as DLC-76/SAILOR.

Section A4

REFERENCES

1. E. A. Straker, G. W. Morrison, and R. H. Odegaarden, "A Coupled Neutron and Gamma-Ray Cross Section Library for Use in Shielding Calculations," *Trans. Am. Nuc. Soc.* 15, 535, 1972. Available from RSIC as DLC-23/CASK.
2. W. E. Ford III and D. H. Wallace, "POPOP4, A Code for Converting Gamma Ray Spectra to Secondary Gamma-Ray Production Cross Sections," CTC-12, 1960.
3. G. L. Simmons and M. L. Gritzner, "Neutron and Gamma-Ray Distributions In and Around a Large Power Reactor During Normal Operations," *Trans. Am. Nuc. Soc.*, 558, 1973.
4. D. Garber, Compiler, "ENDF/B Summary Documentation," BNL 17541 (ENDF-201), Second Edition, ENDF/B-IV, 1975.
5. D. E. Bartine, et al., "Production and Testing of the DNA Few Group Cross Section Library," ORNL/TM/4840, 1975. Available from RSIC as DLC-1/FEWG1.
6. W. E. Ford III, et al., "A 218-Group Neutron Cross Section Library in the AMPX Master Interface format for Criticality Safety Studies," ORNL/CSD/TM-4, 1976. Available from RSIC as DLC-43/CSRL.
7. J. A. Bucholz, "SCALE: A Modular Code System for Performing Standardized Computer Analyses for Licensing Evaluation," NUREG/CR-0200, ORNL/NUREG/CSD-2, Vol. I (to be published).
8. R. J. Barrett and R. E. MacFarlane, "Coupled Neutron and Photon Cross Sections for Transport Calculations," LA-7808-MS, 1979. Available from RSIC as DLC-36B/CLAW-IV.
9. "BUGLE Coupled 45 Neutron, 16 Gamma-Ray,  $P_3$ , Cross Sections for Studies by the ANSI 6.1.2 Shielding Standards Working Group on Multigroup Cross Sections, Informal Notes," 1977. Available from RSIC as DLC-47/BUGLE.
10. R. W. Roussin, et al., "VITAMIN-C: The CTR Processed Multigroup Cross Section Library for Neutronics Studies," ORNL-RSIC-37, 1980. Available from RSIC as DLC-41/VITAMIN-C.
11. N. M. Greene, et al., "AMPX: A Modular Code System for Generating Multigroup Neutron Gamma Libraries from ENDF/B," ORNL-TM-3706, 1976. Available from RSIC as PSR-63/AMPX-II.
12. J. T. West, et al., "Developing an ANS Coupled Cross-Section Standard for Concrete Shielding," *Trans. Am. Nuc. Soc.* 28, 642, 1978.

13. R. W. Roussin, et al., "Comparison of Several Multigroup Libraries for LWR Shielding Problems," Trans. Am. Nuc. Soc. 32, 644, 1979.
14. G. L. Simmons, et al., "PWR and BWR Radiation Environments for Radiation Damage Studies," EPRI NP-152, September 1977.
15. R. W. Roussin, "BUGLE-80, Coupled 47-Neutron, 20-Gamma-Ray,  $P_3$ , Cross Section Library for LWR Shielding Calculations," Informal Notes, 1980. Available from RSIC as DLC-75/BUGLE-80.
16. D. R. Harris, Chairman, "Neutron and Gamma-Ray Cross Sections for Nuclear Radiation Protection Calculations for Nuclear Power Plants," ANSI/ANS 6.1.2 proposed Standard.

Section A5  
BIBLIOGRAPHY

Barrett, R. J. and R. E. MacFarlane, "Coupled Neutron and Photon Cross Sections for Transport Calculations," LA-7808-MS, 1979. Available from RSIC as DLC-36B/CLAW-IV.

Bartine, D. E., et al., "Production and Testing of the DNA Few Group Cross Section Library," ORNL/TM/4840, 1975. Available from RSIC as DLC-1/FEWG1.

Bucholz, J. A., "SCALE: A Modular Code System for Performing Standardized Computer Analyses for Licensing Evaluation," NUREG/CR-0200, ONRL/NUREG/CSD-2, Vol. I (to be published).

"BUGLE Coupled 45 Neutron, 16 Gamma-Ray,  $P_3$ , Cross Sections for Studies by the ANSI 6.1.2 Shielding Standards Working Group on Multigroup Cross Sections, Informal Notes," 1977. Available from RSIC as DLC-47/BUGLE.

Ford, W. E. III, et al., "A 218-Group Neutron Cross Section Library in the AMPX Master Interface format for Criticality Safety Studies," ORNL/CSD/TM-4, 1976. Available from RSIC as DLC-43/CSRL.

Ford, W. E. III and D. H. Wallace, "POPOP4, A Code for Converting Gamma Ray Spectra to Secondary Gamma-Ray Production Cross Sections," CTC-12, 1960.

Garber, D., Compiler, "ENDF/B Summary Documentation," BNL 17541 (ENDF-201), Second Edition, ENDF/B-IV, 1975.

Greene, N. M., et al., "AMPX: A Modular Code System for Generating Multigroup Neutron Gamma Libraries from ENDF/B," ORNL-TM-3706, 1976. Available from RSIC as PSR-63/AMPX-II.

Harris, D. R., Chairman, "Neutron and Gamma-Ray Cross Sections for Nuclear Radiation Protection Calculations for Nuclear Power Plants," ANSI/ANS 6.1.2 proposed Standard.

Roussin, R. W., et al., "VITAMIN-C: The CTR Processed Multigroup Cross Section Library for Neutronics Studies," ORNL-RSIC-37, 1980. Available from RSIC as DLC-41/VITAMIN-C.

Roussin, R. W., et al., "Comparison of Several Multigroup Libraries for LWR Shielding Problems," Trans. Am. Nuc. Soc. 32, 644, 1979.

Roussin, R. W., "BUGLE-80, Coupled 47-Neutron, 20-Gamma-Ray,  $P_3$ , Cross Section Library for LWR Shielding Calculations," Informal Notes, 1980. Available from RSIC as DLC-75/BUGLE-80.

Simmons, G. L. and M. L. Gritzner, "Neutron and Gamma-Ray Distributions In and Around a Large Power Reactor During Normal Operations," Trans. Am. Nuc. Soc., 558, 1973.

Simmons, G. L., et al., "PWR and BWR Radiation Environments for Radiation Damage Studies," EPRI NP-152, September 1977.

Straker, E. A., G. W. Morrison, and R. H. Odegaarden, "A Coupled Neutron and Gamma-Ray Cross Section Library for Use in Shielding Calculations," Trans. Am. Nuc. Soc. 15, 535, 1972. Available from RSIC as DLC-23/CASK.

West, J. T., et al., "Developing an ANS Coupled Cross-Section Standard for Concrete Shielding," Trans. Am. Nuc. Soc. 28, 642, 1978.

Appendix B

AMPX-II JOB STREAMS USED TO  
GENERATE THE SAILOR LIBRARY

```

// ONE EXEC AMPX,GOSIZE=270K,GOTIME=01,SBUF=8148
//GO.FT18F001 DD UNIT=SYSDA,SPACE=(TRK,(1500,50))
//* MASTER NEUTRON LIBRARY
//GO.FT72F001 DD UNIT=3330,VOL=SER=ZX0000,DISP=SHR,
// DSN=JEW.AMPXR2.LIB171N
//* SMALLER NEUTRON LIBRARY
//GO.FT78F001 DD UNIT=3330,VOL=SER=ZX5555,DISP=(NEW,KEEP),
// SPACE=(TRK,(500,100),RLSE),DSN=HEC.GLS.LIB171,
// DCB=(RECFM=VBS,LRECL=X,BLKSIZE=6447,BUFL=8148)
//GO.SYSIN DD *
=AJAX
' GET NEUTRONS OFF OF THE MASTER TAPE
O$$ 78 72 1$$ 1 T
2$$ 72 17 T
3$$ 1269 1273 1276 1191 1192 1190 7141 1261 9262
    1197 1274 1156 1280 1193 1194 1150 1195 T
/*
//TWO EXEC AMPX,GOTIME=08,GOSIZE=550K,SBUF=8148
//GO.FT18F001 DD SPACE=(TRK,(900,60))
//* 171,36 (N,G) MASTER INTERFACE
//GO.FT60F001 DD UNIT=3330,VOL=SER=ZX0000,DSN=JEW.AMPXR2.LIB171NG,
// DCB=(RECFM=VBS,LRECL=X,BLKSIZE=6447,BUFL=8148),DISP=SHR
//* 36 (G) MASTER INTERFACE
//GO.FT61F001 DD UNIT=3330,VOL=SER=ZX0000,DSN=JEW.AMPX0.LIB36G,
// DCB=(RECFM=VBS,LRECL=X,BLKSIZE=6447,BUFL=8148),DISP=SHR
//* 171 (N) MASTER INTERFACE
//GO.FT62F001 DD UNIT=3330,VOL=SER=ZX5555,DSN=HEC.GLS.LIB171,
// DCB=(RECFM=VBS,LRECL=X,BLKSIZE=6447,BUFL=8148),DISP=SHR
//* -----
//* TEMPORARY WORKING STORAGE FOR CHOX WHILE MAKING LIBRARY
//GO.FT70F001 DD UNIT=SYSDA,DSN=&&GLS1,
// DISP=(NEW,PASS),SPACE=(TRK,(500,50)),
// DCB=(RECFM=VBS,LRECL=X,BLKSIZE=6447,BUFL=8148)
//GO.FT71F001 DD UNIT=SYSDA,DSN=&&GLS2,
// DISP=(NEW,PASS),SPACE=(TRK,(500,50)),
// DCB=(RECFM=VBS,LRECL=X,BLKSIZE=6447,BUFL=8148)
//GO.FT72F001 DD UNIT=SYSDA,DSN=&&GLS3,
// DISP=(NEW,PASS),SPACE=(TRK,(500,50)),
// DCB=(RECFM=VBS,LRECL=X,BLKSIZE=6447,BUFL=8148)
//GO.FT73F001 DD UNIT=SYSDA,DSN=&&GLS4,
// DISP=(NEW,PASS),SPACE=(TRK,(500,50)),
// DCB=(RECFM=VBS,LRECL=X,BLKSIZE=6447,BUFL=8148)
//GO.FT74F001 DD UNIT=SYSDA,DSN=&&GLSHB,
// DISP=(NEW,PASS),SPACE=(TRK,(510,50)),
// DCB=(RECFM=VBS,LRECL=X,BLKSIZE=6447,BUFL=8148)
//* WORKING INTERFACE IN AMPX FORMAT.....
//GO.FT75F001 DD UNIT=TAPE62,DISP=(NEW,PASS),LABEL=(4,SL),
// DCB=(RECFM=VBS,LRECL=X,BLKSIZE=6447,BUFL=8148,DEN=4),
// VOL=SER=X23004,DSN=GLS.LWR.MASTER
//* TEMPORARY WORKING STORAGE FOR BONAMI WHILE MAKING LIBRARY

```

```

//GO.FT81F001 DD UNIT=SYSDA,DSN=&&GLSGLS1,
// DISP=(NEW,PASS),SPACE=(TRK,(500,100)),
// DCB=(RECFM=VBS,LRECL=X,BLKSIZE=6447,BUFL=8148)
//GO.FT82F001 DD UNIT=SYSDA,DSN=&&GLSGLS2,
// DISP=(NEW,PASS),SPACE=(TRK,(500,100)),
// DCB=(RECFM=VBS,LRECL=X,BLKSIZE=6447,BUFL=8148)
//GO.FT83F001 DD UNIT=SYSDA,DSN=&&GLSGLS3,
// DISP=(NEW,PASS),SPACE=(TRK,(500,100)),
// DCB=(RECFM=VBS,LRECL=X,BLKSIZE=6447,BUFL=8148)
//GO.FT84F001 DD UNIT=SYSDA,DSN=&&GLSGLS4,
// DISP=(NEW,PASS),SPACE=(TRK,(500,100)),
// DCB=(RECFM=VBS,LRECL=X,BLKSIZE=6447,BUFL=8148)
//GO.SYSIN DD *
=BONAMI
'      PWR FUEL CELL FROM RESAR..WESTINGHOUSE PLANT
0$$ 62 0 18 81
1$$  2  3 10  1  1  2   2**  0.001  1.0  T
3$$ 3R3 4R2 3R1 4$$ 1269 1273 1276 1191 1192 1190 7141 1261 9262 1276
5** 4.714-2 4.2-6 2.357-2   7.64-5 1.45-4 8.77-4 4.27-2
      6.325-4 2.166-2 4.465-2
6$$ 1 2 3
7** 0.41783 0.47498 0.71079
8** 921 672 583
10$$ 8I 10 100 11$$ 0 1 1  T  T
=BONAMI
'      BWR FUEL CELL FROM GESAR 238 GENERAL ELECTRIC
0$$ 62 0 18 82
1$$  2  3  9  1  1  2   2**  0.001  1.0  T
3$$ 2R3 4R2 3R1 4$$ 1269 1276 1191 1192 1190 7141 1261 9262 1276
'      MID PLANE OF REACTOR VOID FRACTION OF 50% IS USED IN WATER
5** 2.475-2 1.2375-2   7.64-5 1.45-4 8.77-4 4.27-2
      4.959-4 2.177-2 4.455-2
6$$ 1 2 3
7** 0.53213 0.6134 0.9174
8** 921 672 551
10$$ 7I 110 190      11$$ 0 1 1  T  T
=BONAMI
'      INFINITE MEDIUM COLLAPSE FOR IRON-WATER MIXTURE
0$$ 62 0 18 83 1$$ 0 1 6 1 1 0 T
3$$ F1
4$$ 1269 1276 1191 1197 1192 1190
'      H      O      CR      MN      FE      NI
5** 1.1785-2 5.8925-3
      1.305-2 1.14-3 4.3725-2 6.4125-2
6$$ 1
7** 10.0
8** 590
10$$ 4I 1400 1900
11$$ 1      T  T
=BONAMI
'      INFINITE MEDIUM COLLAPSE FOR CONCRETE TYPE 04
0$$ 62 0 18 84 1$$ 0 1 10 1 1 0 T
3$$ F1
4$$ 1269 1274 1276 1156 1280 1193
'      H      C      O      NA      MG      AL

```

```

      1194 1150 1195 1192
'      SI      K      CA      FE
5** 8.6-3 1.15-4 4.33-2 9.64-4 1.24-4 1.74-4
      1.66-3 4.6-4 1.5-3 3.45-4
6$$ 1
7** 100.0
8** 300
10$$$ 8I 2000 2900
11$$$ 1          T T
=CHOX
' CREAT INITIAL COUPLED LIBRARY ON LOGICAL 70 WESTINGHOUSE PWR
0$$ 81 60 61 70 E      1$$ 10 0 T
2$$ 8I 10 100 3$$ 1269 1273 1276 1191 1192 1190 7141 1261 1262 1276
4$$ 1 5 8 24 26 28 40 92 92 8 5$$ 8I 10 100 T
=CHOX
' CREATE COUPLE LIBRARY ON LOGICAL 71 GENERAL ELECTRIC BWR
0$$ 82 60 61 71 E      1$$ 3 0 T
2$$ 1I 170 190 3$$ 1261 1262 1276
4$$ 92 92 8 5$$ 110 120 130 T
=CHOX
' CREATE COUPLED LIBRARY ON LOGICAL 72 WATER+STEEL
0$$ 83 60 61 72 E      1$$ 6 0 T
2$$ 4I 1400 1900
3$$ 1269 1276 1191 1197 1192 1190
4$$ 1 8 24 25 26 28
5$$ 4I 200 250 T
=CHOX
' CREATE COUPLED LIBRARY ON LOGICAL 73 CONCRETE FINAL LIBRARY
0$$ 84 60 61 73 E      1$$ 10 0 T
2$$ 8I 2000 2900
3$$ 1269 1274 1276 1156 1280 1193 1194 1150 1195 1192
4$$ 1 6 8 11 12 13 14 19 20 26
5$$ 8I 300 390 T
=CHOX
' CREATE COUPLED LIBRARY ON LOGICAL 74 BOUND H
0$$ 62 60 61 74 E 1$$ 1 0 T
2$$ 1269 3$$ 1269 4$$ 1 5$$ 1269 T
=AJAX
' COPY EVERYTHING FROM UNITS 70,71,72,73, AND 74 TO UNIT 75
0$$ 75 70 1$$ 5 T
2$$ 74 0 T
2$$ 70 0 T
2$$ 71 0 T
2$$ 72 0 T
2$$ 73 0 T
/*
//THREE EXEC AMPX,GOTIME=02,GOSIZE=570K,SBUF=8148
//GO.FT18F001 DD SPACE=(TRK,(900,60))
/* WORKING INTERFACE IN AMPX FORMAT.....
//GO.FT75F001 DD UNIT=TAPE62,DISP=(OLD,PASS),LABEL=(4,SL),
// DCB=(RECFM=VBS,LRECL=X,BLKSIZE=6447,BUFL=8148,DEN=4),
// VOL=SER=X23004,DSN=GLS.LWR.MASTER
/* FILE 76 IS THE XSDRNPM LIBRARY FROM NITAWL
//GO.FT76F001 DD UNIT=3330,DISP=(NEW,KEEP),VOL=SER=ZX5555,
// DCB=(RECFM=VBS,LRECL=X,BLKSIZE=6447,BUFL=8148),

```

```

// DSN=X.HEC15758.XSDRN.GLS,SPACE=(TRK,(100,100),RLSE)
//*
//GO.SYSIN DD *
=NITAWL
' XSDRN LIBRARY WILL BE PRODUCED ON UNIT 76
0$$ 75 A4 76 E 1$$ A2 30 A11 -1 E T
2$$ 1269 111 10 130 4I 200 250 8I 300 390 T
/*
//FOUR EXEC AMPX,GOTIME=12,GOSIZE=770K,SBUF=8148
//* FILE 03 IS A WEIGHTED WORKING LIBRARY FROM XSDRNPM
//GO.FT03F001 DD UNIT=TAPE62,DISP=(NEW,KEEP),LABEL=(5,SL),
// DCB=(RECFM=VBS,LRECL=X,BLKSIZE=6447,DEN=4),
// DSN=X.RWR15758.PWR1,VOL=SER=X23004
//* FILE 04 IS THE XSDRNPM LIBRARY FROM NITAWL
//GO.FT04F001 DD UNIT=3330,DISP=SHR,VOL=SER=ZX5555,
// DCB=(RECFM=VBS,LRECL=X,BLKSIZE=6447),
// DSN=X.HEC15758.XSDRN.GLS
//GO.FT08F001 DD SPACE=(3520,610)
//GO.FT09F001 DD SPACE=(3520,540)
//GO.FT10F001 DD SPACE=(1680,1040)
//* FILE 16 IS THE ANGULAR FLUXES FROM XSDRN CALCULATION
//GO.FT16F001 DD UNIT=TAPE62,VOL=SER=X23285,
// LABEL=(1,SL),DISP=(NEW,KEEP),
// DSN=PWR171.ANG.FLUX,
// DCB=(RECFM=VBS,LRECL=X,BLKSIZE=6447,DEN=4)
//GO.SYSIN DD *
=XSDRNPM
EPRI NP-152 PWR PROBLEM NO PADS 3425 MWT FLAT POWER DIST.
1$$ 2 8 84 1 0
5 33 8 3 0
25 1 0 0 3
2$$ -2 0 0 E
3$$ 1 1 0 0 0
0 0 1 0 0
0 0
4$$ 0 67 0 -2 3
4 70 -1 0
5** 0.001 0.001 7.2676E+17 2Z
1.420892 4Z
0.001 0.75 T
13$$ 8R1 3R2 6R3 6R4 10R5
' FUEL WATER SS304 A533B CONCRETE
14$$ 1269 20 30 70 50 80 90 100
1269 20 210
310 360 220 230 240 250 1Q6
1269 7I 310 390
15** 2.768-2 2.466-6 1.384-2 4.257-3 1.444-5 1.903-4 6.515-3 1.343-2
4.714-2 4.200-6 2.357-2
2.37-4 8.93-4 1.74-2 1.52-3 5.83-2 8.55-3
9.81-4 3.71-4 1.27-4 1.12-3 8.19-2 4.44-4
7.77-3 1.15-4 4.38-2 1.05-3 1.48-4 2.39-3 1.58-2 6.93-4 2.92-3 3.13-4
T
30$$ 15R1 FO
31**
8.196-6 1.407-5 2.346-5 1.676-5 2.120-5 2.669-5 3.318-5 9.212-5

```

1.379-4 2.022-4 2.892-4 4.059-4 5.583-4 7.525-4 9.963-4 1.297-3  
 1.660-3 2.092-3 2.597-3 3.179-3 3.839-3 1.440-3 3.137-3 5.390-3  
 6.274-3 7.224-3 8.229-3 9.282-3 1.037-2 1.148-2 2.632-2 3.072-2  
 3.482-2 1.880-2 1.965-2 2.040-2 2.106-2 2.164-2 2.212-2 1.496-2  
 3.787-3 3.769-3 7.580-3 1.523-2 2.300-2 2.310-2 2.312-2 2.306-2  
 2.290-2 2.266-2 2.237-2 2.202-2 2.162-2 2.111-2 2.066-2 2.006-2  
 1.953-2 1.890-2 3.591-2 1.422-2 1.912-2 1.568-2 1.503-2 1.438-2  
 1.373-2 1.310-2 1.248-2 1.188-2 1.128-2 1.071-2 1.015-2 9.643-3  
 9.099-3 1.672-2 1.488-2 6.804-3 6.405-3 1.168-2 1.031-2 1.110-3  
 4.150-4 8.539-4 2.305-3 4.395-3 7.978-3 3.614-3 3.382-3 3.164-3  
 2.960-3 2.765-3 2.584-3 2.417-3 2.253-3 2.107-3 1.962-3 1.834-3  
 1.708-3 1.595-3 1.487-3 1.383-3 1.291-3 2.853-3 2.386-3 8.013-4  
 5.874-4 1.426-3 8.464-4 1.879-3 6.696-4 9.652-4 8.036-4 9.037-4  
 3.215-4 4.130-4 1.789-4 1.100-4 1.452-4 6.873-5 6.624-5 1.846-4  
 2.654-4 4.036-4 2.781-4 1.916-4 1.319-4 9.077-5 6.245-5 2.768-5  
 1.528-5 1.316-5 1.132-5 5.056-6 4.693-6 8.395-6 7.227-6 1.397-5  
 9.602-6 6.601-6 4.538-6 3.119-6 2.144-6 1.474-6 1.013-6 6.962-7  
 4.784-7 3.290-7 2.260-7 1.553-7 1.067-7 7.339-8 5.044-8 3.396-8  
 2.453-8 1.638-8 1.125-8 7.737-9 5.317-9 3.654-9 2.512-9 1.727-9  
 1.186-9 8.27-10 5.49-10 3.85-10 2.65-10 1.82-10 1.25-10 8.59-11  
 5.91-11 1.14-10 1.54-11 F0

T

33\*\* F0

T

35\*\* 3I 0 4I 120 5I 151.66 2I 168.51 7I 171.40  
 4I 187.96 4I 193.68 9I 200.66 14I 219.71 241.62  
 242 259.5 8I 260 10I 275 300

36\$\$ 15R1 3R2 8R3 5R4 15R5 15R6 3R7 20R8

38\*\* 61R 1 3R 1.0-10 F1

39\$\$ 1 3 2 3 2 4 2 5

40\$\$ F3

51\$\$ 5R1 4R2 4R3 3R4 3R5 5R6 4R7 4R8 3R9 2R10  
 2R11 2R12 13 2R14 3R15 3R16 4R17 5R18 4R19 2R20  
 4R21 4R22 4R23 4R24 10R25 10R26 6R27 4R28 2R29 3R30  
 2R31 2R32 2R33 3R34 4R35 7R36 5R37 3R38 3R39 4R40  
 5R41 3R42 4R43 3R44 3R45 46 47  
 2R48 49 2R50 2R51 2R52 2R53 2R54 2R55 2R56 2R57  
 58 59 60 4R61 2R62 2R63 2R64 2R65 66 67 T T

//

//FIVE EXEC AMPX,GOTIME=20,GOSIZE=980K,SBUF=8148  
 /\*\* FILE 03 IS A WEIGHTED WORKING LIBRARY FROM XSDRNPM  
 //GO.FT03F001 DD UNIT=TAPE62,DISP=(NEW,KEEP),LABEL=(6,SL),  
 // DCB=(RECFM=VBS,LRECL=X,BLKSIZE=6447,DEN=4),  
 // DSN=X.RWR15758.BWR1,VOL=SER=X23004  
 /\*\* FILE 04 IS THE XSDRNPM LIBRARY FROM NITAWL  
 //GO.FT04F001 DD UNIT=3330,DISP=SHR,VOL=SER=ZX5555,  
 // DCB=(RECFM=VBS,LRECL=X,BLKSIZE=6447),  
 // DSN=X.HEC15758.XSDRN.GLS  
 //GO.FT08F001 DD SPACE=(3520,610)  
 //GO.FT09F001 DD SPACE=(3520,540)  
 //GO.FT10F001 DD SPACE=(1680,1040)  
 /\*\* FILE 16 IS THE ANGULAR FLUXES FROM XSDRN CALCULATION  
 //GO.FT16F001 DD UNIT=TAPE62,VOL=SER=X23285,  
 // LABEL=(2,SL),DISP=(NEW,KEEP),  
 // DSN=BWR171.ANG.FLUX,

// DCB=(RECFM=VBS,LRECL=X,BLKSIZE=6447,DEN=4)

//GO.SYSIN DD \*

=XSDRNPM

EPRI NP-152 BWR PROBLEM 3579 MWT GESAR 238" CORE MIDPLANE 50% VOID

1\$\$ 2 7 87 1 0

5 31 8 3 0

25 1 0 0 3

2\$\$ -2 0 0 E

3\$\$ 1 1 0 0 0

0 0 1 0 0

0 0

4\$\$ 0 67 0 -2 3

4 70 -1 0

5\*\* 0.001 0.001 7.46419E+17 2Z

1.420892 4Z

0.001 0.75 T

13\$\$ 7R1 2R2 6R3 6R4 10R5

' FUEL WATER SS304 A533B CONCRETE

14\$\$ 1269 30 70 50 110 120 130

1269 210

310 360 220 230 240 250 1Q6

1269 7I 310 390

15\*\* 1.5354-2 7.677-3 5.7645-3 2.003-5

1.2125-4 5.322-3 1.0884-2

' FUEL MIXTURE ABOVE IS WATER(H+O),ZIRC(ZR+FE) & UO2( 235+238+O)

4.950-2 2.475-2

2.37-4 8.93-4 1.74-2 1.52-3 5.83-2 8.55-3

9.81-4 3.71-4 1.27-4 1.12-3 8.19-2 4.44-4

7.77-3 1.15-4 4.38-2 1.05-3 1.48-4 2.39-3 1.58-2 6.93-4 2.92-3 3.13-4

T

30\$\$ 15R1 FO

31\*\*

8.196-6 1.407-5 2.346-5 1.676-5 2.120-5 2.669-5 3.318-5 9.212-5

1.379-4 2.022-4 2.892-4 4.059-4 5.583-4 7.525-4 9.963-4 1.297-3

1.660-3 2.092-3 2.597-3 3.179-3 3.839-3 1.440-3 3.137-3 5.390-3

6.274-3 7.224-3 8.229-3 9.282-3 1.037-2 1.148-2 2.632-2 3.072-2

3.482-2 1.880-2 1.965-2 2.040-2 2.106-2 2.164-2 2.212-2 1.496-2

3.787-3 3.769-3 7.580-3 1.523-2 2.300-2 2.310-2 2.312-2 2.306-2

2.290-2 2.266-2 2.237-2 2.202-2 2.162-2 2.111-2 2.066-2 2.006-2

1.953-2 1.890-2 3.591-2 1.422-2 1.912-2 1.568-2 1.503-2 1.438-2

1.373-2 1.310-2 1.248-2 1.188-2 1.128-2 1.071-2 1.015-2 9.643-3

9.099-3 1.672-2 1.488-2 6.804-3 6.405-3 1.168-2 1.031-2 1.110-3

4.150-4 8.539-4 2.305-3 4.395-3 7.978-3 3.614-3 3.382-3 3.164-3

2.960-3 2.765-3 2.584-3 2.417-3 2.253-3 2.107-3 1.962-3 1.834-3

1.708-3 1.595-3 1.487-3 1.383-3 1.291-3 2.853-3 2.386-3 8.013-4

5.874-4 1.426-3 8.464-4 1.879-3 6.696-4 9.652-4 8.036-4 9.037-4

3.215-4 4.130-4 1.789-4 1.100-4 1.452-4 6.873-5 6.624-5 1.846-4

2.654-4 4.036-4 2.781-4 1.916-4 1.319-4 9.077-5 6.245-5 2.768-5

1.528-5 1.316-5 1.132-5 5.056-6 4.693-6 8.395-6 7.227-6 1.397-5

9.602-6 6.601-6 4.538-6 3.119-6 2.144-6 1.474-6 1.013-6 6.962-7

4.784-7 3.290-7 2.260-7 1.553-7 1.067-7 7.339-8 5.044-8 3.396-8

2.453-8 1.638-8 1.125-8 7.737-9 5.317-9 3.654-9 2.512-9 1.727-9

1.186-9 8.27-10 5.49-10 3.85-10 2.65-10 1.82-10 1.25-10 8.59-11

5.91-11 1.14-10 1.54-11 FO

T

```

33** FO
  T
35** 0 25 50 100 150 4I 210 4I 225 14I 235.15 2I 253.75
      19I 258.83 15I 302.26 317.5 318 347 4I 347.22 9I 357 390
36$$ 15R1 15R2 3R3 20R4 16R5 3R6 15R7
38** 69R1 3R 1.0-10 F1
39$$ 1 2 3 2 4 2 5
40$$ F3
51$$ 5R1 4R2 4R3 3R4 3R5 5R6 4R7 4R8 3R9 2R10
      2R11 2R12 13 2R14 3R15 3R16 4R17 5R18 4R19 2R20
      4R21 4R22 4R23 4R24 10R25 10R26 6R27 4R28 2R29 3R30
      2R31 2R32 2R33 3R34 4R35 7R36 5R37 3R38 3R39 4R40
      5R41 3R42 4R43 3R44 3R45 46 47
      2R48 49 2R50 2R51 2R52 2R53 2R54 2R55 2R56 2R57
      58 59 60 4R61 2R62 2R63 2R64 2R65 66 67 T T
//
//SIX EXEC AMPX,GOTIME=20,GOSIZE=1080K,SBUF=8148
//* FILE 04 IS THE XSDRNPM LIBRARY FROM NITAWL
//GO.FT04F001 DD UNIT=3330,DISP=SHR,VOL=SER=ZX5555,
// DCB=(RECFM=VBS,LRECL=X,BLKSIZE=6447),
// DSN=X.HEC15758.XSDRN.GLS
//GO.FT08F001 DD SPACE=(3520,610)
//GO.FT09F001 DD SPACE=(3520,540)
//GO.FT10F001 DD SPACE=(2060,830)
//* FILE 16 IS THE ANGULAR FLUXES FROM XSDRN CALCULATION
//GO.FT16F001 DD UNIT=TAPE62,VOL=SER=X23285,
// LABEL=(3,SL),DISP=(NEW,KEEP),
// DSN=BF3171.ANG.FLUX,
// DCB=(RECFM=VBS,LRECL=X,BLKSIZE=6447,DEN=4)
//
//GO.SYSIN DD *
=XSDRNPM
  BROWN'S FERRY-III 3293 MEGAWATTS 50% VOID AT CENTERLINE
1$$ 2 8 103 1 0
     5 31 8 3 0
     25 1 0 0 3
2$$ -2 0 0 E
3$$ 0 1 0 0 0
     0 0 1 0 0
     0 0
5** 0.001 0.001 6.7761E+17 2Z
     1.420892 4Z
     0.001 0.75 T
13$$ 7R1 2R2 6R3 6R4 10R5
     ' FUEL WATER SS304 A533B CONCRETE
14$$ 1269 30 70 50 110 120 130
     1269 210
     310 360 220 230 240 250 1Q6
1269 7I 310 390
15** 1.5354-2 7.677-3 5.7645-3 2.003-5
     1.2125-4 5.322-3 1.0884-2
' FUEL MIXTURE ABOVE IS WATER(H+O),ZIRC(ZR+FE) & UO2( 235+238+O)
4.950-2 2.475-2
2.37-4 8.93-4 1.74-2 1.52-3 5.83-2 8.55-3
9.81-4 3.71-4 1.27-4 1.12-3 8.19-2 4.44-4

```

7.77-3 1.15-4 4.38-2 1.05-3 1.48-4 2.39-3 1.58-2 6.93-4 2.92-3 3.13-4 T

30\$\$ 21R1 FO

31\*\*

8.196-6 1.407-5 2.346-5 1.676-5 2.120-5 2.669-5 3.318-5 9.212-5  
1.379-4 2.022-4 2.892-4 4.059-4 5.583-4 7.525-4 9.963-4 1.297-3  
1.660-3 2.092-3 2.597-3 3.179-3 3.839-3 1.440-3 3.137-3 5.390-3  
6.274-3 7.224-3 8.229-3 9.282-3 1.037-2 1.148-2 2.632-2 3.072-2  
3.482-2 1.880-2 1.965-2 2.040-2 2.106-2 2.164-2 2.212-2 1.496-2  
3.787-3 3.769-3 7.580-3 1.523-2 2.300-2 2.310-2 2.312-2 2.306-2  
2.290-2 2.266-2 2.237-2 2.202-2 2.162-2 2.111-2 2.066-2 2.006-2  
1.953-2 1.890-2 3.591-2 1.422-2 1.912-2 1.568-2 1.503-2 1.438-2  
1.373-2 1.310-2 1.248-2 1.188-2 1.128-2 1.071-2 1.015-2 9.643-3  
9.099-3 1.672-2 1.488-2 6.804-3 6.405-3 1.168-2 1.031-2 1.110-3  
4.150-4 8.539-4 2.305-3 4.395-3 7.978-3 3.614-3 3.382-3 3.164-3  
2.960-3 2.765-3 2.584-3 2.417-3 2.253-3 2.107-3 1.962-3 1.834-3  
1.708-3 1.595-3 1.487-3 1.383-3 1.291-3 2.853-3 2.386-3 8.013-4  
5.874-4 1.426-3 8.464-4 1.879-3 6.696-4 9.652-4 8.036-4 9.037-4  
3.215-4 4.130-4 1.789-4 1.100-4 1.452-4 6.873-5 6.624-5 1.846-4  
2.654-4 4.036-4 2.781-4 1.916-4 1.319-4 9.077-5 6.245-5 2.768-5  
1.528-5 1.316-5 1.132-5 5.056-6 4.693-6 8.395-6 7.227-6 1.397-5  
9.602-6 6.601-6 4.538-6 3.119-6 2.144-6 1.474-6 1.013-6 6.962-7  
4.784-7 3.290-7 2.260-7 1.553-7 1.067-7 7.339-8 5.044-8 3.396-8  
2.453-8 1.638-8 1.125-8 7.737-9 5.317-9 3.654-9 2.512-9 1.727-9  
1.186-9 8.27-10 5.49-10 3.85-10 2.65-10 1.82-10 1.25-10 8.59-11  
5.91-11 1.14-10 1.54-11 FO T

33\*\* FO T

35\*\* 3I 0 3I 168 7I 207 4I 231.65 3I 237.744 3I 242 3I 254

4I 258.064 8I 263.144 19I 271 9I 313 4I 318.77 4I 322

4I 330 334.264 335 364 364.744 6I 365.374 380

36\$\$ 21R1 12R2 5R3 39R4 15R5 3R6 7 7R8

38\*\* 92R1 3R1.0-10 F1

39\$\$ 1 2 3 2 4 2 4 5

40\$\$ F3 T

//SEVEN EXEC AMPX,GOTIME=15,GOSIZE=540K,SBUF=8148

//GO.FT18FOO1 DD SPACE=(TRK,(900,60))

/\*\*

/\*\* FILES 70,71,72,73,74 ARE USED AS TEMPORARY STORAGE BY MALOX

//GO.FT70FOO1 DD UNIT=SYSDA,DSN=&&GLS1,

// DISP=(NEW,PASS),SPACE=(TRK,(500,50)),

// DCB=(RECFM=VBS,LRECL=X,BLKSIZE=6447,BUFL=8148)

//GO.FT71FOO1 DD UNIT=SYSDA,DSN=&&GLS2,

// DISP=(NEW,PASS),SPACE=(TRK,(500,50)),

// DCB=(RECFM=VBS,LRECL=X,BLKSIZE=6447,BUFL=8148)

//GO.FT72FOO1 DD UNIT=SYSDA,DSN=&&GLS3,

// DISP=(NEW,PASS),SPACE=(TRK,(500,50)),

// DCB=(RECFM=VBS,LRECL=X,BLKSIZE=6447,BUFL=8148)

//GO.FT73FOO1 DD UNIT=SYSDA,DSN=&&GLS4,

// DISP=(NEW,PASS),SPACE=(TRK,(500,50)),

// DCB=(RECFM=VBS,LRECL=X,BLKSIZE=6447,BUFL=8148)

//GO.FT74FOO1 DD UNIT=SYSDA,DSN=&&GLSHB,

// DISP=(NEW,PASS),SPACE=(TRK,(510,50)),

// DCB=(RECFM=VBS,LRECL=X,BLKSIZE=6447,BUFL=8148)

/\*\* MASTER INTERFACE IN AMPX FORMAT.....

//GO.FT75FOO1 DD UNIT=TAPE62,DISP=(OLD,PASS),LABEL=(1,SL),

// DCB=(RECFM=VBS,LRECL=X,BLKSIZE=6447,BUFL=8148,DEN=4),

```

// VOL=SER=X23004,DSN=GLS.LWR.MASTER
//* FILE 76 IS THE COLLAPSEDMASTER OUT OF LAST AJAX
//GO.FT76F001 DD UNIT=3330,DISP=(NEW,KEEP),VOL=SER=ZX5555,
// DCB=(RECFM=VBS,LRECL=X,BLKSIZE=6447,BUFL=8148),
// DSN=X.RWR15758.COLLAP.GLS,SPACE=(TRK,(100,100))
//* UNITS 81,82,83,84 ARE TEMPORARY STORAGE FOR AJAX RUNS
//GO.FT81F001 DD UNIT=SYSDA,DSN=&&GLSGLS1,
// DISP=(NEW,PASS),SPACE=(TRK,(500,100)),
// DCB=(RECFM=VBS,LRECL=X,BLKSIZE=6447,BUFL=8148)
//GO.FT82F001 DD UNIT=SYSDA,DSN=&&GLSGLS2,
// DISP=(NEW,PASS),SPACE=(TRK,(500,100)),
// DCB=(RECFM=VBS,LRECL=X,BLKSIZE=6447,BUFL=8148)
//GO.FT83F001 DD UNIT=SYSDA,DSN=&&GLSGLS3,
// DISP=(NEW,PASS),SPACE=(TRK,(500,100)),
// DCB=(RECFM=VBS,LRECL=X,BLKSIZE=6447,BUFL=8148)
//GO.FT84F001 DD UNIT=SYSDA,DSN=&&GLSGLS4,
// DISP=(NEW,PASS),SPACE=(TRK,(500,100)),
// DCB=(RECFM=VBS,LRECL=X,BLKSIZE=6447,BUFL=8148)
//GO.SYSIN DD *
=AJAX
1$$ 1 0$$ 81 75 T
2$$ 75 10 T
3$$ 1269 7I20 100 4$$ 8I 10 100 T
=AJAX
1$$ 1 0$$ 82 75 T
2$$ 75 3 T
3$$ 110 120 130 T
=AJAX
1$$ 1 0$$ 83 75 T
2$$ 75 7 T
3$$ 1269 3I 210 250 310 4$$ 5I 200 260 T
=AJAX
1$$ 1 0$$ 84 75 T
2$$ 75 10 T
3$$ 1269 7I 310 390 4$$ 8I 300 390 T
=MALOCS
' BWR CALCULATION AT CORE CENTER AT INTERVAL #8 DEC 20, 1979
1$$ 171 47 36 20 0 0 2$$ 82 71 3$$ 0 0 1 1 FO T
4$$ 5R1 4R2 4R3 3R4 3R5 5R6 4R7 4R8 3R9 2R10
2R11 2R12 13 2R14 3R15 3R16 4R17 5R18 4R19 2R20
4R21 4R22 4R23 4R24 10R25 10R26 6R27 4R28 2R29 3R30
2R31 2R32 2R33 3R34 4R35 7R36 5R37 3R38 3R39 4R40
5R41 3R42 4R43 3R44 3R45 46 47
6$$ 2R1 2 2R3 2R4 2R5 2R6 2R7 2R8 2R9 2R10
11 12 13 4R14 2R15 2R16 2R17 2R18 19 20
5** 6.063E+08 1.072E+09 1.600E+09 1.371E+09 1.658E+09 2.062E+09
2.553E+09 7.319E+09 1.050E+10 1.473E+10 2.086E+10 3.128E+10 4.161E+10
5.650E+10 7.612E+10 9.640E+10 1.220E+11 1.574E+11 1.933E+11 2.278E+11
2.925E+11 1.120E+11 2.522E+11 4.256E+11 4.705E+11 5.418E+11 6.664E+11
6.962E+11 8.185E+11 8.722E+11 1.947E+12 2.117E+12 2.345E+12 1.435E+12
1.756E+12 1.774E+12 1.872E+12 2.053E+12 2.074E+12 1.454E+12 3.963E+11
4.070E+11 7.956E+11 1.406E+12 1.924E+12 1.868E+12 1.837E+12 1.793E+12
2.157E+12 2.066E+12 1.996E+12 2.049E+12 2.141E+12 2.111E+12 1.768E+12
2.268E+12 2.300E+12 2.083E+12 3.370E+12 1.328E+12 2.248E+12 2.158E+12
2.498E+12 2.740E+12 2.596E+12 2.432E+12 2.362E+12 2.315E+12 2.241E+12

```

2.175E+12 2.120E+12 2.058E+12 1.956E+12 3.003E+12 2.649E+12 1.458E+12  
 1.492E+12 3.418E+12 3.334E+12 3.736E+11 1.398E+11 2.886E+11 7.948E+11  
 1.556E+12 2.963E+12 1.417E+12 1.371E+12 1.332E+12 1.297E+12 1.260E+12  
 1.227E+12 1.197E+12 1.165E+12 1.139E+12 1.109E+12 1.085E+12 1.061E+12  
 1.039E+12 1.018E+12 9.953E+11 9.777E+11 2.361E+12 2.258E+12 8.329E+11  
 6.401E+11 1.674E+12 1.092E+12 2.775E+12 1.152E+12 1.870E+12 1.816E+12  
 2.459E+12 1.028E+12 1.487E+12 7.175E+11 4.691E+11 6.546E+11 3.255E+11  
 3.242E+11 9.651E+11 1.585E+12 3.095E+12 3.011E+12 2.943E+12 2.888E+12  
 2.849E+12 2.807E+12 1.661E+12 1.101E+12 1.090E+12 1.062E+12 5.415E+11  
 5.655E+11 1.058E+12 1.094E+12 2.640E+12 2.632E+12 2.628E+12 2.579E+12  
 2.548E+12 2.518E+12 2.496E+12 2.486E+12 2.423E+12 2.415E+12 2.378E+12  
 2.178E+12 2.375E+12 2.262E+12 2.256E+12 2.131E+12 2.075E+12 2.190E+12  
 1.816E+12 2.024E+12 1.997E+12 1.938E+12 1.472E+12 1.565E+12 1.749E+12  
 1.751E+12 1.791E+12 1.717E+12 1.741E+12 1.707E+12 1.670E+12 1.661E+12  
 1.636E+12 1.597E+12 1.350E+13 1.842E+13  
 7\*\* 4.509E+02 6.746E+06 5.562E+09 1.809E+10 3.696E+10 6.978E+10  
 2.138E+11 2.862E+11 4.154E+11 5.413E+11 1.539E+12 2.281E+12 3.392E+12  
 6.087E+12 1.153E+13 1.043E+13 5.807E+12 7.239E+12 1.715E+13 1.263E+13  
 7.103E+12 7.703E+12 6.725E+12 3.912E+12 4.722E+12 3.485E+12 5.862E+12  
 3.890E+12 7.829E+11 3.030E+11 9.872E+10 2.231E+10 8.672E+09 2.194E+10  
 5.560E+08 2.107E+08 T

=MALOCS

' PWR CORE CALCULATION AT INTERVAL #8 OF CORE

1\$\$ 171 47 36 20 0 0 2\$\$ 81 70 3\$\$ 0 0 1 1 FO T  
 4\$\$ 5R1 4R2 4R3 3R4 3R5 5R6 4R7 4R8 3R9 2R10  
 2R11 2R12 13 2R14 3R15 3R16 4R17 5R18 4R19 2R20  
 4R21 4R22 4R23 4R24 10R25 10R26 6R27 4R28 2R29 3R30  
 2R31 2R32 2R33 3R34 4R35 7R36 5R37 3R38 3R39 4R40  
 5R41 3R42 4R43 3R44 3R45 46 47  
 6\$\$ 2R1 2 2R3 2R4 2R5 2R6 2R7 2R8 2R9 2R10  
 11 12 13 4R14 2R15 2R16 2R17 2R18 19 20

5\*\* 9.049E+08 1.604E+09 2.363E+09 2.053E+09 2.477E+09 3.073E+09  
 3.802E+09 1.095E+10 1.561E+10 2.170E+10 3.056E+10 4.619E+10 6.105E+10  
 8.288E+10 1.117E+11 1.404E+11 1.769E+11 2.286E+11 2.801E+11 3.278E+11  
 4.224E+11 1.616E+11 3.648E+11 6.125E+11 6.703E+11 7.692E+11 9.500E+11  
 9.811E+11 1.156E+12 1.225E+12 2.717E+12 2.915E+12 3.199E+12 3.195E+12  
 2.394E+12 2.406E+12 2.530E+12 2.766E+12 2.776E+12 1.947E+12 5.350E+11  
 5.496E+11 1.061E+12 1.865E+12 2.543E+12 2.461E+12 2.414E+12 2.349E+12  
 2.819E+12 2.677E+12 2.575E+12 2.636E+12 2.747E+12 2.687E+12 2.249E+12  
 2.864E+12 2.880E+12 2.603E+12 4.198E+12 1.657E+12 2.785E+12 2.625E+12  
 3.002E+12 3.253E+12 3.054E+12 2.854E+12 2.754E+12 2.696E+12 2.608E+12  
 2.523E+12 2.452E+12 2.375E+12 2.252E+12 3.516E+12 3.126E+12 1.720E+12  
 1.764E+12 3.961E+12 3.834E+12 4.286E+11 1.602E+11 3.298E+11 9.042E+11  
 1.765E+12 3.384E+12 1.615E+12 1.559E+12 1.522E+12 1.478E+12 1.433E+12  
 1.405E+12 1.381E+12 1.331E+12 1.310E+12 1.269E+12 1.237E+12 1.227E+12  
 1.197E+12 1.176E+12 1.147E+12 1.124E+12 2.717E+12 2.599E+12 9.464E+11  
 7.579E+11 1.927E+12 1.273E+12 3.210E+12 1.330E+12 2.171E+12 2.104E+12  
 2.850E+12 1.190E+12 1.684E+12 8.137E+11 5.917E+11 7.954E+11 3.849E+11  
 3.793E+11 1.127E+12 1.851E+12 3.615E+12 3.533E+12 3.457E+12 3.391E+12  
 3.365E+12 3.318E+12 1.969E+12 1.312E+12 1.298E+12 1.281E+12 6.415E+11  
 6.602E+11 1.267E+12 1.301E+12 3.169E+12 3.154E+12 3.150E+12 3.108E+12  
 3.079E+12 3.054E+12 3.031E+12 3.028E+12 2.972E+12 2.962E+12 2.930E+12  
 2.731E+12 2.925E+12 2.811E+12 2.808E+12 2.694E+12 2.599E+12 2.760E+12  
 2.344E+12 2.578E+12 2.543E+12 2.483E+12 1.964E+12 2.104E+12 2.295E+12  
 2.292E+12 2.342E+12 2.249E+12 2.282E+12 2.243E+12 2.201E+12 2.191E+12

2.162E+12 2.116E+12 1.852E+13 2.685E+13  
 7\*\* 2.372E+02 1.174E+07 3.854E+10 4.007E+11 1.058E+11 1.278E+11  
 4.012E+11 5.900E+11 7.308E+11 9.633E+11 2.579E+12 3.794E+12 5.718E+12  
 1.014E+13 1.918E+13 1.715E+13 9.696E+12 1.222E+13 2.910E+13 2.171E+13  
 1.210E+13 1.304E+13 1.128E+13 6.597E+12 8.455E+12 5.900E+12 1.004E+13  
 6.682E+12 1.332E+12 4.955E+11 1.243E+11 2.287E+10 9.512E+09 1.207E+10  
 8.811E+08 6.318E+08 T

=MALOCS

' COLLAPSE OVER A PWR WATER SPECTRA BETWEEN BARREL AND PV INTER. # 38

1\$\$ 171 47 36 20 0 0 2\$\$ 83 72 3\$\$ 0 0 1 1 FO T  
 4\$\$ 5R1 4R2 4R3 3R4 3R5 5R6 4R7 4R8 3R9 2R10  
 2R11 2R12 13 2R14 3R15 3R16 4R17 5R18 4R19 2R20  
 4R21 4R22 4R23 4R24 10R25 10R26 6R27 4R28 2R29 3R30  
 2R31 2R32 2R33 3R34 4R35 7R36 5R37 3R38 3R39 4R40  
 5R41 3R42 4R43 3R44 3R45 46 47

6\$\$ 2R1 2 2R3 2R4 2R5 2R6 2R7 2R8 2R9 2R10

11 12 13 4R14 2R15 2R16 2R17 2R18 19 20

5\*\* 8.433E+06 1.567E+07 1.630E+07 1.950E+07 2.322E+07 2.813E+07  
 3.421E+07 1.047E+08 1.289E+08 1.537E+08 2.006E+08 3.309E+08 3.996E+08  
 5.244E+08 6.969E+08 7.969E+08 9.312E+08 1.181E+09 1.364E+09 1.420E+09  
 1.885E+09 7.154E+08 1.627E+09 2.610E+09 2.502E+09 2.672E+09 3.428E+09  
 3.002E+09 3.570E+09 3.578E+09 7.089E+09 6.351E+09 6.263E+09 3.771E+09  
 5.059E+09 5.264E+09 5.485E+09 5.977E+09 5.826E+09 4.357E+09 1.405E+09  
 1.564E+09 2.575E+09 4.476E+09 5.664E+09 5.257E+09 5.159E+09 4.888E+09  
 6.119E+09 5.605E+09 5.201E+09 5.286E+09 5.379E+09 5.381E+09 4.231E+09  
 5.489E+09 5.692E+09 5.071E+09 7.757E+09 2.982E+09 5.122E+09 4.668E+09  
 5.198E+09 5.351E+09 4.987E+09 4.851E+09 4.721E+09 4.665E+09 4.576E+09  
 4.491E+09 4.342E+09 4.212E+09 3.997E+09 6.338E+09 5.789E+09 3.201E+09  
 3.236E+09 6.923E+09 6.658E+09 7.449E+08 2.797E+08 5.775E+08 1.577E+09  
 3.087E+09 5.946E+09 2.869E+09 2.800E+09 2.740E+09 2.679E+09 2.621E+09  
 2.569E+09 2.527E+09 2.468E+09 2.425E+09 2.374E+09 2.330E+09 2.291E+09  
 2.258E+09 2.221E+09 2.181E+09 2.143E+09 5.193E+09 5.016E+09 1.856E+09  
 1.458E+09 3.759E+09 2.481E+09 6.332E+09 2.633E+09 4.323E+09 4.219E+09  
 5.749E+09 2.421E+09 3.502E+09 1.703E+09 1.145E+09 1.630E+09 8.107E+08  
 7.964E+08 2.350E+09 3.836E+09 7.525E+09 7.502E+09 7.436E+09 7.350E+09  
 7.364E+09 7.373E+09 4.431E+09 2.966E+09 2.966E+09 2.961E+09 1.476E+09  
 1.472E+09 2.946E+09 2.982E+09 7.484E+09 7.495E+09 7.494E+09 7.556E+09  
 7.603E+09 7.647E+09 7.649E+09 7.757E+09 7.810E+09 7.853E+09 7.900E+09  
 7.944E+09 7.990E+09 8.037E+09 8.084E+09 8.131E+09 7.973E+09 8.425E+09  
 8.266E+09 8.307E+09 8.352E+09 8.392E+09 8.432E+09 8.471E+09 8.508E+09  
 8.544E+09 8.723E+09 8.466E+09 8.641E+09 8.668E+09 8.696E+09 8.717E+09  
 8.737E+09 8.754E+09 1.042E+11 1.210E+12

7\*\* 6.553E+04 1.841E+07 9.219E+10 1.346E+11 4.555E+10 2.815E+10  
 4.262E+10 4.921E+10 3.550E+10 3.961E+10 5.593E+10 6.080E+10 8.510E+10  
 1.082E+11 5.596E+11 1.920E+11 1.021E+11 1.207E+11 2.888E+11 2.532E+11  
 1.461E+11 1.733E+11 1.840E+11 9.930E+10 3.868E+11 2.046E+11 5.406E+11  
 9.284E+11 7.443E+11 1.097E+12 7.214E+11 4.828E+11 4.486E+11 2.100E+11  
 1.767E+10 1.767E+08 T

=MALOCS

' COLLAPSE OVER 1/4 T PRESSURE VESSEL OF A PWR INTERVAL # 51

1\$\$ 171 47 36 20 0 0 2\$\$ 83 73 3\$\$ 0 0 1 1 FO T  
 4\$\$ 5R1 4R2 4R3 3R4 3R5 5R6 4R7 4R8 3R9 2R10  
 2R11 2R12 13 2R14 3R15 3R16 4R17 5R18 4R19 2R20  
 4R21 4R22 4R23 4R24 10R25 10R26 6R27 4R28 2R29 3R30  
 2R31 2R32 2R33 3R34 4R35 7R36 5R37 3R38 3R39 4R40

5R41 3R42 4R43 3R44 3R45 46 47  
6\$\$ 2R1 2 2R3 2R4 2R5 2R6 2R7 2R8 2R9 2R10  
11 12 13 4R14 2R15 2R16 2R17 2R18 19 20  
5\*\* 1.078E+06 2.040E+06 1.757E+06 2.298E+06 2.868E+06 3.519E+06  
4.252E+06 1.331E+07 1.490E+07 1.618E+07 2.019E+07 3.432E+07 4.050E+07  
5.169E+07 6.752E+07 7.415E+07 8.308E+07 1.024E+08 1.149E+08 1.158E+08  
1.506E+08 5.647E+07 1.279E+08 2.057E+08 1.912E+08 1.914E+08 2.374E+08  
2.051E+08 2.300E+08 2.406E+08 4.611E+08 4.158E+08 4.319E+08 2.428E+08  
3.109E+08 3.664E+08 3.990E+08 4.568E+08 4.340E+08 3.313E+08 1.130E+08  
1.282E+08 1.918E+08 4.352E+08 5.558E+08 5.124E+08 5.320E+08 5.848E+08  
6.806E+08 6.621E+08 6.193E+08 6.166E+08 6.685E+08 8.117E+08 7.434E+08  
6.981E+08 1.021E+09 9.272E+08 1.503E+09 6.073E+08 1.182E+09 7.785E+08  
9.469E+08 7.345E+08 7.667E+08 1.139E+09 1.201E+09 1.667E+09 1.766E+09  
1.408E+09 1.252E+09 1.172E+09 9.487E+08 2.116E+09 1.334E+09 6.491E+08  
1.317E+09 2.797E+09 3.147E+09 4.618E+08 1.454E+08 2.204E+08 3.919E+08  
5.772E+08 1.756E+09 9.232E+08 6.579E+08 8.504E+08 6.254E+08 4.156E+08  
5.390E+08 1.111E+09 6.604E+08 9.067E+08 5.639E+08 3.104E+08 6.295E+08  
5.916E+08 9.603E+08 7.821E+08 6.016E+08 1.137E+09 7.523E+08 1.458E+08  
7.515E+08 5.371E+08 9.452E+08 1.308E+09 4.391E+08 9.115E+08 7.373E+08  
6.763E+08 2.180E+08 1.012E+08 3.836E+07 1.271E+08 1.174E+09 7.882E+08  
4.190E+08 8.408E+08 8.865E+08 1.111E+09 9.354E+08 5.923E+08 3.231E+08  
7.897E+08 8.408E+08 4.403E+08 3.182E+08 2.979E+08 2.599E+08 1.125E+08  
9.156E+07 1.480E+08 2.146E+08 6.880E+08 6.946E+08 5.075E+08 5.031E+08  
5.051E+08 4.968E+08 3.119E+08 4.061E+08 4.571E+08 4.829E+08 5.015E+08  
5.168E+08 5.264E+08 5.348E+08 5.390E+08 5.399E+08 5.245E+08 5.456E+08  
5.241E+08 5.126E+08 4.984E+08 4.810E+08 4.608E+08 4.380E+08 4.125E+08  
3.856E+08 3.622E+08 3.210E+08 2.953E+08 2.639E+08 2.329E+08 2.027E+08  
1.738E+08 1.471E+08 4.221E+08 3.805E+08  
7\*\* 7.358E+03 2.022E+06 9.507E+09 1.418E+10 5.442E+09 3.840E+09  
5.459E+09 6.283E+09 5.254E+09 5.895E+09 7.754E+09 8.801E+09 1.144E+10  
1.438E+10 3.174E+10 2.203E+10 1.176E+10 1.406E+10 3.373E+10 2.925E+10  
1.638E+10 1.911E+10 2.010E+10 2.324E+10 2.204E+10 2.064E+10 5.279E+10  
8.197E+10 5.305E+10 4.458E+10 7.919E+09 8.636E+08 5.932E+07 3.169E+06  
6.234E+05 1.278E+05 T

=MALOCS

' COLLAPSE OVER A CONCRETE SPECTRA 10 CM INTO CONCRETE INTER. # 71

1\$\$ 171 47 36 20 0 0 2\$\$ 84 74 3\$\$ 0 0 1 1 FO T

4\$\$ 5R1 4R2 4R3 3R4 3R5 5R6 4R7 4R8 3R9 2R10

2R11 2R12 13 2R14 3R15 3R16 4R17 5R18 4R19 2R20

4R21 4R22 4R23 4R24 10R25 10R26 6R27 4R28 2R29 3R30

2R31 2R32 2R33 3R34 4R35 7R36 5R37 3R38 3R39 4R40

5R41 3R42 4R43 3R44 3R45 46 47

6\$\$ 2R1 2 2R3 2R4 2R5 2R6 2R7 2R8 2R9 2R10

11 12 13 4R14 2R15 2R16 2R17 2R18 19 20

5\*\* 3.087E+04 5.980E+04 4.163E+04 5.856E+04 7.631E+04 9.475E+04  
1.152E+05 3.766E+05 3.942E+05 4.010E+05 4.779E+05 8.293E+05 9.341E+05  
1.173E+06 1.540E+06 1.655E+06 1.771E+06 2.138E+06 2.327E+06 2.289E+06  
2.992E+06 1.156E+06 2.664E+06 4.091E+06 3.628E+06 3.770E+06 4.957E+06  
4.161E+06 4.642E+06 4.766E+06 9.520E+06 8.331E+06 7.996E+06 5.291E+06  
7.570E+06 8.570E+06 9.821E+06 1.190E+07 1.154E+07 1.064E+07 3.581E+06  
4.720E+06 7.369E+06 1.290E+07 1.480E+07 1.317E+07 1.118E+07 1.097E+07  
2.096E+07 1.716E+07 1.581E+07 1.736E+07 1.935E+07 2.120E+07 1.509E+07  
2.379E+07 2.843E+07 2.686E+07 3.193E+07 1.068E+07 2.413E+07 2.867E+07  
3.265E+07 3.838E+07 4.423E+07 4.739E+07 4.999E+07 5.929E+07 6.843E+07  
7.119E+07 6.178E+07 7.108E+07 6.856E+07 9.044E+07 6.633E+07 3.598E+07

```

3.883E+07 1.035E+08 1.183E+08 1.415E+07 5.373E+06 1.096E+07 2.974E+07
6.016E+07 1.200E+08 5.957E+07 5.884E+07 5.323E+07 5.154E+07 4.937E+07
5.262E+07 6.499E+07 7.287E+07 7.761E+07 7.178E+07 6.718E+07 6.599E+07
7.358E+07 7.573E+07 6.729E+07 6.846E+07 1.636E+08 1.431E+08 5.354E+07
4.718E+07 1.205E+08 7.979E+07 2.052E+08 8.345E+07 1.423E+08 1.377E+08
1.718E+08 7.974E+07 1.188E+08 5.540E+07 3.832E+07 5.587E+07 2.905E+07
2.838E+07 8.391E+07 1.391E+08 2.736E+08 2.694E+08 2.619E+08 2.639E+08
2.607E+08 2.614E+08 1.534E+08 9.319E+07 8.646E+07 6.604E+07 4.381E+07
5.486E+07 1.190E+08 1.159E+08 2.775E+08 2.686E+08 2.645E+08 2.633E+08
2.625E+08 2.619E+08 2.610E+08 2.605E+08 2.598E+08 2.590E+08 2.583E+08
2.574E+08 2.565E+08 2.556E+08 2.545E+08 2.536E+08 2.460E+08 2.573E+08
2.498E+08 2.484E+08 2.471E+08 2.455E+08 2.440E+08 2.424E+08 2.406E+08
2.388E+08 2.410E+08 2.309E+08 2.328E+08 2.305E+08 2.282E+08 2.257E+08
2.231E+08 2.202E+08 1.823E+09 1.005E+10
7**      3.202E+03 1.070E+06 9.371E+07 2.946E+08 1.057E+08 5.911E+07
2.392E+08 1.499E+08 1.269E+08 3.148E+08 2.072E+08 4.167E+08 2.497E+08
3.045E+08 6.558E+08 4.094E+08 1.851E+08 1.876E+08 4.548E+08 3.683E+08
2.311E+08 2.510E+08 2.704E+08 2.581E+08 3.077E+08 2.768E+08 7.490E+08
1.333E+09 1.077E+09 1.674E+09 9.985E+08 4.746E+08 1.848E+08 1.952E+07
5.421E+05 5.835E+04 T

```

=AJAX

0\$\$ 76 70 1\$\$ 5 T

2\$\$ 70 0 T

2\$\$ 71 0 T

2\$\$ 72 0 T

2\$\$ 74 0 T

2\$\$ 73 5 T

3\$\$ 3I 220 260 4\$\$ 3I 400 440 T

/\*

//EIGHT EXEC AMPX,GOTIME=010,GOSIZE=550K,SBUF=8148

//GO.FT18F001 DD SPACE=(TRK,(900,60))

/\*

/\* 171,36 (N,G) MASTER INTERFACE

//GO.FT60F001 DD UNIT=3330,VOL=SER=ZX0000,DSN=JEW.AMPXR2.LIB171NG,

// DCB=(RECFM=VBS,LRECL=X,BLKSIZE=6447,BUFL=8148),DISP=SHR

/\* 36 (G) MASTER INTERFACE

//GO.FT61F001 DD UNIT=3330,VOL=SER=ZX0000,DSN=JEW.AMPX0.LIB36G,

// DCB=(RECFM=VBS,LRECL=X,BLKSIZE=6447,BUFL=8148),DISP=SHR

/\* 171 (N) MASTER INTERFACE

//GO.FT62F001 DD UNIT=3330,VOL=SER=ZX0000,DSN=JEW.AMPXR2.LIB171N,

// DCB=(RECFM=VBS,LRECL=X,BLKSIZE=6447,BUFL=8148),DISP=SHR

/\* 70 STORES 15 ISOTOPES FROM 171 LIBRARY

//GO.FT70F001 DD UNIT=SYSDA,DSN=&&GLS1,

// DISP=(NEW,PASS),SPACE=(TRK,(500,50)),

// DCB=(RECFM=VBS,LRECL=X,BLKSIZE=6447,BUFL=8148)

/\* UNIT 71 CONTAINS THE OUTPUT FROM BONAMI-SELF SHIELDED

//GO.FT71F001 DD UNIT=SYSDA,DSN=&&GLS2,

// DISP=(NEW,PASS),SPACE=(TRK,(500,50)),

// DCB=(RECFM=VBS,LRECL=X,BLKSIZE=6447,BUFL=8148)

/\* UNIT 72 CONTAINS U,PU,NP,O FROM BONAMI, FOLLOWING AJAX

//GO.FT72F001 DD UNIT=SYSDA,DSN=&&GLS3,

// DISP=(NEW,PASS),SPACE=(TRK,(500,50)),

// DCB=(RECFM=VBS,LRECL=X,BLKSIZE=6447,BUFL=8148)

/\* UNIT 73 CONTAINS THE 9 ISOTOPES IN COUPLED FORMAT

//GO.FT73F001 DD UNIT=SYSDA,DSN=&&GLS4,

```

// DISP=(NEW,PASS),SPACE=(TRK,(500,50)),
// DCB=(RECFM=VBS,LRECL=X,BLKSIZE=6447,BUFL=8148)
/** UNIT 74 IS THE OLD 171/36 WORKING LIBRARY
//GO.FT74F001 DD UNIT=3330,DISP=SHR,VOL=SER=ZX5555,
// DSN=X.HEC15758.XSDRN.GLS,
// DCB=(RECFM=VBS,LRECL=X,BLKSIZE=6447,BUFL=8148)
/** UNIT 75 CONTAINS COLLAPSED DATA FROM MALOCS RUN
//GO.FT75F001 DD UNIT=SYSDA,DSN=&&GLSHB,
// DISP=(NEW,PASS),SPACE=(TRK,(510,50)),
// DCB=(RECFM=VBS,LRECL=X,BLKSIZE=6447,BUFL=8148)
/** UNIT 76 IS THE OLD COLLAPSED MASTER INTERFACE
//GO.FT76F001 DD UNIT=3330,DISP=SHR,VOL=SER=ZX5555,
// DSN=X.RWR15758.COLLAP.GLS,
// DCB=(RECFM=VBS,LRECL=X,BLKSIZE=6447,BUFL=8148)
/** UNIT 77 CONTAINS THE MERGED OLD AND NEW COLLAPSED MASTERS
//GO.FT77F001 DD UNIT=SYSDA,DSN=&&GLS7,
// DISP=(NEW,PASS),SPACE=(TRK,(500,50)),
// DCB=(RECFM=VBS,LRECL=X,BLKSIZE=6447,BUFL=8148)
//GO.FT81F001 DD UNIT=TAPE62,DISP=(NEW,PASS),LABEL=(7,SL),
// DCB=(RECFM=VBS,LRECL=X,BLKSIZE=6447,BUFL=8148,DEN=4),
// VOL=SER=X23004,DSN=GLS.LWR171.WORK
//GO.FT82F001 DD UNIT=TAPE62,DISP=(NEW,PASS),LABEL=(1,SL),
// DCB=(RECFM=VBS,LRECL=X,BLKSIZE=6447,BUFL=8148,DEN=4),
// VOL=SER=X23285,DSN=GLS.LWR171.ANISN.BINARY
//GO.FT83F001 DD UNIT=TAPE62,DISP=(NEW,PASS),LABEL=(8,SL),
// DCB=(RECFM=VBS,LRECL=X,BLKSIZE=6447,BUFL=8148,DEN=4),
// VOL=REF=*.FT81F001,DSN=GLS.LWR47.WORK
//GO.FT84F001 DD UNIT=TAPE62,DISP=(NEW,PASS),LABEL=(2,SL),
// DCB=(RECFM=VBS,LRECL=X,BLKSIZE=6447,BUFL=8148,DEN=4),
// VOL=REF=*.FT82F001,DSN=GLS.LWR47.ANISN.BINARY
//GO.SYSIN DD *
=AJAX
' 15 ISOTOPES WRITTEN ON UNIT 70, READ FROM 62
0$$ 70 70 1$$ 1 T
2$$ 62 15 T
3$$ 1161 1163 1263 1264 1265 1266
' PU242 U236 NP237 PU239 PU240 PU241
    1269 1273 1276 1191 1192 1196 7141 1261 9262
' H B-10 0 CR FE NI ZR U235 U238
4$$ 131 1 15 T
=BONAMI
' READ FROM UNIT 70 & WRITE SELF SHIELDED ON 71
0$$ 70 0 18 71 1$$ 2 3 16 1 1 2 2** 0.001 1.35 T
3$$ 9R1 4R2 3R3
4$$ 14 2 15 4 5 6 1 3 9 10 11 12 13 7 8 9
' U235 U236 U238 PU239 PU240 PU241 PU242 NP237 0
' CR FE NI ZR H B-10 0
5** 5.052-4 1.985-5 2.131-2 4.074-5 3.976-6 9.973-7
    4.661-8 2.930-7 4.465-2
    7.64-5 1.45-4 8.77-4 4.27-2 4.788-2 3.003-6 2.394-2
6$$ 1 2 3 7** 0.41783 0.47498 0.71079 8** 921 672 580
10$$ 14I 1 16 11$$ 0 1 1 T
=AJAX
' READ 9 ISOTOPES FROM UNIT 71 & WRITE THEM ON 72
0$$ 72 72 1$$ 1 T

```

```

2$$ 71 9 T
3$$ 7I 1 9 4$$ 7I 500 580 T
=CHOX
' COUPLE CROSS SECTIONS N(72),NG(60),G(61), COUPLED(73)
0$$ 72 60 61 73 E 1$$ 9 0 T
2$$ 7I 500 580 3$$ 1261 0 1262 1264 1265 0 0 0 1276
4$$ 3R92 4R94 94 8 5$$ 7I 500 580 T
=NITAWL
' UNIT 73 IS 9 ELEMENT COUPLED, 74 IS PREVIOUS WORKING LIB(30 ELEMENT)
' XSDRN WORKING LIBRARY ON 81, ANISN BINARY ON 82 171N/36G
0$$ 73 74 A4 81 A9 82 1$$ A2 9 30 0 2 3 4 A11 -1 E T
2$$ 7I 500 580 1269 11I 10 130 4I 200 250 8I 300 390 T
=MALOCS
' PWR CORE CALCULATION AT INTERVAL #8 OF CORE
' COLLAPSE 9 ELEMENTS OVER PWR SPECTRUM..PU FUEL..
1$$ 171 47 36 20 0 0 2$$ 73 75 3$$ 0 0 1 1 FO T
4$$ 5R1 4R2 4R3 3R4 3R5 5R6 4R7 4R8 3R9 2R10
2R11 2R12 13 2R14 3R15 3R16 4R17 5R18 4R19 2R20
4R21 4R22 4R23 4R24 10R25 10R26 6R27 4R28 2R29 3R30
2R31 2R32 2R33 3R34 4R35 7R36 5R37 3R38 3R39 4R40
5R41 3R42 4R43 3R44 3R45 46 47
6$$ 2R1 2 2R3 2R4 2R5 2R6 2R7 2R8 2R9 2R10
11 12 13 4R14 2R15 2R16 2R17 2R18 19 20
5** 9.049E+08 1.604E+09 2.363E+09 2.053E+09 2.477E+09 3.073E+09
3.802E+09 1.095E+10 1.561E+10 2.170E+10 3.056E+10 4.619E+10 6.105E+10
8.288E+10 1.117E+11 1.404E+11 1.769E+11 2.286E+11 2.801E+11 3.278E+11
4.224E+11 1.616E+11 3.648E+11 6.125E+11 6.703E+11 7.692E+11 9.500E+11
9.811E+11 1.156E+12 1.225E+12 2.717E+12 2.915E+12 3.199E+12 1.954E+12
2.394E+12 2.406E+12 2.530E+12 2.766E+12 2.776E+12 1.947E+12 5.350E+11
5.496E+11 1.061E+12 1.865E+12 2.543E+12 2.461E+12 2.414E+12 2.349E+12
2.819E+12 2.677E+12 2.575E+12 2.636E+12 2.747E+12 2.687E+12 2.249E+12
2.864E+12 2.880E+12 2.603E+12 4.198E+12 1.657E+12 2.785E+12 2.625E+12
3.002E+12 3.253E+12 3.054E+12 2.854E+12 2.754E+12 2.696E+12 2.608E+12
2.523E+12 2.452E+12 2.375E+12 2.252E+12 3.516E+12 3.126E+12 1.720E+12
1.764E+12 3.961E+12 3.834E+12 4.286E+11 1.602E+11 3.298E+11 9.042E+11
1.765E+12 3.384E+12 1.615E+12 1.559E+12 1.522E+12 1.478E+12 1.433E+12
1.405E+12 1.381E+12 1.331E+12 1.310E+12 1.269E+12 1.237E+12 1.227E+12
1.197E+12 1.176E+12 1.147E+12 1.124E+12 2.717E+12 2.599E+12 9.464E+11
7.579E+11 1.927E+12 1.273E+12 3.210E+12 1.330E+12 2.171E+12 2.104E+12
2.850E+12 1.190E+12 1.684E+12 8.137E+11 5.917E+11 7.954E+11 3.849E+11
3.793E+11 1.127E+12 1.851E+12 3.615E+12 3.533E+12 3.457E+12 3.391E+12
3.365E+12 3.318E+12 1.969E+12 1.312E+12 1.298E+12 1.281E+12 6.415E+11
6.602E+11 1.267E+12 1.301E+12 3.169E+12 3.154E+12 3.150E+12 3.108E+12
3.079E+12 3.054E+12 3.031E+12 3.028E+12 2.972E+12 2.962E+12 2.930E+12
2.731E+12 2.925E+12 2.811E+12 2.808E+12 2.694E+12 2.599E+12 2.760E+12
2.344E+12 2.578E+12 2.543E+12 2.483E+12 1.964E+12 2.104E+12 2.295E+12
2.292E+12 2.342E+12 2.249E+12 2.282E+12 2.243E+12 2.201E+12 2.191E+12
2.162E+12 2.116E+12 1.852E+13 2.685E+13
7** 2.372E+02 1.174E+07 3.854E+10 4.007E+11 1.058E+11 1.278E+11
4.012E+11 5.900E+11 7.308E+11 9.633E+11 2.579E+12 3.794E+12 5.718E+12
1.014E+13 1.918E+13 1.715E+13 9.696E+12 1.222E+13 2.910E+13 2.171E+13
1.210E+13 1.304E+13 1.128E+13 6.597E+12 8.455E+12 5.900E+12 1.004E+13
6.682E+12 1.332E+12 4.955E+11 1.243E+11 2.287E+10 9.512E+09 1.207E+10
8.811E+08 6.318E+08 T
=AJAX

```

```

MERGE 2 COLLAPSED MASTERS TOGETHER UNIT76(35),75(9)
TOTAL OF 44 ELEMENTS ARE WRITTEN ON UNIT 77
0$$ 77 77 1$$ 2 T
2$$ 76 0 T
2$$ 75 0 T
=NITAWL
MASTER ON UNIT 77, WORKING LIB WRITTEN TO 83, ANISN BINARY TO 84
0$$ 77 A4 83 A9 84 1$$ 0 44 A5 2 3 4 A11 -1 E T
2$$ 11I 10 130 5I200 260 13I 300 440 7I 500 580 T
/*
//NONE EXEC AXMIY
//GO.FT83FO01 DD UNIT=TAPE62,DISP=(NEW,PASS),LABEL=(9,SL),
// DCB=(RECFM=VBS,LRECL=X,BLKSIZE=6447,BUFL=8148,DEN=4),
// VOL=SER=X23004,DSN=GLS.LWR47.ANISN.MIX
//GO.FT82FO01 DD UNIT=TAPE62,DISP=(OLD,PASS),LABEL=(2,SL),
// DCB=(RECFM=VBS,LRECL=X,BLKSIZE=6447,BUFL=8148,DEN=4),
// VOL=SER=X23285,DSN=GLS.LWR47.ANISN.BINARY
// GO.FTOSFO01 DD*
MIX ANISN CROSS SECTIONS 47N/20G MAKE CARD IMAGE TAPE FOR SAILWR LIB
1$$ 67 70 70 2 176 0 0 0 114 234 1 0 3 40
2$$ 0 0 3 4 0 0 0 0
3$$ 0 0 82 83 5 6 0 0 T
10$$ 54I 179 234 2R-179 6R-183 6R-187 6R-191
10R-195 4R-199 3R-203 3R-207 3R-211 3R-215 3R-219 3R-223
3R-227 3R-231
11$$ 56Z 55 59 79 107 63 67 71 75
139 107 123 127 131 135 139 107 123 127 131 135 81 83 119
2I 15 27 43 47 51 3Q3 31 35 39 3Q3
12** 56Z 0.06686 0.03343
2.37-4 8.93-4 1.74-2 1.52-3 5.83-2 8.55-3
9.81-4 3.71-4 1.27-4 1.12-3 8.19-2 4.44-4
9.37-4 5.06-4 3.37-4 5.34-4 8.21-2 6.05-4
7.77-3 1.15-4 4.38-2 1.05-3 1.48-4 2.39-3 1.58-2 6.93-4 2.29-3
3.13-4
7.64-5 1.48-4 8.77-4 4.27-2
1.874-4 2.616-2 2.322-2 4.697-4 2.589-2 2.322-2
5.604-4 2.580-2 2.322-2 5.951-4 2.576-2 2.322-2
6.938-4 2.566-2 2.322-2 8.006-4 2.556-2 2.322-2
8.806-4 2.550-2 2.322-2 2.133-2 1.708-3 2.322-2
16$$ 232I 1 234 18$$ F-1
13$$
2I 1 4 2I 7 10 2I 13 16 2I 19 22 2I 25 28 2I 31 34
2I 37 40 2I 43 46 2I 49 52 2I 55 58 2I 61 64 2I 67 70
2I 73 76 2I 79 82 2I 85 88 2I 91 94 2I 97 100 2I103 106
2I109 112 2I115 118 2I121 124 2I127 130 2I133 136 2I139 142
2I145 148 2I151 154 2I157 160 2I163 166 2I169 172 2I175 178
2I181 184 2I187 190 2I193 196 2I199 202 2I205 208 2I211 214
2I217 220 2I223 226 2I229 232 2I235 238 2I241 244 2I247 250
2I253 256 2I259 262 T

```